UNIVERSITY OF BORÅS
SCHOOL OF ENGINEERING

Enhanced Butanol Production by Free and Immobilized *Clostridium* sp. Cells Using Butyric Acid as Co-Substrate

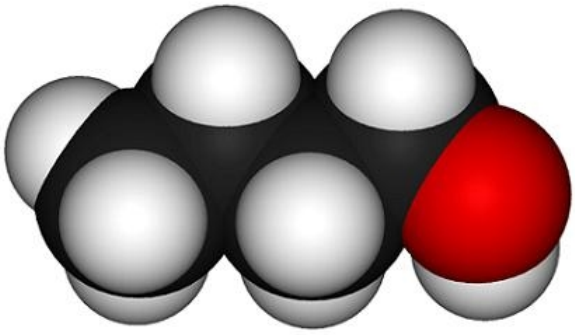

Laili Gholizadeh

This thesis comprises 30 ECTS credits and is a compulsory part in the Master of Science with a Major in Chemical Engineering – Applied Biotechnology 120 ECTS credits No. 10/2009

Title: Enhanced Butanol Production by Free and Immobilized *Clostridium* sp. Cells using Butyric Acid as Co-Substrate.

Author: Laili Gholizadeh Baroghi (e-mail: leili.gholizadeh@gmail.com)

Master Thesis

Subject Category: Biotechnology (Bioprocess Engineering – Biofuels)

University College of Borås
School of Engineering
SE-501 90 BORÅS
Telephone: (+46) 033 435 4640

Examiner:	Prof. Mohammad Taherzadeh
Supervisor and Thesis Advisor:	Prof. Shang–Tian Yang
Supervisor Address:	OSU–Ohio State University 125 Koffolt Laboratories 140 West 19th Ave. Columbus, OH 43210–1185, USA
Client:	Ohio State University (OSU), Chemical & Biomolecular Engineering Department Prof. Shang–Tian Yang Columbus, Ohio; USA.
Date:	08–12–2009
Keywords:	Bio-butanol • Acetone–Butanol–Ethanol (ABE) • ABE-fermentation • Butyric acid • *Clostridium* • *C. acetobutylicum* ATCC 824 • *C. beijerinckii* ATCC 55025 • *C. beijerinckii* BA 101 • *C. beijerinckii* NCIMB 8052 • Fibrous-bed Bioreactor (FBB) • Batch • Suspended cell culture • Immobilized cell system.

DEDICATION

I would like to dedicate this M.Sc. Thesis to my beloved Family for all their love and encouragement and for always been supportive of my choices.

"I am among those who think that science has great beauty. A scientist in his laboratory is not only a technician: he is also a child placed before natural phenomena, which impress him like a fairy tale."

– Marie Curie

ABSTRACT

Butanol production by four different *Clostridium* sp. strains was investigated using glucose P2-medium supplemented with increasing concentrations of butyric acid, added as co-substrate. Batch fermentations were carried out in serum bottles (freely-suspended cell cultures) and fibrous-bed bioreactor (FBB) with medium recirculation (immobilized cells). Butyric acid clearly revealed to inhibit cellular growth with all specific growth rates declining upon the increase of butyrate concentrations. However, the presence of low and moderate levels in the medium can readily enhance the ABE-fermentation and increase butanol production through a shift induction towards the solventogenic phase controlled by the medium pH. In all cases it was found that 4.0 $g \cdot l^{-1}$ is the optimal concentration of butyrate that maximizes the yields for all ABE-solvents and butanol productivities. The non-mutant C. *acetobutylicum* ATCC 824 was singled out as the most efficient butanol productive strain among all bacteria tested (10.3 $g \cdot l^{-1}$ butanol *versus* 0.72 $g \cdot l^{-1}$ with and without 4.0 $g \cdot l^{-1}$ butyrate, respectively) showing a productivity augment in the order of 0.078 $g \cdot l^{-1} \cdot h^{-1}$ (78.5%) and yields of 0.3 $g \cdot g^{-1}$ from substrate and 7.6 $g \cdot g^{-1}$ from biomass *versus* 0.072 $g \cdot g^{-1}$ and 0.41 $g \cdot g^{-1}$ with and without the optimal butyrate concentration, respectively. This strain also revealed the best overall tolerance over increasing butyrate concentrations up to ~6.0 $g \cdot l^{-1}$ and the highest glucose uptake (65.5%) among all bacteria. Furthermore, the beneficial effects of butyric acid were also observed through the use of a fibrous bed-bioreactor when the mutated strains of *C. beijerinckii* ATCC 55025 and BA 101 were tested. The use of this immobilized cell system effectively improved butanol production over the free system with butanol titers in the fermentation broth around 11.5 $g \cdot l^{-1}$ and 9.4 $g \cdot l^{-1}$ for the two bacteria, respectively, roughly doubling the values attained with the corresponding suspended cell cultures when the media were supplemented with 4.0 $g \cdot l^{-1}$ of butyrate. All these results confirm the enhancement of butanol formation using either free or immobilized cell cultures supplemented with butyric acid concentrations up to 4.0 $g \cdot l^{-1}$ in the media.

Keywords: Bio-butanol • Acetone–Butanol–Ethanol (ABE) • ABE-fermentation • Butyric acid • *Clostridium* •*C. acetobutylicum* ATCC 824 • *C. beijerinckii* ATCC 55025 • *C. beijerinckii* BA 101 • *C. beijerinckii* NCIMB 8052 • Fibrous-bed Bioreactor (FBB) • Batch • Suspended cell culture • Immobilized cell system.

Acknowledgments

I would like to deeply thank several people who have played a decisive role during the several months in which this work lasted, providing me with useful and helpful assistance. Without their patience and understanding, this dissertation would likely not have been materialized.

In first place, I would like gratefully acknowledge to Professor Shang-Tian Yang for being my supervisor and thesis advisor at the Chemical and Bimolecular Engineering Department of Ohio State University (OSU). I would like to express my special gratitude to him for providing me the opportunity of performing my master thesis work within his research group. I am sincerely grateful for his attentive supervision and guidance throughout this work – It has been a true privilege.

To my fellow colleagues Wei-Lun Chang and Jingbo Zhao, I am thankful for their support and incentive, as well as Thanks to other colleagues at Koffolt Laboratories for all their friendship and support and for the really great times spent in and outside the laboratory.

And last but not the least; I would like to hugely thank my exceptional family, especially to my husband, my parents and my brother and sisters for all their love, never-ending support and encouragement.

Table of Contents

List of Figures

List of Tables

Abbreviations and Terms

ΔP/Δt: Average Butanol Formation Rate (or Observable Butanol Formation Rate)

ΔpH: Variation in pH value

ΔS/Δt: Observable Substrate (Glucose) Consumption Rate

$\left(Y_{P/X}\right)$: Butanol or/and ABE-solvents Yields from Biomass

$\left(Y_{P/S}\right)$: Butanol or/and ABE-solvents Yields from Substrate

$\frac{dP}{dt}$: Instantaneous Butanol Formation Rate

ABE: Acetone–Butanol–Ethanol

ATCC: American Type Culture Collection

BA: Butyric Acid (Butyrate)

BTU: British Thermal Units

BuOH: Butanol

CoA: Coenzyme A

DCW: Dry Cell Weight

FBB: Fibrous-Bed Bioreactor

HC: Hierarchical Clustering

k_S: First-order Rate Constant for Glucose Consumption

NCIMB: National Collection of Industrial, Marine and Food Bacteria

OD: Optical Density

PABA: *p*-Amino benzoic acid

PC: Principal Component

PCA: Principal Component Analysis

q_p: Specific Butanol Formation Rate

q_S: Specific Glucose Consumption Rate

RVP: Reid Vapor Pressure

SD: Standard Deviation

SEM: Scanning Electron Microscopy

STP: Standard Temperature and Pressure Conditions

SVD: Single Value Decomposition

USD: United States Dollar ($)

YE: Yeast Extract

Chapter 1 – Introduction

1. INTRODUCTION

Due to the continual rise in the cost of crude oil as main energy source, research into sustainable economical and environmental alternatives to fossil fuels is continuously becoming more and more important. One set of promising alternatives to petroleum derived fuels are *biofuels*, especially those produced via fermentation processes from renewable resources, such as butanol (biobutanol) [1]. Biofuels are generally considered as fuel additives rather than petroleum substitutes (Davis and Morton III, 2008).

Even though commercial butanol is nearly exclusively produced from petrochemical routes nowadays, its production via microbial fermentation is not a recent matter. The so-called acetone–butanol–ethanol (ABE) fermentation promoted by bacteria of the genus *Clostridium* sp., particularly *acetobutylicum* (Lin and Blaschek, 1983), is in fact one of the oldest known anaerobic industrial fermentations. It was ranked in second place just behind ethanol fermentation by the yeast *Saccharomyces cerevisiae* in its scale of production, and is still one of the largest biotechnological processes ever known (Ramey and Yang, 2004 (report)). This fermentation was widely carried out industrially up to the first half of the 20th Century with 66% of the butanol consumed worldwide being produced from biotechnological means (Dürre, 2008). However, with the advent of the Second World War and the escalating development of the Petrochemical Industry, its production rapidly started to cease. By the 1960s, totally efficient production of ABE by the oil industry along with the higher costs of carbohydrate sources as feed substrate, combined with even lower sugar content in the case of molasses (main substrate at that time), have resulted in the complete eradication of this industrial activity. However, as the oil prices started to increase from the beginning of the 1970s due to the "oil crisis" coupled with the uncertainty of petroleum supplies in more and more energy driven worldwide societies, and the emergent environmental awareness, have lead to the concomitant revival and interest of this bio-industry (Dürre, 1998; Dürre, 2008). Since then, substantial research efforts on ABE-producing clostridia have been carried out in multiple fields, namely in Microbial Technology, to improve solvent yields, low volumetric productivities and final product concentration. These are focused in the selection and physiological improvement of microbial cultures by genetic and metabolic engineering (Desai *et al*., 1999; Nölling *et al*., 2001; Scotcher and Bennett, 2005; Papoutsakis, 2008), fermentation engineering and technology including upstream processing and

media optimization, and the development of integrated low energy separation–extraction–purification techniques (downstream processing) (Ezeji *et al*., 2004; Liu and Fan, 2004; Ezeji *et al*., 2007; Lee *et al*., 2008a).

Like in every bioprocess, ABE-fermentation manifests several drawbacks in terms of economical competitiveness over pure chemical processes. The main disadvantage in this case concerns the rather complex metabolic pathway that governs butanol production by these bacteria (Fig. 1).

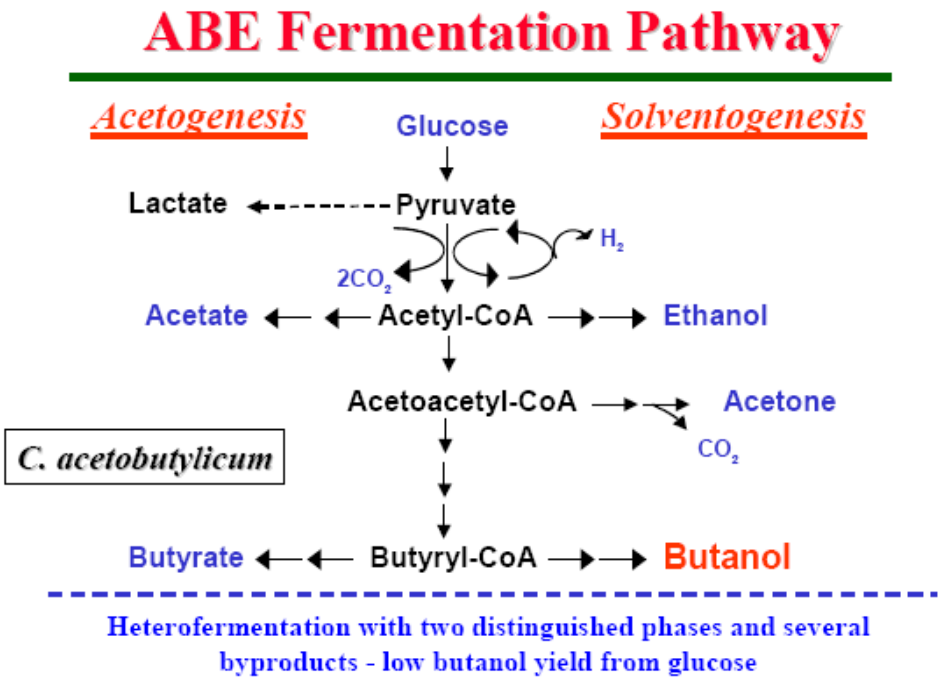

Figure 1. Two-phase ABE Fermentation pathways in *C. acetobutylicum* (adapted from Ramey and Yang, 2004 (report). Reprint used with permission from the authors.

In a typical batch ABE-fermentation from carbohydrates, butyric, propionic and acetic acids are firstly produced by *C. acetobutylicum* (acidogenesis) in the exponential phase of cell growth with the culture then undergoing a metabolic shift towards the formation of acetone, butanol and ethanol as main product solvents in the approximate 3:6:1 ratio when the stationary phase is reached (solventogenesis) (Fond *et al*., 1985). This shift induction is controlled either by the decrease in pH (< 5) at the end of the exponential phase and increase of butyric acid concentration (> 2 $g \cdot l^{-1}$) (Gottschalk and Morris, 1981; Gottwald and Gottschalk, 1985; Monot *et al*., 1984). However, the actual fermentation is rather complex and very delicate to be controlled

efficiently (Chauvatcharin *et al*., 1998). Therefore, in conventional ABE fermentations the butanol yield from glucose is in general quite low, typically around 15% (w/w) and seldom exceeding the 25% wt. Also, butanol production is limited by severe product inhibition (toxicity) that stops cell growth ceasing the fermentation. In fact, these bacteria can hardly sustain butanol concentrations above 10 $g \cdot l^{-1}$; and as a result butanol concentrations in usual ABE fermentative broths are usually below 13 $g \cdot l^{-1}$. In the past these two factors combined with low cell densities made butanol production from glucose by ABE-fermentation uneconomical (Maddox, 1989). Since then, various systems for ABE production have been developed in an attempt to solve these problems (Groot *et al*., 1992), including: batch culture (Ishizaki *et al*., 1999; Qureshi and Blaschek, 1999) or fed-batch culture (Yang and Tsao, 1995; Qureshi and Blaschek, 2000; Ezeji *et al*., 2004) integrated with a process of butanol removal and continuous culture (Godin and Engasser, 1990; Mutschlechner *et al*., 2000). Cell-recycle and cell immobilization have also been utilized in order to increase cell density and bioreactor productivity and the introduction of extractive fermentation to reduce the effect of solvent inhibition, have also been tentatively explored (Geng and Park, 1994; Groot *et al*., 1991a/b; Maddox *et al*, 1995; Mollah and Stuckey, 1993; Mulchandani and Volesky, 1994; Park *et al*., 1990; Qureshi and Blaschek, 1999; Qureshi and Maddox, 1995; Yang and Tsao, 1995). Cell immobilization, while increasing volumetric productivities and rapid bioconversion due to the accumulation of high amount of cells per mass unit of support material, coupled with cell-retention inside the bioreactor, also simplifies downstream-processing by producing cell-free product streams. *In-situ* recovery of butanol by extractive fermentation has been shown to improve the fermentation productivity and butanol yield by twofold. However, despite of all these attempts butanol titer, productivity and yield still remain relatively low (20 $g \cdot l^{-1}$ in concentration from the fermentation broth; 4.5 $g \cdot l^{-1} \cdot h^{-1}$ in productivity; and less than 25% wt in yield from glucose) (Ramey and Yang, 2004 (report)).

Of the several factors that affect ABE fermentation in the production of butanol, the medium pH and the concentration of butyric and acetic acids are categorically the most important ones (Bahl *et al*., 1982; Yu and Saddler, 1983; Monot *et al*., 1984; Ammouri *et al*., 1987; Assobhei *et al*., 1998; Chen and Blaschek, 1999; Tashiro *et al*., 2004; Lee *et al*., 2008b). It has been demonstrated that during the acidogenesis phase of cell growth the intracellular pH follows the decrease of the external pH due to the formation of acids, but this parallel trend is controlled

internally with the cells keeping a constant ΔpH between 0.9 and 1.3 when the medium pH varied from 5.9–4.3 (Gottwald and Gottschalk, 1985; Terracino and Kashket, 1986).

Therefore, the purpose of the present study is to provide further insights on the particular effects of butyric acid added as co-metabolic substrate in the fermentation medium in the formation of butanol and total ABE-solvents using four different ABE-producing strains of clostridia: *C. acetobutylicum* ATCC 824, *C. beijerinckii* ATCC 55025, *C. beijerinckii* BA 101 and *C. beijerinckii* NCIMB 8052. These bacteria, commonly used in many research studies, are firstly going to be compared and characterized in terms of butanol and ABE-solvents production, and the impact of butyric acid addition on their individual cell growth patterns and fermentation parameters, such as yield from substrate (and biomass), volumetric productivity, and butanol/ABE-solvents concentration will be evaluated. Secondly, a preliminary comparison attempt between suspended cell culture fermentation in serum bottles and immobilized cell system involving a fibrous-bed bioreactor (FBB) with medium recirculation, both operating in batch mode, are going to be performed for the mutant strains *C. beijerinckii* ATCC 55025 and *C. beijerinckii* BA 101. Preliminary results shown herein reveal that butyric acid has an inhibitory effect on cell growth but lower levels in the media can effectively improve ABE-fermentation and increase butanol production for all species tested, especially when an optimal 4.0 $g \cdot l^{-1}$ of butyric acid is supplemented in the medium.

Chapter 2 – Literature Review

2. LITERATURE SURVEY

2.1 Butanol

Butanol (IUPAC nomenclature, 1-butanol; CAS no. 71-36-3) also commonly known as butyl alcohol, *n*-butanol or methylolpropane, is a linear 4-carbon aliphatic alcohol (primary alcohol) having the molecular formula of C_4H_9OH (MW 74.12 $g \cdot mol^{-1}$). Butanol is a colorless, flammable, slightly hydrophobic liquid with a distinct banana-like aroma and strong alcoholic odor. In direct contact it may irritate the eyes and skin. Its vapor has an irritant effect on mucous membranes and a narcotic effect when inhaled in high concentrations. It is completely miscible with most common organic solvents, but only sparingly soluble in water (Lee *et al*., 2008a; Dürre, 2008). Other chemicals in the same alcohol family include methanol (1-carbon), ethanol (2-carbon), and propanol (3-carbon) (Kristin Brekke, 2007). Table 2.1 summarizes the distinctive characteristics of butanol over other fuels.

2.2. Butanol as Fuel

One of the major preeminent roles of biobutanol (bio-based butanol) is its appliance in the next generation of motor-fuels. While ethanol has received most of the attention as a fuel additive for many reasons (Hansen *et al*., 2005 and Niven, 2005), butanol could be a better direct option due to its own intrinsic physical and chemical properties (Huber *et al*., 2006) and energy content as compared to ethanol (Table 2.1). This means butanol consumption is close to that of pure gasoline whereas ethanol-gasoline blends are consumed much faster to obtain the same power input. Additionally, butanol can be mixed with common gasoline at any percentage ratio (Atsumi *et al*., 2008) in a similar way as with existing gasoline-ethanol blends (e.g., 23% in Brazil and 10% in United States and some parts of Europe). Also, butanol usage does not require any modifications in car engines or substitutions, producing similar mileage performance to gasoline. For instance, in 2005, David Ramey, drove a 13-year old Buick across the United States, fueled just by pure butanol with only a 9% consumption increase as compared to standard gasoline (petrol) [1]. Despite this small increase in biofuel consumption the emissions of CO, hydrocarbons and NO_x pollutants were drastically reduced. This has a tremendous positive impact on the global environment.

Table 2.1. Physical and chemical properties of butanol (adapted from Davis and Morton III, 2008; Lee *et al*., 2008a; [4] and [5]).

Properties	**Butanol**	**Chemical Structure**
Melting point (°C)	- 89.3	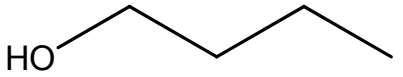
Specific gravity	0.810– 0.812	
Ignition temperature (°C)	35–37	
Auto-ignition temperature (°C)	343–345	1-butanol
Flash point (°C)	25–29	
Relative density (water: 1.0)	0.81	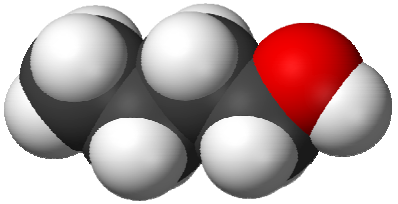
Critical pressure (hPa)	48.4	
Critical temperature (°C)	287	
Explosive limits (vol. % in air)	1.4–11.3	
Water solubility	9.0 ml/100 ml (7.7 g/100 ml at 20°C)	
Relative vapor density (air: 1.0)	2.6	
Vapor pressure (kPa at 20°C)	0.58	

	Butanol	**Gasoline**	**Ethanol**	**Methanol**
Boiling point (°C)	117–118	27–221	78	64.7
Density at 20°C (g/ml)	0.8098	0.7–0.8	0.7851	0.7866
Solubility in 100 g of water	immiscible	immiscible	miscible	miscible
Energy density ($MJ \cdot l^{-1}$)	27–29.2	32	19.6	16
Energy content/value (BTU/gal)	110000	115000	84000	76000
Air-fuel ratio	11.2	14.6	9	6.5
Heat of vaporization (MJ/kg)	0.43	0.36	0.92	1.2
Liquid Heat capacity (Cp) at STP (kJ/k-mol.ºK)	178	160–300	112.3	81.14
Research octane number	96	91–99	129	136
Motor octane number	78	81–89	102	104
Octanol/Water Partition Coefficient (as $logP_{o/w}$)[a]	0.88	3.52±0.62	-0.31	-0.77
Dipole moment (polarity)	1.66	n.a.	1.7	1.6
Viscosity (10^{-3} Pa.s)	2.593	0.24–0.32	1.078	0.5445

[a)] LogP is a measure of hydrophobicity (lipophilicity) and is similar to polarity. These published values were obtained from Hansch *et al*., (1995) for the three alcohols. In gasoline the LogP was roughly estimated as the weigh average of main representative components.

Other important advantages over ethanol include: (a) the lower volatility (less explosive). Butanol has a Reid Vapor Pressure (RVP) 7.5 times lower than ethanol (S.-T. Yang, 2008); (b) it does not readily adsorb moisture (lower hygroscopicity), so is less affected by weather changes; (c) less corrosive (Dürre, 2007); (d) is safer than ethanol because of its high flash point and lower vapor pressure; (e) it has a higher octane rating; (f) butanol has approximately 30% more energy/BTU accumulated per gallon (around 110.000 BTU per gallon, as opposed to ethanol, which has 84.000 BTU per gallon); and (g) complete miscibility with gasoline and diesel fuel. This allows butanol to be a much safer fuel that can be dispersed through existing pipelines and filling stations (S.-T. Yang, 2008) with simple integration into the present fuel delivery and storage infrastructure (pipelines, storage tanks, filling stations, etc.). Ethanol, on the other hand, can only be added shortly prior to use. The vapor pressure of butanol (4 mmHg at 20°C) is 11 times lower than ethanol (45 mmHg at 20°C) enabling it to be directly added to gasoline without regarding evaporation emissions and consequent related complications. Also, the physical-chemical properties of butanol makes possible the blending with gasoline with no phase-separation in the presence of water (less readily contaminated with water) than other biofuel/gasoline blends. However, the viscosity of butanol is twice of that of ethanol and 5–7 times that of gasoline (Wackett, 2008). Other physical properties of butanol, such as density and heat capacity, are somewhat comparable to that of ethanol (Table 2.1).

2.3. Main Applications of Butanol

Besides the expected role as engine-biofuel, butanol is actually an important bulk chemical with a broad range of industrial uses. Almost half of the worldwide production is used in the form of butyl acrylate and methacrylate esters used in the production latex surface coatings, enamels, nitrocellulose lacquers, adhesives/scalants, elastomers, textiles, super absorbents, flocculants, fibers, and plastics. Other important butanol derived compounds are butyl glycol ether, butyl acetate and plasticizers. Compounds of minor applicability are butyl amines and amino resins. Butanol and derived compounds are excellent diluents in paint thinners, hydraulic and brake fluid formulations. It is also used as solvent in the perfume industry and for the manufacturing of antibiotics, vitamins and hormones. Other applications include the manufacture of safety glass, detergents, flotation aids (e.g., butyl xanthate), deicing fluids, cosmetics (eye makeup, nail-care

products, shaving and personal hygiene products. It is also commonly used as extracting agent and in food and flavor industries) (Lee *et al*., 2008a and Dürre 2008).

2.4. Chemical Synthesis of Butanol

Butanol has been made industrially using three major chemical processes: Oxo synthesis, Reppe synthesis, and crotonaldehyde hydrogenation (Fig.2.1). In oxo synthesis (hydroformylation), carbon monoxide and hydrogen are added to an unsaturation using metal catalysts such as Co, Rh, or Ru substituted hydrocarbonlyls (Falbe, 1970). Aldehyde mixtures are obtained in the first reaction step, which is followed by hydrogenation for the production of butanol. Depending on the reaction conditions such as pressure, temperature and type of catalyst, different isomeric ratios of butanol can be obtained. In the Reppe synthesis, propylene, carbon monoxide and water are reacted together in the presence of a catalyst (Bochman *et al*., 1999) generating a mixture of *n*-butaraldehyde and isobutaraldehyde where the former is reduced to *n*-butanol (Wackett, 2008). The Reppe process directly produces butanol at low temperature and pressure. However, this process has not been commercially successful since it requires expensive technology. Until a few decades ago, the common route for butanol synthesis was from acetaldehyde using crotonaldehyde hydrogenation. The process consists of aldol condensation, dehydration, and hydrogenation (Bochman *et al*., 1999). Although rarely utilized nowadays, it may again become significant in the future. While other processes rely completely on petroleum, the crotonaldehyde hydrogenation process provides an alternative route from ethanol which can be produced from biomass. In this case, ethanol is dehydrogenated to form acetaldehyde from which the synthesis can proceed (Swodenk, 1983).

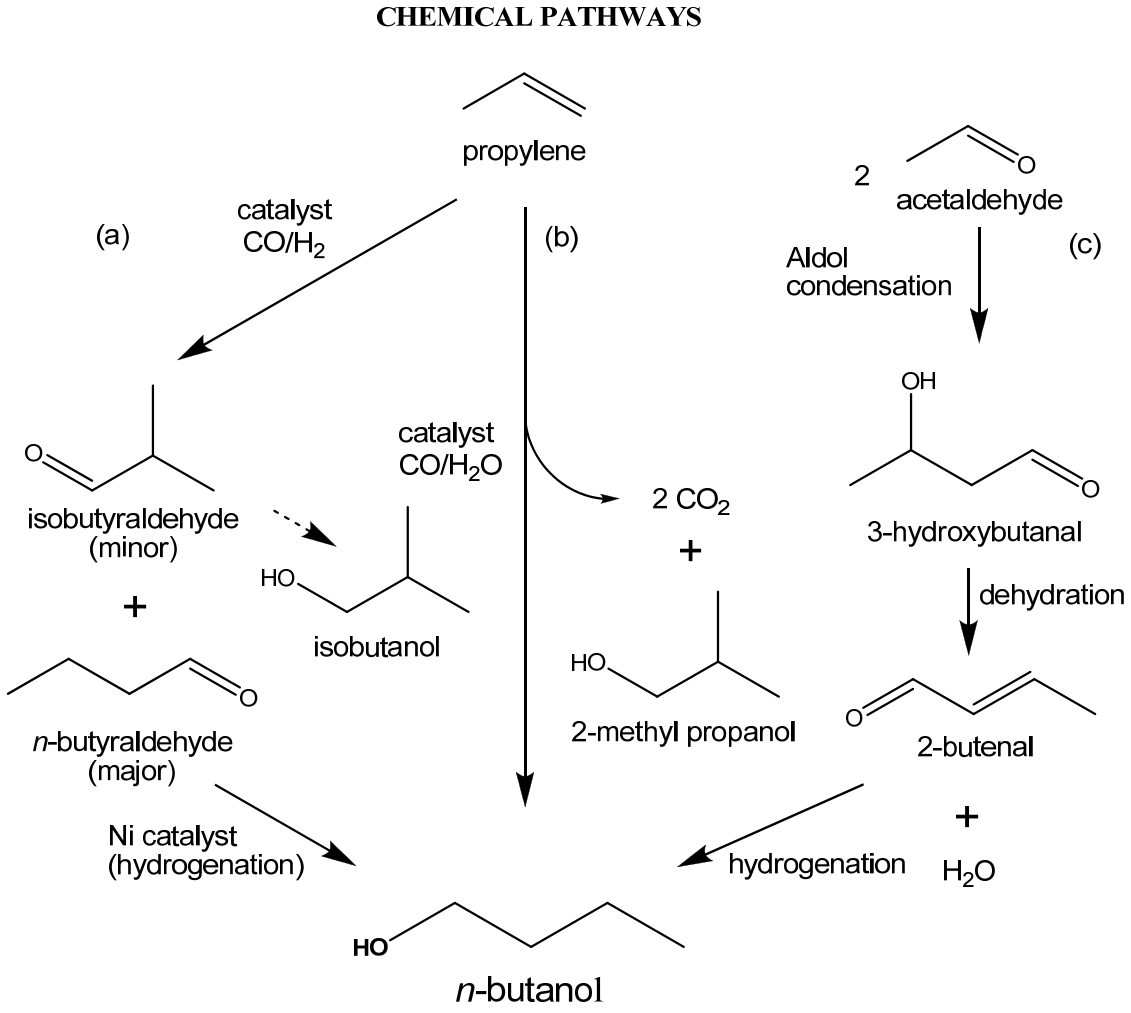

Figure 2.1. Industrial synthesis of butanol and secondary by-products. Chemical routes: (a) Oxo synthesis, (b) Reppe process, and (c) crotonaldehyde hydrogenation (adapted from Lee, 2008a and Wackett, 2008).

2.5. Economics of the ABE-Fermentation

In 1996, the worldwide annual production of butanol was 2.49×10^6 tons (Lee *et al*., 2008a). It has been estimated that around 10–12 billion pounds of butanol is produced annually (Donaldson *et al*., 2007), which accounts for 7–8.4 billion dollar (USD) market at current price. Butanol has a projected market expansion of 3% annually (Kirschner, 2006). Butanol production by regions in the world is shown in Table 2.2.

Table 2.2. World production of butanol by region (1996 data*).

Region	Butanol (kg)
North America	1.17×10^9
South America	5.12×10^7
Europe	8.43×10^8
Asia	4.30×10^8
TOTAL	2.49×10^9

*Adapted from Qureshi and Blaschek, (2001a).

In recent years several economic studies have been conducted on the production of butanol from various substrate sources and process layouts (Lenz and Moreira, 1980; Qureshi and Blaschek, 2001a/b). In these studies it was found that recovery of butanol from the fermentation broth by distillation is totally uneconomical when compared with petrochemically derived butanol. Nonetheless, studies employing *C. beijerinckii* BA101, *C. acetobutylicum* P260, hydrolyzed DDGS (corn stover, corn fiber, and fiber-rich distillers dried grains and solubles) and wheat straw suggest that commercial production of biobutanol from agricultural wastes is moving closer (Ezeji *et al*., 2007). For instance, DuPont (US) and British Petroleum/BP (UK) have recently teamed up in a major effort to further develop and commercialize 1-butanol as well as other higher octane biobutanol isomers. Both companies also announced that testing of these advanced biofuels demonstrates the use of biobutanol can increase the blending of biofuels in

gasoline beyond the current 10 percent limit for ethanol without compromising performance [1]. It is expected that the first plants would focus on sugar or corn starch; but, it is likely that agricultural waste residues, or their derived hydrolysates, would become a potential carbon source instead due to their high abundance (Ezeji *et al*., 2007). If produced directly from a biomass source, there is no net carbon dioxide production.

Several recent advances have been performed including the development and optimization of microbial cultures (metabolic/genetic engineering and media formulation), process technologies, and use of waste substrates. However, all these advances will need to be translated into developable technologies and processes that can compete directly with the established petrochemical routes for butanol production. For example, many upstream studies have been focusing on the utilization of low cost by-products from various industrial activities as potential feedstock substrates. Some of these include: industrial wastewater from palm oil (Hipolito *et al*., 2008), corn steep medium (Parekh *et al*., 1998 and Parekh *et al*., 1999), blackstrap molasses (a secondary product of sugar industries) (Syed *et al*., 2008), corn fiber hydrolysate (Qureshi *et al*., 2008), degermed corn (Campos *et al*., 2002 and Ezeji *et al*., 2007), soy molasses (Qureshi *et al*., 2001b), wheat straw hydrolysate (Qureshi *et al*., 2007 and Qureshi *et al*., 2008a/b), corn steep water (Parekh *et al*., 1999), whole potato media (Nimcevic *et al*., 1998), and hemicelulose hydrolysates from the wood and paper industries (Mes-Hartree and Saddler, 1982). It is anticipated that future research might focus on the development of second-generation cultures (as compared to the existing strains of *C. beijerinckii* BA101, *C. acetobutylicum* PJC4BK, and *C. acetobutylicum* P260, which hyper-produce total ABE-solvents on the order of 25–33 $g \cdot l^{-1}$ (Qureshi *et al*., 2005 and Ezeji *et al*., 2006). Another way where technological advances could be made involves the recovery of fermentation by-products (large waste water streams, cell mass, CO_2, and H_2) for further revenue. For instance, CO_2 can be converted into algal biomass and oil when exposed to sunlight. The use of carbon dioxide would benefit the biobutanol industry quite significantly since it is produced at zero cost. Moreover, H_2 gas can be separated and burned to generate electricity (Ezeji *et al*., 2007). Several studies are available regarding the economical evaluation and feasibility of the ABE-fermentation process (Qureshi and Blaschek, 2001a–c; Lenz and Moreira, 1980; and Ramey and Yang, 2004 (report)).

2.6. Short Description of the Species

Individual vegetative cells of *Clostridium acetobutylicum* are straight rod-shaped bacillus ranging in size of 0.5–1.5×1.5–6 μm (Robinson, 2000) (Fig. 1.3). They are Gram-positive in growing cultures but Gram-negative in older cultures, typically strictly anaerobes (oxygen free), heterofermentative, spore-forming and motile by peritrichous flagella. During sporulation, cells swell markedly and store granulose, a polysaccharide based material that serves has carbon and energy source during solventogenesis. Spores are oval and subterminal (Fig. 1.3b). The optimum growth temperature is 37°C, and biotin and 4-aminobenzoate are usually required as growth factors. ABE-clostridial strains are generally classified into four distinct groups based on their biochemical and genetic characteristics (Woods, 1995). The best known groups are the mesophiles *C. acetobutylicum* and *C. beijerinckii* (formerly known as *C. butylicum*) and one of the most documented strains in ABE-fermentation research studies (Karakashev *et al*., 2007).

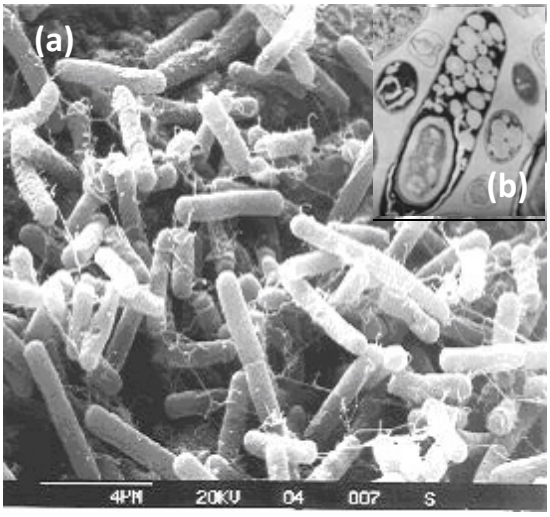

Figure 2.2. Scanning Electron Micrographs (SEM) of *C. acetobutylicum* (also called the "*Weizman organism*") showing the different stages of spore formation: vegetative cells (a) and spore formed cells (b). Image (a) was taken from [2] and image (b) was taken from [3] (image: Courtesy Andrew Goldenkranz).

2.7. Characterization of Butanol–producing Strains of *Clostridium*

A large number of solventogenic clostridia have been reported over the years (Johnson and Chen, 1995; Zverlov *et al*., 2006). *C. acetobutylicum* harbors a large plasmid which carries the genes for solventogenesis. Loss of the plasmid causes instability leading to degeneration of the bacteria during long fermentation periods which is characterized by acid accumulation without any switch to solventogenesis (Kashket and Cao, 1995; Cornillot *et al*., 1997). In *C. beijerinckii*, and most probably also in other butanologenic species, the solventogenic genes are localized in the chromosome (Wilkinson *et al*., 1995). Both the chromosome and megaplasmid of *C. acetobutylicum* have been totally sequenced (Nölling *et al*., 2001) and the genes involved in acid and solvent production have been identified (Dürre 1998).

The primary type strain, *C. acetobutylicum* ATCC 824, was firstly isolated in 1924 from garden soil in Connecticut (Weyer and Rettger, 1927) and is one of the best-studied ABE-solventogenic clostridia along with the *C. beijerinckii* NCIMB 8052 counterpart. Strain relationships among solventogenic clostridia have been analyzed (Cornillot and Soucaille, 1996, Johnson and Chen, 1995 and Jones and Keis, 1995), and the ATCC 824 strain was shown to be strongly correlated to the historical wild type "Weizmann strain". The ATCC 824 wild-type strain has been physiologically characterized and used in a variety of molecular biology and metabolic engineering studies both in Europe and United States (Bahl *et al*., 1995, Dürre *et al*., 1995, Girbal and Saucaille, 1998, Papoutsakis and Bennett, 1999 and Petitdemange *et al*., 1997). DNA sequence analysis of the 16s rRNA gene of several representative strains have shown that the amylolytic *C. acetobutylicum* ATCC 824 is phylogenetically distant from the saccharolytic strains, including *C. beijerinckii* NCIMB 8052. A number of reports suggest that *C. beijerinckii* might have greater potential for the industrial production of solvents than does the previously sequenced *C. acetobutylicum* since the former has a wider substrate range and pH optimum for growth and solvent formation (Ezeji *et al*., 2004a). The ATCC 824 wild-type strain is well known to metabolize a broad range of monosaccharides, disaccharides, starches, and other substrates, such as inulin, pectin, whey, and xylan, but not crystalline cellulose (Lee *et al*., 1985 and Mitchell, 1998).

A promising route to improve ABE-fermentation is the development of metabolic and genetically-modified clostridia with increased solvent production due to reutilization of carboxylic acids accumulated during the acidogenic phase of carbohydrate uptake, and increased resistance to product inhibition. Metabolic engineering allows the channeling of substrate consumption just to the formation of a specific solvent (e.g., butanol), if desired, resulting in high yields.

The *C. acetobutylicum* ATCC 824 strain has been transformed with a 192-kb megaplasmid designated by pSOL1 (Scotcher and Bennett, 2005), which carries a synthetic *operon* constructed to over-express three homologous acetone-formation genes: *ctfA* and *ctfB* encoding a multifunctional coenzyme A (CoA) transferase which transfers the CoA-moiety from acetoacetyl-CoA to acetate or butyrate, and *adc* encoding acetoacetate decarboxylase (Mermelstein and Papoutsakis 1993). Subsequently, acetoacetate is decarboxylated to form acetone, and acetyl-CoA and butyryl-CoA are converted to ethanol and butanol (Scotcher and Bennett, 2005). Therefore, overexpression of those genes results in significant increase in ABE-solvents formation and decrease in carboxylic acids concentrations. For a more detailed description of clostridial biochemistry review the paper by Mitchell (1998). Modification in solvent production in genetically manipulated strains of *C. acetobutylicum* ATCC 824 due to induced suppression of the solventogenic genes has also been described (Nair *et al*. 1999). Contrary to the super-expression of the solventogenic genes, the prior induction of those genes (suppressed solvent synthesis) resulted in highest solvent production and butanol tolerance reported up till now. Therefore, this strategy appears to be the most promising biotechnological approach for strain enhancement in future commercial applications of ABE-fermentation.

The hyper-amylolytic/butanolagenic *C. beijerinckii* BA101 strain was generated from *C. beijerinckii* NCIMB 8052 (formerly just *C. acetobutylicum*) using chemical mutagenesis (Annous and Blaschek, 1991). Even though the hyper-butanol producing *C. beijerinckii* is slightly more tolerant to butanol than the 8052 parent strain, it does not means that it produces more butanol. Recently, pilot plant studies on butanol production by *C. beijerinckii* NCIMB 8052 parent and mutant BA101 strain in inexpensive glucose/corn steep water medium has been

described. The results confirm that *C. beijerinckii* BA101 grows well and is easy to handle in this simple, cheap medium which is suitable for industrial application (Parekh *et al*., 1999). Moreover, *C. beijerinckii* BA101 may be more adaptable to continuous processes than *C. acetobutylicum* ATCC 824, since it appears to be more stable with respect to strain degeneration. Availability of the genome sequence between these two strains will enable the application of DNA microarrays, gene expression profiling, and comparative genomics in order to better understand the phenotypic differences that exist between *C. beijerinckii* NCIMB 8052 and *C. acetobutylcium* ATCC 824 (Ezeji *et al*., 2004a).

The bacterium *C. beijerinckii* ATCC 55025 was derived from the *C. acetobutylicum* ATCC 4259 parental strain by treating the cells with aqueous ethyl methane sulfonate (mutagen). The resulting mutant is asporogenic, revealed high butyrate uptake rate, and good tolerance to high initial substrate levels and solvents produced (Jain *et al*., 1993).

2.8. Advanced Fermentation–separation Methods

Batch reactors are usually desired in the industry due to its simple mode of operation while reducing the contamination risk. However, the productivity attainable in a batch reactor is generally low due to the lag phase, product inhibition effects as well as the *downtime* for harvesting, cleaning, sterilizing, and re-filling the reactor. The preparation time and lag phase can be surpassed by using continuous operation and the problem of product inhibition can be resolved through the incorporating an *in situ* product removal system. One should note that a single-stage continuous operation is not feasible given to the complexity of butanol production by clostridia. To circumvent substrate inhibition and to increase the biomass, fed-batch mode of operation with intermittent or continuous feeding of nutrients has been used for butanol production. Moreover, immobilized cell reactors and cell recycle reactors have also been applied in order to increase the productivity. For instance, cells of *C. beijerinckii* BA101 have been successfully immobilized onto clay brick particles for ABE-solvents production (Qureshi *et al*., 2000). At a dilution rate of 2.0 h^{-1}, a solvent productivity of 15.8 $g{\cdot}l^{-1}{\cdot}h^{-1}$ was attained with a yield of 0.38 $g{\cdot}g^{-1}$ and concentration of 7.9 $g{\cdot}l^{-1}$. Both yield and concentration were increased by

lowering the dilution rate. This indicates that immobilized cell continuous reactors can be strong candidates for the industrial ABE-fermentation.

Membrane cell recycle reactors are another alternative to improve productivity. A hollow-fiber ultrafilter was applied to separate and recycle the biomass in a continuous fermentation (Pierrot *et al*., 1986). At a dilution rate of 0.5 h^{-1}, cell mass, solvent concentration, and solvent productivity of 20 $g \cdot l^{-1}$, 13 $g \cdot l^{-1}$, and 6.5 $g \cdot l^{-1} \cdot h^{-1}$ h were achieved, respectively. However, fouling of the membrane with the fermentation broth occurred revealing to be a major obstacle for this system. Lipnizki and co-workers (2000) proposed a way of overcoming this problem by allowing only the fermentation broth to undergo filtration by using the immobilized cell system (Lipnizki *et al*., 2000).

2.8.1. Cell Immobilization and Fibrous–Bed Bioreactor (FBB)

Whole-cell immobilization is presently a widespread technique for laboratory studies in many research fields also with reasonable application in large-scale industrial processes. Generally, cell immobilization can be defined as the physical confinement or localization of cells inside a bioreaction system, with preservation of its catalytic activity and stability, and which can be used repeatedly and continuously (Lima *et al*., 2003). Immobilization allows cells to get confined in a favorable and compatible micro-environment, protecting them from potential harmful reaction media (e.g., organic solvents) and against external shear-stress forces developed inside biocatalytic reactors when freely-suspended cell cultures are utilized (Kourkoutas *et al*., 2004). This methodology is not only applicable to microbial cells but also to purified enzymes and animal and plant tissues or even to cell organelles. The industrial use of immobilized cell systems is still limited though, including in ABE-fermentation, and further application will depend upon the optimization of immobilization procedures that can be readily affordable for scaling up.

Fibrous matrices have been developed as support material for cell immobilization because they provide high specific surface area, high void volume, low cost, high mechanical strength, high permeability, and low pressure drop inside reactors. The fibrous bed bioreactor (FBB) with cells

immobilized in the fibrous matrix packed in a column reactor has been successfully employed for several organic acid fermentations, such as butyric and lactic acids, with large increased reactor productivity, final product concentration and yield. Other advantages of the FBB include efficient and continuous mode of operation without the need of repeated cell inoculation, elimination of the lag phase, good long-term stability, while enabling simplified downstream processing. The high reactor performance of the FBB can be attributed mainly to the high viable cell density maintained within the bioreactor as a result of the exclusive cell immobilization mechanism on the porous fibrous matrix. Conventional immobilized cell systems normally lose fermentation productivity over long operation periods when the cells are used continually or repeatedly in a continuous or fed-batch fermentation, due to restricted mass transfer and the buildup of dead biomass. Reactor blockage and channeling effects are also frequent to occur, resulting in reactor deterioration with consequent efficiency loss and inoperability. Thus, for stable long-term bioreactor performance, the cells must be renewed continuously to maintain high productivity and avoid culture degeneration. Another advantage of the FBB is that aged, latent, non-viable and non-productive cells can be immediately removed from the fermentation system and the cell density inside the bioreactor can be adjusted to prevent clogging (Ramey and Yang, 2004 (report)).

Cell immobilization by adsorption onto fibrous matrices usually occurs through three stages: transport of the freely-suspended cells from the bulk liquid onto the fiber surface, cell adhesion at the surface and consequent colonization along the surface. Cell growth in the fibrous matrix can be controlled by the supply of growth nutrients available in the fermentation medium. Upon cell growth the cells get gradually retained at the solid surface until all the available area for immobilization is completely exhausted. The cell-to-fiber adhesion is carried out by simple physical adsorption due to long-range forces such as van der Waals forces and electrostatic (ionic) interactions, and short-range interactions, e.g., dipole interactions and covalent binding established between the bacterial cell wall and the fiber surface (Ramey and Yang, 2004 (report)). In other cell immobilization systems involving absorption a multiple cell-layer often develops forming a thick biofilm (Kourkoutas *et al*., 2004). Although easy to perform, mild on the cells, non-specific character, and potentially free of diffusion limitations, this adsorption

method presents some constraints. Since the adhesion process depends on the balance between opposing attraction and repulsion forces in both electrostatic and hydrophobic interactions; changes in the pH, temperature, ionic strength, surfactant concentration, culture age, and the presence of shearing forces may easily lead to cell leakage from the support. Cell detachment can be overcome partially by using fibers with irregular surface or tailor-made surfaces such as modified cotton fabric (Ramey and Yang, 2004 (report)).

The diagrams shown in (Fig. 2.3) illustrate the basic conceptual design of a Fibrous Bed Bioreactor (FBB). In this bioreactor the cells are immobilized in a loosely convoluted fibrous matrix and then packed inside a columnar vessel (Silva, 1995). The large inflow channels in between the matrices layers enable completely free axial flow of fermentation broth and gases that can be withdrawn from the reactor outlet while inert suspended particles, such as excess of dead biomass, are settled at the bottom of the reactor where they are continually removed. This unique feature avoids directly clogging and fouling problems with severe pressure drops which are very common in traditional immobilized cell systems (e.g., packed-bed, encapsulated-bed and membrane bioreactors). Due to the high cell densities achieved (ranging from 40–100 $g \cdot l^{-1}$), coupled with the high permeability of the immobilized cell matrix, the feed stream nutrients can be consumed fast as they re-circulate through the system resulting in high volumetric productivities. Depending on the design, the transport of nutrients to the cell matrix can occur either by diffusion or convection which greatly enhances the volumetric mass transfer rate, making this reactor one of the most efficient in terms of hydrodynamics and mass transfer. The bioreactor can be operated either continuously or as repeated batch and fed-batch for prolonged periods due to continued cell renewal. More details can be found in Ramey and Yang, 2004 (report).

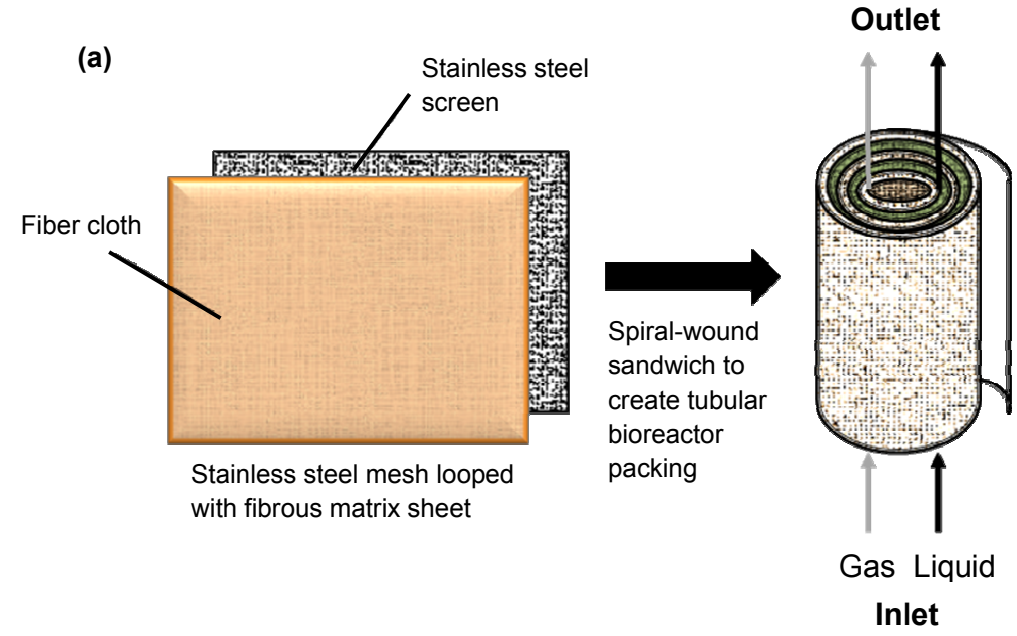

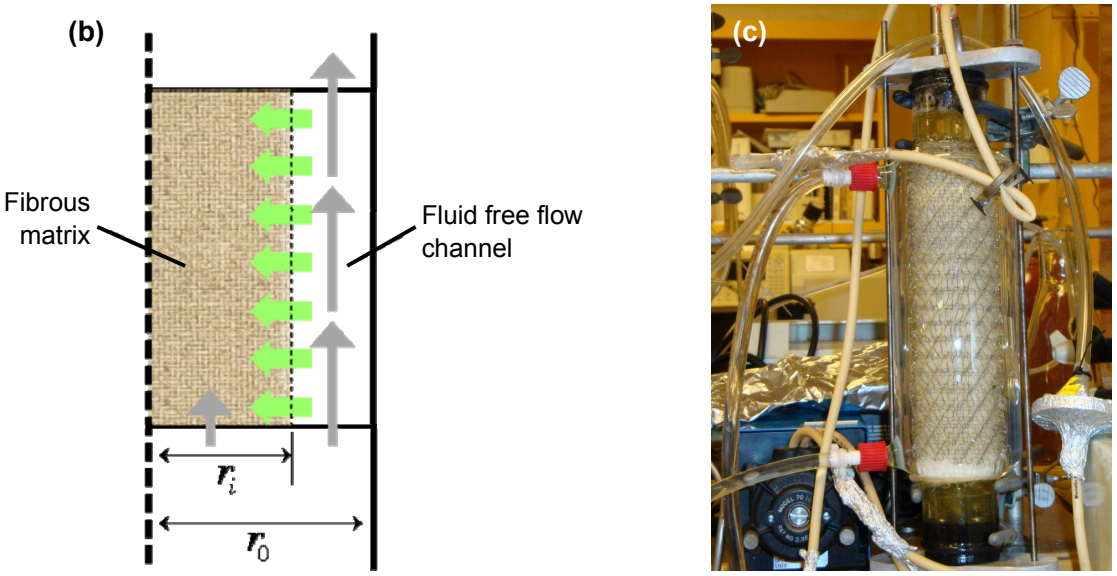

Figure 2.3. Convoluted Fibrous-Bed Bioreactor (FBB). Legend: (a) construction schematics of a spiral-wound fibrous matrix showing the tubular packing design; (b) liquid flow pattern (grey arrows) developed within the looped structure with inward direction of feed stream nutrients (green arrows); (c) photograph of a jacketed glass column packed with the spiral-wound module (inside volume, ~450 ml). The drawings (a) and (b) were adapted from Ramey and Yang, 2004 (report). More details can be found in Appendix A.

2.8.2. Butanol Recovery Techniques

High product recovery cost is another problem in the microbial production of butanol. The traditional recovery by using distillation (extraction) suffers from a high operation cost due to the low titer of butanol in the fermentation broth caused by product inhibition. In addition to low product concentration, the boiling point of butanol is higher than that of water (118°C). The usual concentration of total solvents in the fermentation broth is between 18–33 $g \cdot l^{-1}$ (using starch or glucose) of which butanol is only about 13–18 $g \cdot l^{-1}$. This makes butanol recovery by distillation very demanding energetically. Philips and Humphrey (1985) evaluated the economics of butanol recovery from fermentation broth using distillation showing that energy savings by a factor of several orders of magnitude can be attained if the final concentration of butanol is increased from 10 to 40 $g \cdot l^{-1}$ (Philips and Humphrey, 1985). At a 10 $g \cdot l^{-1}$ feed butanol concentration, the ratio of tons of oil used for fuel to tons of 100% recovered butanol is 1.5, while at a 40 $g \cdot l^{-1}$ feed butanol concentration, this ratio is 0.25. This factor suggests that an enormous amount of energy can be saved if the butanol concentration in the fermentation broth is increased threefold. In order to improve recovery performance and reduce the costs, multiple complementary techniques have been thus investigated including condensation (*in situ* gas stripping and pervaporation), liquid–liquid extraction, adsorption, and reverse osmosis (Dürre, 1998). Details on how these separation techniques operate on solvent removal have been described elsewhere (Maddox, 1989; Groot *et al*., 1992 and Dürre 1998).

From an economical perspective, reverse osmosis is most attractive. However, it has disadvantages of membrane blockage and fouling. On the other hand, liquid–liquid extraction has high capacity and selectivity, although it can be expensive to perform (Dürre, 1998). Thus, there are advantages and disadvantages of using each recovery technique, which need to be carefully analyzed.

Gas stripping is a simple and efficient way to recover butanol from the fermentation broth. The fermentation gas is bubbled through the fermentation liquid and then passed through a condenser for solvent recovery. The stripped gas is then recycled back to the fermentor and the process continues until all the sugar in the liquid medium is consumed. Gas stripping enables the use of a

concentrated sugar solution in the fermentor (Qureshi and Blaschek, 2001d) and a reduction in butanol inhibition and high sugar utilization (Maddox *et al*., 1995). Gas stripping was applied to a batch reactor to recover solvents from the fermentation broth of *C. beijerinckii* BA101 (Ezeji *et al*., 2003). A 161.7 $g \cdot l^{-1}$ sugar solution was successfully fermented and 75.9 $g \cdot l^{-1}$ total solvent produced in the integrated process. Fed-batch fermentation was also integrated with gas stripping to reduce substrate inhibition and increase cell mass (Ezeji *et al*., 2004a). In this system, 500 g glucose was consumed and 233 g solvent was produced with the productivity of 1.16 $g \cdot l^{-1} \cdot h^{-1}$ and the yield of 0.47 $g \cdot g^{-1}$. In the case of continuous fermentation integrated with gas stripping, 460 g of total solvent was produced from 1163 g glucose with a productivity of 0.91 $g \cdot l^{-1} \cdot h^{-1}$.

Liquid–liquid extraction is another efficient technique to remove solvents from the fermentation broth. This approach takes advantage of the differences in the distribution coefficients of the chemicals. Because butanol is more soluble in the extractant (organic phase) than in the fermentation broth (aqueous phase), it is selectively accumulated in the extractant. Common extractants include decanol and oleyl alcohol (Evans and Wang, 1988). Liquid–liquid extraction has critical problems, however, such as the toxicity of the extractant to the cell and emulsification. These problems can be overcome if the fermentation broth and the extractant are separated by a membrane that provides high surface area for butanol exchange between the two immiscible phases; this method is named ‘‘*perstraction*’’ (Ezeji *et al*., 2007a). *C. acetobutylicum* has been cultivated in a continuously operated membrane bioreactor connected to a four-stage mixer-settler cascade (Eckert and Schügerl, 1987). In this system, butanol was extracted with *n*-decanol (extractant) from the cell-free fermentation broth, which was re-fed into the fermentor. This system allowed the production of solvents with a high productivity of 3.08 $g \cdot l^{-1} \cdot h^{-1}$. Among the several extractants reported, oleyl alcohol, being a good extractant, is the most promising for *C. beijerinckii* BA 101 because of its relative non-toxicity (Ezeji *et al*., 2007a).

Pervaporation is a membrane-based process that allows selective the removal of volatile compounds from the fermentative broth. The membrane is placed in contact with the fermentation broth and the volatile liquids or solvents diffuse through the membrane as a vapor which is recovered by condensation. Both liquid and solid pervaporation membranes have been

used. A liquid membrane containing oleyl alcohol was used in pervaporation of dilute aqueous butanol solutions (Matsumura *et al*., 1988). The selectivity of this liquid membrane was better than that of a silicon rubber membrane. When pervaporation using an oleyl alcohol liquid membrane was employed for the pretreatment of butanol purification, the energy requirement was ten times less of that of conventional distillation. To develop a stable membrane having a high degree of selectivity, Qureshi and co-workers (1999) synthesized a siliconsilicalite-1 composite membrane which showed a 2.2-fold enhancement in selectivity. Using this membrane in an integrated batch-pervaporation process with *C. beijerinckii* BA101, a twofold increase in the total solvent concentration (from 24.2 in control batch to 51.5 $g \cdot l^{-1}$ in batch pervaporation) was achieved (Qureshi and Blaschek, 1999). The pervaporation condition did not affect the growth of *C. beijerinckii* BA101. Since the membrane permeate contains acetone, butanol, and ethanol, distillation is still required for further purification. Pervaporation was also applied to a fed-batch reactor resulting in increased solvent productivity from 0.35 $g \cdot l^{-1} \cdot h^{-1}$ (batch reactor) to 0.98 $g \cdot l^{-1} \cdot h^{-1}$ (fed-batch reactor) due to the reduction in product inhibition (Qureshi and Blaschek, 2000). Recently, the overall solvent productivity in continuous fermentation of *C. acetobutylicum* was increased up to 2.34 $g \cdot l^{-1} \cdot h^{-1}$ by integrating with a pervaporation system using an ionic liquid polydimethylsiloxane ultrafiltration membrane (Izák *et al*., 2008).

It should be highlighted that the recovery and purification processes are directly affected by the performance of fermentation, which in turn is affected by the strain characteristics. For example, when a strain is metabolically engineered to produce butanol without or much less acetone and ethanol, the purification process will be considerably simplified. When the butanol tolerance of a strain is increased by metabolic engineering, this will also facilitate the recovery process as higher butanol concentration can be achieved during the fermentation. Thus, the overall process needs to be optimized from strain development to fermentation to downstream processes. This will lead to the reduction in overall production costs. More details on this subject can be found on an excellent review by Ezeji *et al*. (2004a).

Chapter 3 – Experimental

3. MATERIALS AND METHODS

3.1. Chemicals

Dextrose (food grade) was obtained from Cargill Foods, K_2HPO_4, KH_2PO_4, $MgSO_4.7H_2O$, $MnSO_4.H_2O$, NaCl, $FeSO_4.7H_2O$, sodium butyrate reagent grade (Aldrich Chemical Co.), Butyric Acid and Phosphoric Acid.

3.2. Medium Preparation

The P2-medium was prepared according to the following formulation (components per liter of distilled water):

- 3.0 g of yeast extract (YE);
- 0.5 g of phosphates (K_2HPO_4 and KH_2PO_4);
- Vitamins: 0.001 g of *p*-Amino benzoic acid (PABA), 0.001 g of thiamine and 0.0001 g of biotin;
- Trace elements/metals: 0.2 g of $MgSO_4.7H_2O$, 0.01 g of $MnSO_4.H_2O$, 0.01 g of $FeSO_4.7H_2O$, and 0.01 g of NaCl;
- A dextrose solution was prepared separately, sterilized by autoclaving at 121°C, 15 psig for 20-min and later on mixed to obtain a final glucose concentration of ~50 $g \cdot l^{-1}$ in P2-medium.

3.3. Microorganisms and inocula Preparation

Four different bacterial strains of the *Clostridium* genus were used in the present study. *C. acetobutylicum* ATCC 824 and *C. beijerinckii* ATCC 55025, BA101 were obtained from the American Type Culture Collection (ATCC). *C. beijerinckii* NCIMB 8052 was obtained from The National Collection of Industrial, Marine and Food Bacteria (NCIMB). All bacteria were maintained in P2-medium at 4°C as stock cultures.

To prepare inocula of all 4-strains in totally anoxic conditions the following procedure was employed: serum tubes containing 5.0 ml of P2-medium were first purged with sterile nitrogen gas for 5-min. To prevent caramelization of sugar, a browning reaction, a separate 50 $g \cdot l^{-1}$ dextrose solution in distilled water was prepared in a 100 ml serum bottle and purged with

nitrogen gas for 15-min again to attain perfect anaerobic conditions. Both vessels were tightly sealed with rubber stoppers and aluminum crimps to prevent ingress of air and contamination with oxygen. Both liquids were sterilized by autoclaving at 121°C, 15 psig for 20-min after which they were left at room temperature for cooling. 1.0 ml of dextrose solution was then added to the first tube followed by cell inoculation with 1/30 volume of each original stock culture. Anaerobic stock cultures for all strains were taken from an original serum tubes stored at 4 °C. Prior to inoculation the stock culture tubes were left resting at room temperature for 30-min in order to pre-activate the cells. The pre-culture was incubated at 37°C during 16-hours for cell growth followed by another inoculation round in order to obtain final fresh cell culture inocula.

3.4. Bacterial Cultures and Medium

P2-medium was used for all four clostridia strains for experiments in serum bottles and immobilized cell bioreactor system with and without added butyric acid.

P2-medium supplemented with different concentration of butyrate ranging from 0–12 $g \cdot l^{-1}$ were added initially into the serum bottles and adjusted to pH 5.0 using a sodium butyrate/butyric acid buffer solution (pH 5.0). For the strains BA 101 and NCIMB 8052 the initial pH was adjusted to 6.4 instead of 5.0 using a corresponding sodium butyrate/butyric acid buffer solution (pH 6.4). Each serum bottle was purged with nitrogen for 15-min to attain total anaerobic conditions, subsequently sealed, autoclaved at 121°C, 15 psig for 20-min and placed at room temperature. Dextrose solution was subsequently added in order to obtain a final glucose concentration of ~50 $g \cdot l^{-1}$ followed by the inoculation with 3.0 ml of fresh culture of the corresponding strain. The final volume of cell suspension in P2-medium was 100 ml. All serum bottles with different butyrate concentrations were incubated at 37ºC for different fermentation periods (according to each bacterial strain) and suspension samples were taken periodically to measure pH, optical density, residual glucose concentration, acids and solvents produced. All incubations were performed in triplicate except for the strain NCIMB 8052 where only one fermentation run was conducted.

3.5. Fibrous-Bed Bioreactor Fermentation

The fibrous-bed bioreactor (FBB) was made of a glass column packed with spiral wound cotton towel and had a working volume of ~450 ml (see Figs. A1 and A2 in Appendix A). Detailed description of the reactor construction, start-up and operation can be found in Appendix A. The column reactor was aseptically connected to a spinner-flask fermentor (μ-Carrier BELLCO 1965-00500) containing the liquid medium through a recirculation loop (~1.5 m long, tubing i.d.: 3.1 mm; Microflex Norprene 06402-16, Cole Parmer, Chicago, IL) and operated under perfectly-mixed conditions (120 rpm) with controlled temperature at 35ºC unless stated otherwise. Anaerobiosis was reached by sparging the medium with sterile nitrogen gas. The FBB was operated at a repeated 2-cycle batch mode with cell growth coupled with immobilization in order to increase the cell density in the fibrous-bed. Initial pH values in the system were adjusted to 5.0 and 6.4 for the strains ATCC 55025 and BA 101, respectively by using a corresponding sodium butyrate/butyric acid buffer solution. After the first stage of operation, when sugar in the fermentation broth was stabilized to a minimum residual level, the spent medium in the system was completely replaced with newly fresh P2-medium supplemented with glucose (~50 $g \cdot l^{-1}$) and butyrate (4.0 $g \cdot l^{-1}$) to start a new fermentation batch (2^{nd} cycle). Samples were taken at regular time intervals throughout the fermentation course for the analysis of biomass, substrate and product(s) concentrations.

3.6. Analytical Methods

For the suspended cell culture (serum bottles) and immobilized cell system (FBB), 3.0 ml liquid samples were taken aseptically at specific time intervals. The cell density was analyzed by measuring the optical density of the cell suspension at a wavelength of 600 nm (OD_{600}) with a spectrophotometer (Model UV-1601 SHIMADZU). The pH was measured with a hand-held potentiometer (pH-meter Model EW-35614-20, Cole Parmer, Vernon Hills, IL). After measured OD and pH, cells were immediately centrifuged at 13200 rpm (16100 g), 21°C for 5-min in a centrifuge (Model 5415D, Eppendorf), the clear supernatant removed from the cell pellet, diluted at the ratio of 1/30-1/25 with phosphate buffer solution (K_2HPO_4/KH_2PO_4, 0.5 M, pH 7.0) and used for analysis of residual glucose and product concentrations. Glucose concentration was measured using the YSI 2700 Select™ Biochemistry Analyzer following the manufacturer's

instructions (Yellow Spring Instruments, Inc., OH). Acetone, butanol, ethanol, acetic acid and butyric acid concentrations were quantified by gas chromatography. The chromatographic system (Shimadzu GC-2014) was equipped with a flame ionization detector FID, SPL 2014 integrator and Stabilwax-DA column (Restek) using helium as the carrier gas at the flow rate of 2.0 ml·min^{-1}. The injector temperature and the detector temperature were set to 200°C. The column temperature was programmed as the followings: 80°C hold for 3-min, and then increased to 150 °C at 30°C·min^{-1} and hold at 150°C for 4-min.

3.7. Calculations

3.7.1. *Reaction rate estimation*

For reaction rate determinations the experimental data corresponding to butanol production (g·l^{-1}) were interpolated using several approaches. One of them was by smoothing cubic *B*-splines using the procedure *interpolate/extrapolate* built-in in the software OriginLab® v. 8.0 (Origin® 8). This method executes discrete data-fitting in a piecewise fashion using a 3rd order Bezier spline polynomial to approximate the data. In most cases, where the product distribution profile showed less oscillation behavior, a non-linear dynamic fit of sigmoid growth type (*S*-shaped curve) was used instead to reveal the most probable trend of the data (from OriginLab® v. 8.0., and/or SigmaPlot® v. 11.0 mathematical softwares). A fitting-power no less than 0.97 (Adj. R^2) was pre-required in this case. The reaction rate was evaluated by the first derivative of the adjusted curve showing the product accumulation dynamics. The specific butanol production rate, q_p (g·g^{-1}·h^{-1}) was subsequently predicted by applying the following formula (Tashiro *et al*., 2004):

$$q_p = \frac{1}{\bar{X}} \cdot \frac{\Delta P}{\Delta t} \tag{1}$$

Where $\bar{X}$ denotes the average cell concentration obtained in the interval Δt: $t_1 \le \bar{X} \le t_2$ and P represents the concentration of butanol at each time instant, t. The specific butanol formation rate is expressed in terms of mean weighted rate based on time intervals and averaged biomass

concentration obtained from each interval. The term ($\Delta P/\Delta t$) represents the observable rate of butanol formation.

3.7.2. *Biomass concentration estimation*

Biomass concentration for each bacterial strain was estimated by dry cell weight (DCW) measurements using a predetermined correlation curve obtained between the absorbance measured at 600 nm and the cell dry weight ($g \cdot l^{-1}$). One unit of OD_{600} was roughly equivalent to 0.79 $g \cdot l^{-1}$ of DCW for cells of *C. acetobutylicum* ATCC 824 grown in P2-medium while for cells of *C. beijerinckii* ATCC 55025, BA 101 and NCIMB 8052 was 0.53 $g \cdot l^{-1}$ grown in the same medium (see more details in Appendix C1). The pre-established calibration curves were as follows:

- *C. acetobutylicum* ATCC 824:

$$\mathrm{DCW}\left(\mathrm{g} \cdot \mathrm{l}^{-1}\right) = 0.7881\left(\pm 0.0614\right) \cdot \mathrm{OD}_{600} \tag{2}$$

- *C. beijerinckii* ATCC 55025, BA 101 and NCIMB 8052:

$$\mathrm{DCW}\left(\mathrm{g} \cdot \mathrm{l}^{-1}\right) = 0.5343\left(\pm 0.0429\right) \cdot \mathrm{OD}_{600} \tag{3}$$

The maximal specific growth rate, $\mu_{\max}$ (expressed in reciprocal hours, h^{-1}) was determined from the semi-logarithmic plot described by equation (4) for data taken exclusively in the exponential phase of cell growth using a minimum requirement of three experimental data points:

$$\ln OD_t = \mu_{\max} \cdot t + \ln OD_i \tag{4}$$

The turbidity parameter, OD, represents the optical density (absorbance) of the cell suspension measured at 600 nm of wavelength, and t is the sampling time (hours). In some cases, where the minimum requirement for balanced fitting was not satisfied, the following alternative equation was employed in the linear range of the plot $\ln OD$ *versus* time:

$$\mu_{\max} = \frac{\Delta \ln OD}{\Delta t} = \frac{\ln\left(OD_t / OD_i\right)}{t_f - t_i} \tag{5}$$

3.7.3. *Yields from substrate and biomass*

To estimate the overall solvent yields based on glucose plus butyric acid utilizations $\left(Y_{\text{P/S}}\right)$ and biomass produced $\left(Y_{\text{P/X}}\right)$, the two following equations were utilized (Tashiro *et al*., 2004):

$$Y_{\text{P/S}} = \frac{P}{S_c} \tag{6}$$

$$Y_{\text{P/X}} = \frac{P}{X_{\max}} \tag{7}$$

Where P is the solvent production ($g \cdot l^{-1}$), S_c is the substrate consumed (S_c = [glucose]$_c$ + 0.5 × [butyrate]$_c$), and $X_{\max}$ is the maximum biomass concentration attained during cell growth ($g \cdot l^{-1}$). The overall solvent yields based solely on glucose utilization were also calculated but revealed no demarked difference from the previous yields determined from the inclusion of butyrate consumption (see regression analysis in Appendices C3 and C4 for more details).

3.7.4. *Glucose consumption kinetics*

The maximum volumetric glucose consumption rate ($g \cdot l^{-1} \cdot h^{-1}$) was predicted considering that glucose uptake by the cells followed a first-order exponential decay kinetics (8) which is based on the differential consumption model (9) where the linear form is given by equation (10):

$$S(t) = S_0 \cdot \exp\left(-k_s \cdot t\right) \tag{8}$$

$$\frac{dS(t)}{dt} = -k_s \cdot S(t), \text{ with } S(0) = S_0 \tag{9}$$

$$\ln S(t) = -k_s \cdot t + \ln S_0 \tag{10}$$

The quantity $S(t)$ denotes the concentration of glucose over time (t), S_0 is the initial glucose concentration attained immediately before the linear range of glucose depletion was achieved (in the corresponding exponential decay), and k_s is the first-order rate constant for glucose consumption (with reciprocal units of h^{-1}). The proposed approximation was based on the assumption that the most intensive depletion profile is inversely proportional to the profile of biomass formation (exponential cell growth) coupled with the individual profiles for solvents production. The first-order decay constant $(-k_s)$ was estimated through linear calibration (regression) of the experimental points in the approximate linear range of the semi-log plot $\ln S(t)$ *versus* time (see the descriptive example given in Appendix D2). The negative slope of the straight-calibration line indicated the approximate value of k_s.The maximum observable glucose consumption rate $\left(\frac{\Delta S}{\Delta t}\right)$ was then calculated using the glucose concentrations obtained at the same time interval where the regression analysis was performed. Therefore this maximum rate should be considered as an observable or *averaged* uptake rate given that it was determined considering a finite time interval where the decaying profile had its steeper region. The specific glucose consumption rate (q_s) (in reciprocal hours, h^{-1}) was evaluated according to the following equation (Görgens *et al*., 2005):

$$q_s = \exp\left(\frac{\Delta \ln\left(S/\Delta X\right)}{\Delta t}\right) \tag{11}$$

Where $\Delta X = X - X_0$ is the net biomass concentration, and S is the glucose concentration, both quantities attained at each time interval, Δt. The specific glucose utilization rate (h^{-1}) is actually defined as the mass of glucose consumed per mass of biomass formed at each hour ($g_{glucose} \cdot g_{biomass}^{-1} \cdot h^{-1}$). A fairly accurate linear correlation between $\left(\frac{\Delta S}{\Delta t}\right)$ and k_s is represented in Appendix C3 including all the strains simultaneously. These two entities give a measure of the efficiency in glucose consumption while q_s quantifies the glucose uptake effectiveness in terms of biomass formed. Since all biomass formation profiles are dependent on the type of medium, experimental conditions and perturbations into the system; the specific glucose uptake rate is

therefore more selective and discriminative in the analysis since it incorporates via biomass the metabolic state of the bacterial culture which is directly affected by these factors. The specific glucose consumption rate was determined geometrically through the maximum negative slope of the plot $\ln\left(\frac{S}{X-X_0}\right)$ *versus* time:

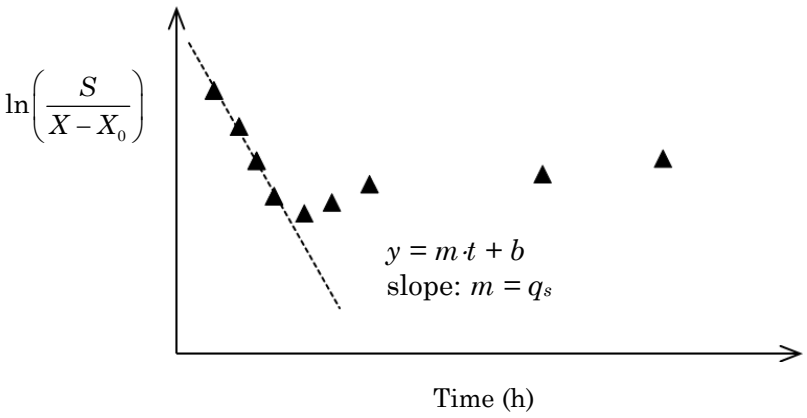

Figure 3.1. Logarithmic Method used for the calculation of the specific glucose consumption rate in the natural logarithmic domain. (▲) ln(glucose/net biomass formation). The slope of the calibration line indicates the specific consumption rate. Slope values for all strains at different butyric acid concentrations are given in Table D5 available in Appendix D.

Chapter 4 – Results and Discussion

4. RESULTS AND DISCUSSION

4.1. Batch Fermentation with Suspended Cell Culture

4.1.1. Fermentation Kinetics in Serum Bottles

Butyric acid in fermentation broth has been shown to activate solvents production by cells of *C. acetobutylicum* (Bahl *et al*., 1982; Yu and Saddler, 1983; Holt *et al*., 1984; Monot *et al*., 1984; Ammouri *et al*., 1987). Additionally, increased yields and production of solvents has been reported following the feeding of butyric and acetic acid to cultures of *C. beijerinckii* and *C. acetobutylicum* (Chen and Blaschek, 1999; Lee *et al*., 2008b).

In order to further investigate the specific effect of externally added butyrate on the fermentation kinetics by the four clostridia strains, individual batch cultures were carried out in chemically defined P2-medium (performed in serum bottles) containing glucose (~50 $g \cdot l^{-1}$) and supplemented with 2.0, 4.0, 6.0, 8.0, 10.0 and 12.0 $g \cdot l^{-1}$ of butyric acid. In graphs from Figs. 4.1–4.4 (A1–D2) are shown the individual kinetic profiles for each bacterial strain, unaffected by the addition of butyrate (control cultures). Check in Appendix B for the corresponding activity profiles over fermentation time with increasing butyric acid concentrations initially added in the medium.

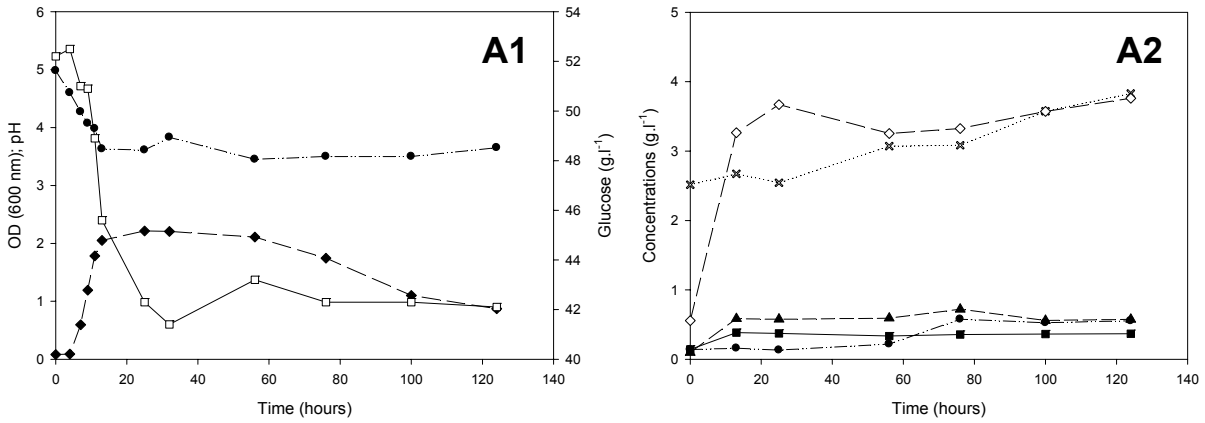

Figure 4.1. Time–course studies of various activities for *C. acetobutylicum* **ATCC 824** fermentation; Legend: A1: medium pH (●), cell density (by OD_{600nm}) (◆), and glucose (□); A2: concentrations of butanol (▲), ethanol (■), acetic acid (✕), butyric acid (◇), and acetone (✹).

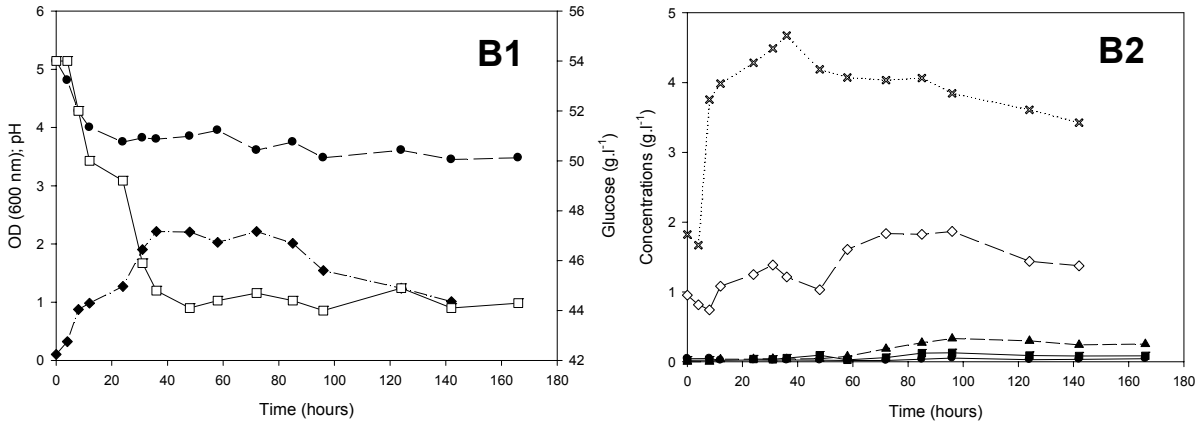

Figure 4.2. Time–course studies of various activities for *C. beijerinckii* **ATCC 55025** fermentation; Legend: B1: medium pH (●), cell density (by OD_{600nm}) (◆), and glucose (□); B2: concentrations of butanol (▲), ethanol (■), acetic acid (✕), butyric acid (◇), and acetone (✹).

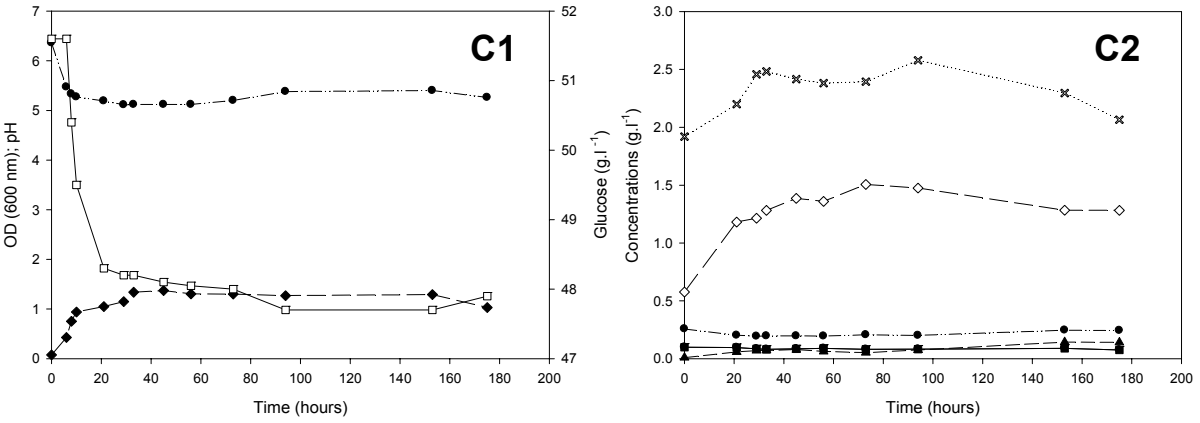

Figure 4.3. Time–course studies of various activities for *C. beijerinckii* **BA 101** fermentation; Legend: C1: medium pH (●), cell density (by OD_{600nm}) (◆), and glucose (□); C2: concentrations of butanol (▲), ethanol (■), acetic acid (✕), butyric acid (◇), and acetone (✹).

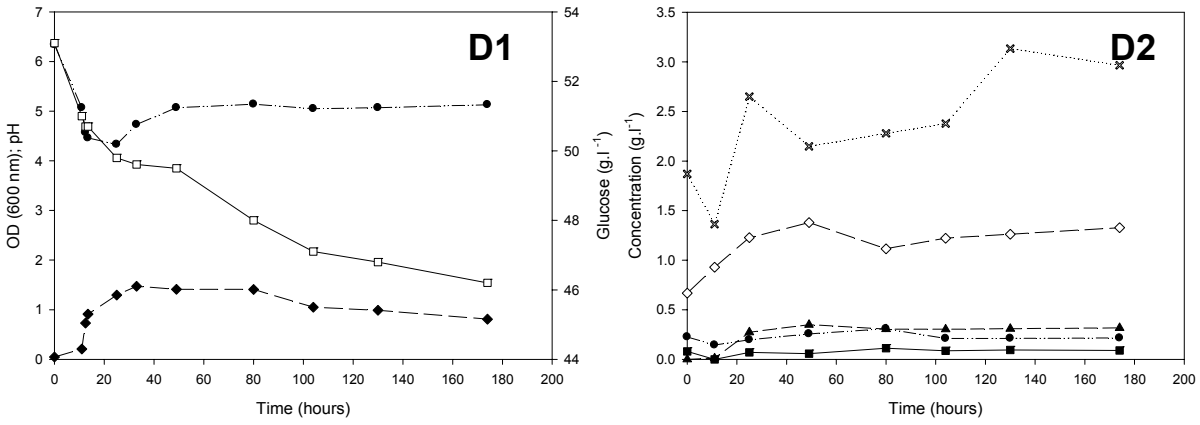

Figure 4.4. Time–course studies of various activities for *C. beijerinckii* **NCIMB 8052** fermentation; Legend: D1: medium pH (●), cell density (by OD_{600nm}) (◆), and glucose (□); D2 - concentrations of butanol (▲), ethanol (■), acetic acid (✕), butyric acid (◇), and acetone (✹).

As fully expected, all bacteria exhibited a biphasic metabolic pattern strongly influenced by the medium pH. As general trend, initially cells consume glucose to grow producing and excreting organic acids (butyrate and acetate) as primary metabolites (acidogenesis), those of which when accumulated to certain levels result in a drop of the medium pH. This increase in broth acidity shifts the formation of acids towards the production of solvents when the culture reaches the stationary phase of cell growth (solventogenesis). At high pH, organic acids are mainly formed, whereas at low pH, solvent production is stimulated. When acids are reutilized for the formation of solvents the medium pH raises again. Despite this common behavior, the nature of metabolic shift and kinetic pattern of solvent formation are markedly strain dependent given that each bacterium exhibits its own intrinsic genetic and metabolic characteristics. It is not the purpose of this study to give an extensive explanation based on these inherent physiologic properties but to assign possible causes for the effects observed, supported by available studies documented in the literature.

As result from the production of acids coupled with cell growth, *C. acetobutylicum* ATCC 824 (graph A1) revealed a pH drop value around 3.5 (ΔpH of 1.5 starting from 5.0) while in *C. beijerinckii* ATCC 55025 (graph B1), BA 101 (graph C1) and NCIMB 8052 (graph D1) the pH values were about 3.6 (ΔpH of 1.4 starting from 5.0), 5.1 (ΔpH of 1.3 starting from 6.4) and 4.3

(ΔpH of 2.1 starting from 6.4), respectively. These differences in pH regulate the temporal switch associated with solvent formation for each strain. Usually an external pH below 5.0 (optimal around pH 4.3) (Gottschalk and Morris, 1981; Gottwald and Gottschalk, 1985; Monot *et al*., 1984) and an endogenous pH greater than 5.5 are required to induce solventogenesis (Terraciano and Kashket, 1986). Yet, it can be seen that without any supplementary butyrate, the formation of alcohols and acetone is very low when compared to the formation of acids. Only residual levels of solvents were produced for all cases (less than 0.5 $g \cdot l^{-1}$). The reason for this is that acidogenesis is predominant in this case with the cells not switching to significantly to the solventogenic phase given that higher pH values than those obtained are usually required. Conversely, when feeding with butyric acid that started at 2.0 $g \cdot l^{-1}$, the pH did not drop as much as in control inducing a clear shift from acidogenesis to solventogenesis. This fact combined with butyric acid consumption by the cells as co-substrate resulted in more production of solvents including butanol as the most formed (for comparison see all kinetic profiles in the graphs of Appendix B for the four strains). The initial values observed in the graphs for both organic acids, result from pre-culture inoculation effects since the cellular inocula were metabolically in the acidogenic phase (after 16-hours of cell growth).

4.1.2. Influence of Butyric Acid on Cell Growth

Butyric acid has previously been reported to inhibit cell growth (de Mattos *et al*., 1994). To examine in more detail the effect of added butyrate, the cell growth profiles (based on optical density measurements) for the four strains were compared as described by the graphs (a–d) of (Fig. 4.5.) during the first 50-hours of fermentation.

The batch fermentation results show that irrespective of the bacterial strains used there was a gradual inhibition of cell growth, with no realistic growth observed whatsoever for butyric acid concentrations above 10 $g \cdot l^{-1}$. To better quantify this inhibitory effect, the maximal specific growth rates were determined for all bacteria from kinetic data taken in the exponential growth phase and plotted against the concentration of added butyrate (Fig. 4.6.) (Check in Appendix C2 for more details). The results demonstrate that butyric acid has effectively a prominent inhibitory effect on cell growth with all specific growth rates declining with increasing butyrate concentrations. This finding confirms previous results obtained with *Clostridium butyricum*

grown in a glucose-limited chemostat culture (de Mattos *et al*., 1994). While cells from *C. beijerinckii* BA 101 could be considered the most resistant ones to critical concentrations of butyrate (10 $g \cdot l^{-1}$), cells of *C. beijerinckii* ATCC 55025 evidenced a better "apparent" tolerance in the butyric acid region between 2–8 $g \cdot l^{-1}$.

In an attempt to evaluate the four species together regarding the overall effect of butyric acid on their growth efficiency, *Principal Component Analysis* (PCA) and *Hierarchical Clustering* (HC) were employed as parallel multivariate techniques using butyrate concentrations (mean values) as input variables (Figs 4.7. and 4.8., respectively). PCA works as a multidimensional least squares fit of natural variables where the correlation level among objects (bacteria) is found in the form of projected variables called principal components. This statistical tool attempts to reduce a large or moderate set of variables to a smaller and more meaningful set of independent ones that may represent more clearly the underlying ("hidden") properties that explain the observed phenomena. If *m* observations are taken from *n* variables, PCA may reduce the dimensionality of the initial data matrix ($m \times n$) by finding new *v* variables in a lower number than *n*. The principal components that are generated (i.e., the new *v* variables) should represent the correlation between the objects, since they result from a linear combination of the original variables. Together, they should preserve as much variance as possible of the original *n* variables, while remaining mutually independent and orthogonal. The first principal component (PC1) represents the most variance in the data. The second principal component (PC2) is perpendicular to PC1, and represents the maximum amount of variance not explained by PC1 and so forth (Esbensen, 2001). HC performs an agglomerative hierarchical grouping of the objects according to their degree of similarity (Miller J.N. and Miller, J.C., 2000). Together, these techniques help reveal the general clustering, groupings, trends and patterns among the objects described by the original variables without prior knowledge.

A comparative analysis of both plots clearly reveal one major cluster composed by the mutant strains ATCC 55025 and BA 101 of *C. beijerinckii*, both of them showing a very similar overall tolerance to increasing butyrate concentrations when comparing with the two wild type bacteria (see Appendix C5 for extra details). PC1 accounts for the largest variance (62.2%) of the initial dataset and it explains the global resistance strength towards increasing butyrate concentrations. PC2 accounts for the second largest variance (~25%) and represents the

resistance shape exhibited by the four strains. In general, *C. acetobutylicum* ATCC 824, *C. beijerinckii* ATCC 55025 and *C. beijerinckii* BA 101 behave similarly in deactivation when compared with *C. beijerinckii* NBIMB 8052 and are therefore positioned in the positive side of PC1. Also, based on the data shown in Fig. 4.6 it appears that there was no statistically significant difference among the mutant strains and non-mutated *C. acetobutylicum* ATCC 824. However, in terms of resistance pattern *C. acetobutylicum* ATCC 824 reveals to behave inversely from the mutated bacteria especially upon addition of low butyrate levels up to ~6.0 $g \cdot l^{-1}$. *C. beijerinckii* NCIMB 8052 was shown globally to be the less resistant bacteria towards butyric acid addition with low specific growth rates, also decreasing as a function of butyrate concentrations, and is thus located in the negative side of PC1, far apart from the other strains.

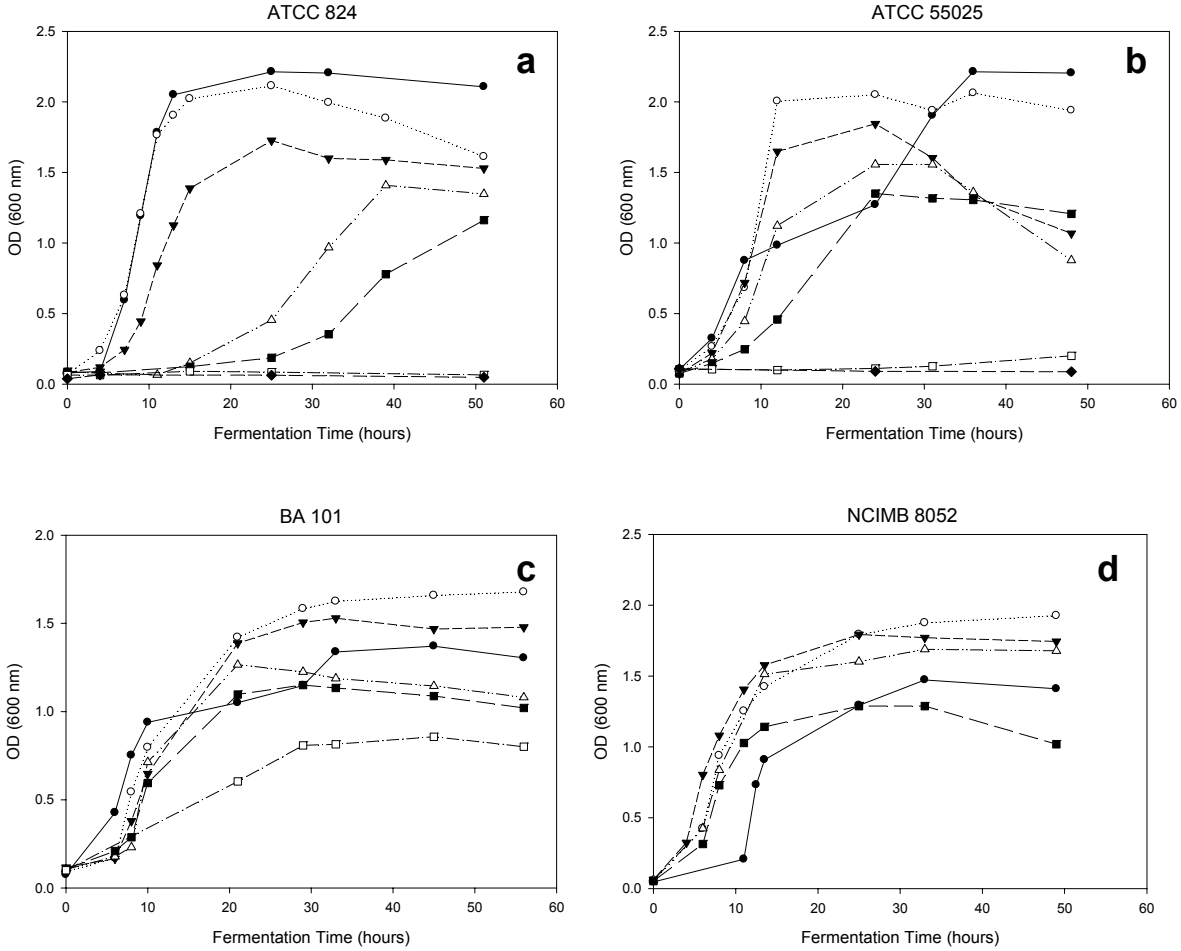

Figure 4.5. The effect of butyric acid concentration (BA) on the bacterial growth profiles obtained in the first 50-hours of fermentation. Legend: (●) control (BA 0 $g \cdot l^{-1}$); (○) BA 2.0 $g \cdot l^{-1}$; (▼) BA 4.0 $g \cdot l^{-1}$; (△) BA 6.0 $g \cdot l^{-1}$; (■) BA 8.0 $g \cdot l^{-1}$; (□) BA 10.0 $g \cdot l^{-1}$; and (◆) BA 12.0 $g \cdot l^{-1}$.

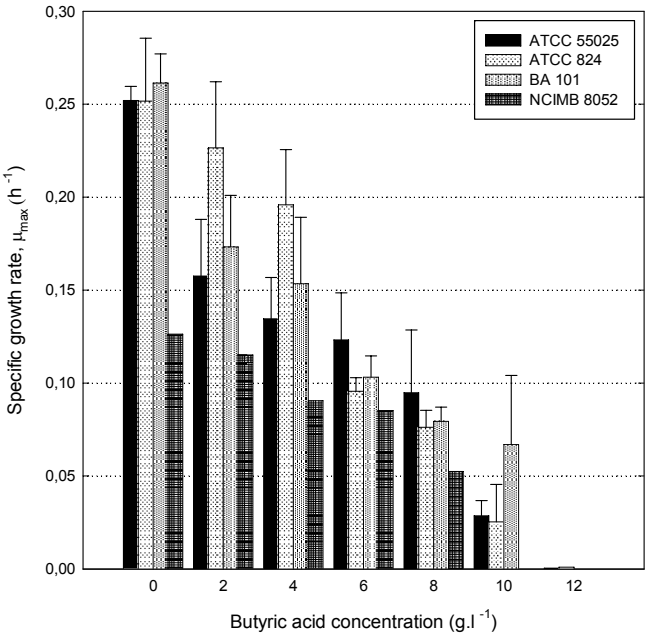

Figure 4.6. The effect of butyric acid addition on the maximal specific growth rate for the four clostridia strains. Each specific growth rate was estimated from the slope of the corresponding semi-logarithmic plot of optical density (OD) *versus* time (see example in Appendix C2). Errors in bars are expressed in terms of Standard Deviation (SD) from calculations of three independent fermentation replicates for the clostridia strains ATCC 55025, ATCC 824 and BA 101. The effect of butyric acid was not evaluated in NCIMB 8052 for concentrations above 8.0 $g \cdot l^{-1}$. Additionally, one single fermentation experiment was conducted for this strain.

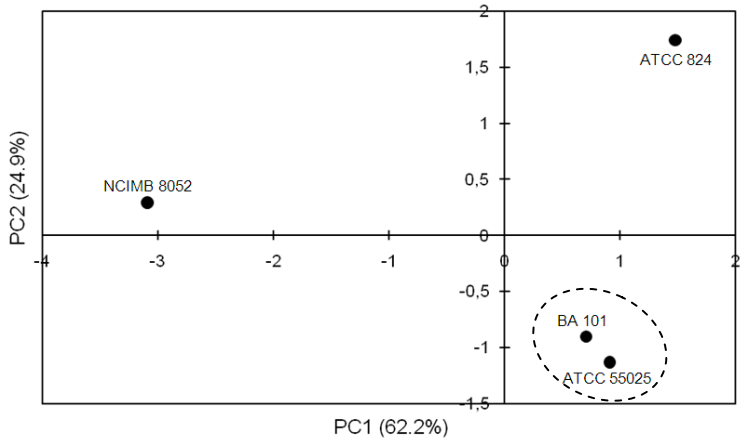

Figure 4.7. Principal Component Analysis (PCA) score plot. Data are represented and plotted orthogonally (projection) according to the first (PC1) and second (PC2) principal components. Percentages denote the statistical variance associated with each principal component. PC1 and PC2 cover a total accumulated variance of 87.1%. PC3 (not shown here) covered the remaining "residual" variance (12.9%). This scatter plot reveals the closeness (correlation wise) between the four bacterial strains based on their specific growth rates expressed as a function of increasing butyrate concentrations. The dotted line encloses the cluster. PCA output data was generated using the Single Value Decomposition (SVD) algorithm built-in the software SCAN from Minitab® (1995).

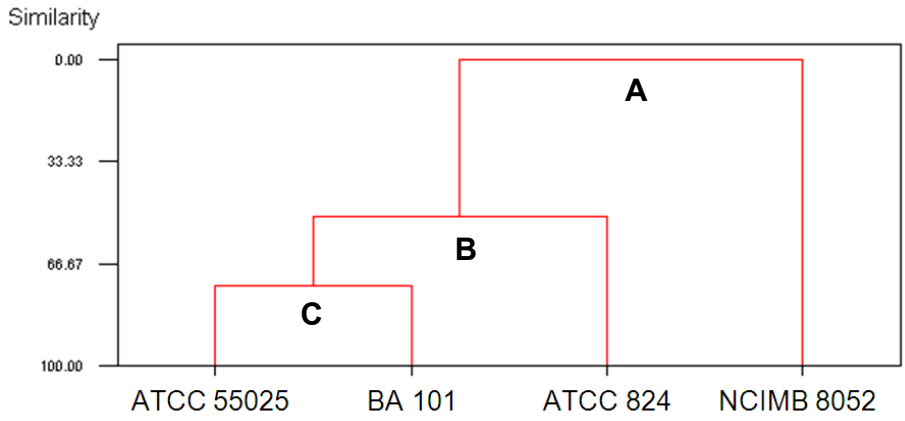

Figure 4.8. Hierarchical Clustering Analysis (HCA) illustrating the stages of clustering for Fig. 4.7. Data are represented in a binary tree plot (dendrogram) revealing the similarity level among all bacteria based on their individual specific growth rates as a function of butyric acid concentrations. Clusters (similarity percentage): A: 0.0%; B: 51.27%; and C: 73.75% respectively (based on Euclidean distance–complete linkage). Output data from HCA was generated using the SCAN package (SCAN for Windows release v. 1.1.) from Minitab® (1995).

4.1.3. Effect of Butyric Acid Addition on Solvent Production

Production of solvents, especially butanol, is manifestly influenced by butyric acid. Besides shifting the metabolic stage of the culture due to a decrease in medium pH, butyric acid is also utilized by the cells as co-substrate in the formation of butanol (Tashiro *et al*., 2004). As such, the regulation of butyrate amounts in the culture media is of great industrial importance. Fig. 4.9 shows the effect of increasing butyric acid concentrations on the batch efficiency parameters (yield from substrate and productivity) for the four clostridia. In all cases it was found that 4.0 $g \cdot l^{-1}$ is the most favorable concentration of butyric acid that maximizes the yield for all ABE-solvents and butanol productivities. Table 4.1 compares the values of the main fermentation parameters based on kinetic data from Appendix B for all bacteria. Clearly, *C. acetobutylicum* ATCC 824 produces more butanol without supplemented butyrate (0.72 ± 0.076 $g \cdot l^{-1}$) than the other strains. By adding butyric acid into the medium the production of butanol was significantly improved attaining globally a maximal concentration of 10.29 ± 0.34 $g \cdot l^{-1}$ in the fermentation broth for this bacterium. This resulted in a 4-fold increase in butanol yield from substrate (0.29 $g \cdot g^{-1}$) coupled with 4.7-times more productivity (~0.1 $g \cdot l^{-1} \cdot h^{-1}$). The production of total ABE-solvents were also considerably enhanced, attaining an optimal yield of ~0.45 $g \cdot g^{-1}$ with almost 3-fold increase when compared to the control culture (~0.16 $g \cdot g^{-1}$). However, if the analysis is

based solely on the increase of butanol yield and corresponding productivity at 4.0 $g \cdot l^{-1}$, then the results show that *C. beijerinckii* ATCC 55025, *C. beijerinckii* BA 101 and *C. beijerinckii* NCIMB 8052 have better efficiency (in ascending order) when compared to *C. acetobutylicum* ATCC 824.

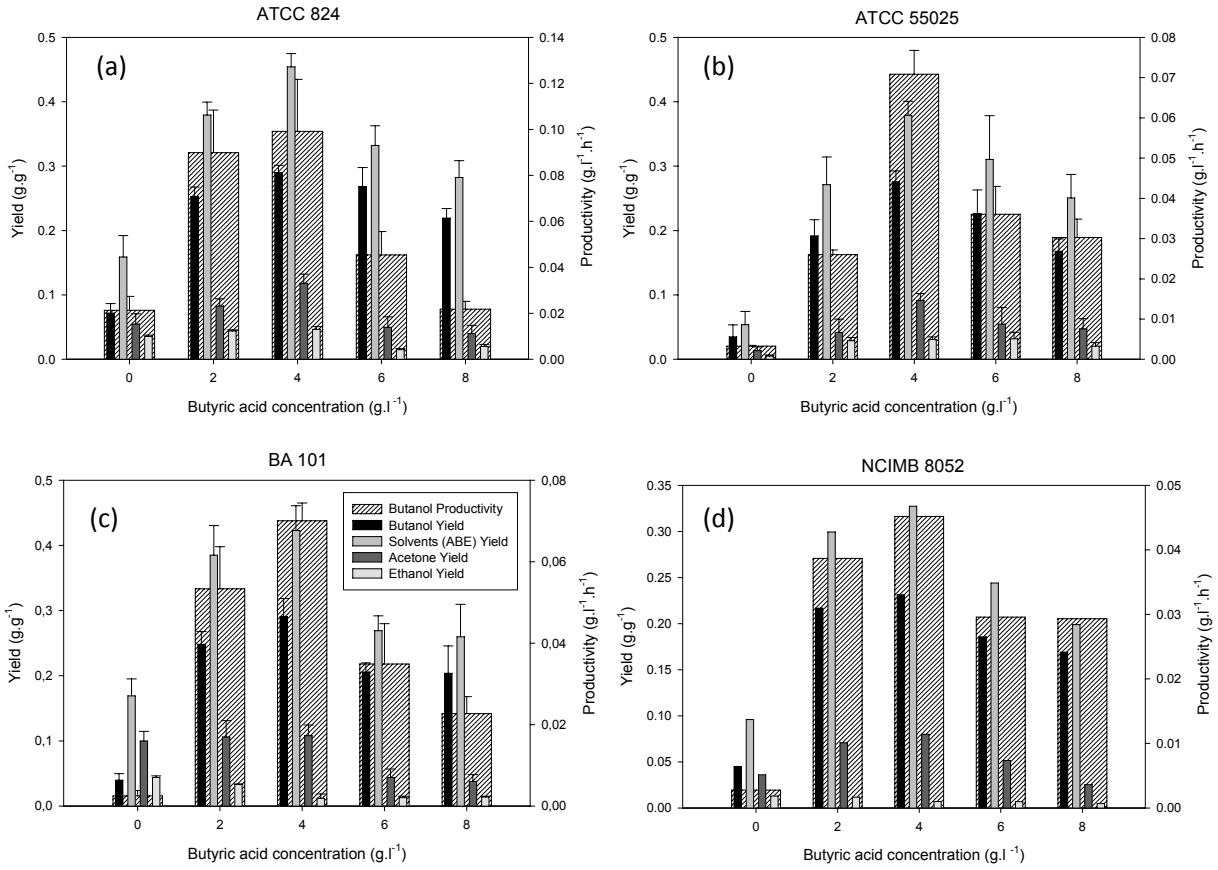

Figure 4.9. The effect of increasing butyric acid concentrations on ABE–fermentation yields from substrate (small front columns) and butanol productivity (large backside columns). Error bars represent Std. Deviation (SD) obtained from three independent fermentations for each strain: (a) *C. acetobutylicum* ATCC 824, (b) *C. beijerinckii* ATCC 55025, and (c) *C. beijerinckii* BA 101. Individual yields were calculated based on glucose consumed as limiting substrate plus half of butyric acid utilized as co-substrate (see subsection 3.7.3. from Materials and Methods). The effect of butyric acid was not tested for the strain *C. beijerinckii* NCIMB 8052 for concentrations above 8.0 $g \cdot l^{-1}$; and only one fermentation run was performed for this case (d). Legend for all graphs is given on the inset of (c).

In order to find the best trade-off between both fermentation parameters and better visualize the effect of butyric acid on each culture performance, butanol yield from substrate and productivity

were combined and plotted together as a function of butyrate concentration (Fig. 4.10). The 3D-graph immediately reveals that *C. acetobutyricum* ATCC 824 is in fact the most butanol productive strain in the range of butyrate concentrations studied, followed by the mutants *C. beijerinckii* ATCC 55025 and *C. beijerinckii* BA 101 at the optimal (4.0 $g \cdot l^{-1}$) butyric acid concentration. It is very likely that the effect of relatively moderate cell growth inhibition at optimal butyrate concentration plus the dominant solventogenic phase are two possible factors that may have contributed synergistically to this outcome in efficiency when compared with the rest of the strains. At 2.0 $g \cdot l^{-1}$ of butyrate added *C. actobutylicum* ATCC 824 and *C. beijerinckii* BA 101 showed approximately the same level of butanol yield from substrate (~0.25 $g \cdot g^{-1}$) but revealed different productivities as well increases in yield and productivity (see Table 4.1).

The yield from biomass also provides a quantitative assessment of the fermentation performance and/or efficiency since it is directly related with the amount biomass produced. Biomass formation in the fermentation broth is strongly affected by the type of culture medium utilized, pH variations, main carbon source (limiting substrate) used for energy generation, co-substrate(s), substrate and product levels (inhibition), temperature, etc (Doran, 1995). Therefore, these disturbances into the system are immediately reflected in terms of yield from biomass. Graphs (a) and (b) from Fig. 4.11 show the direct influence of butyric acid concentration in butanol yield and total ABE-solvents yields from maximal biomass, respectively. When high cellular concentrations in the media are attained coupled with very low butanol (or solvents) formation the resulting yields from biomass are tremendously low. This is particularly evident for the strains ATCC 824 and ATCC 55025 in the case where no butyric acid was initially added in the medium. Both strains revealed the highest maximal biomass concentration also with the greatest specific growth rates. The fact that these bacteria were metabolically inactive for solvent production due to low butyric acid levels and suboptimal pHs necessary for solvent(s) production, reflected into high cell growth rates with resultant high biomass levels in the system. Conversely, when butyric acid was slightly added in the media before the optimal point was reached, solvents production was stimulated at the cost of lower specific cell growth rates but with moderate biomass levels. The outcome was a significant increase in the solvent(s) yields from biomass for all bacteria. Again, *C. acetobutylicum* ATCC 824 revealed to be the most butanol productive bacteria attaining a maximal butanol yield of ~7.6 $g \cdot g^{-1}$ at the optimal

butyrate concentration (4.0 $g \cdot l^{-1}$), corresponding to 22.4-times greater in magnitude than the corresponding control. Above the optimal level of butyric acid concentration, the yield values decrease as a direct consequence of gradual cell growth inhibition by the co-substrate with concomitant low biomass concentration coupled by low levels of butanol produced. The only exception seems to be for the strain NCIMB 8052 which revealed no demarked difference from the yields values at the optimal butyrate concentration (see the graphs from Fig. 4.11 and Table 4.2 for values). In all cases one can see that butyrate addition favors ABE-solvents production over the control cultures. Above the optimal butyrate concentration cell growth is strongly inhibited lessening butanol yields and productivities for all strains.

The kinetic profiles for the limiting substrate (this case glucose) can also provide relevant information about the fermentation efficiency since they are straightly connected with cell growth (with concomitant production of organic acids) and maintenance activities within the cell (Doran, 1995). Several studies have reported that increasing the concentration of butyric acid in the culture also favors the consumption rate of glucose (de Mattos *et al*., 1994 and Lee *et al*., 2008b). The graphs (a) and (b) from Fig. 4.12 reflect the effect of butyric acid addition on the first-order rate constant for glucose consumption and specific glucose uptake rate (based on biomass) for the four bacterial strains, respectively (consult Table D5 in Appendix D for the corresponding values). In graph (a) the results show that while glucose was only slightly consumed in cultures where butyrate was absent, the concentration of glucose decreased abruptly when butyrate was added. This was clearly evident for the non-mutant *C. acetobutylicum* ATCC 824, which revealed a higher glucose consumption rate (~0.72 $g \cdot l^{-1} \cdot h^{-1}$) when 2.0 $g \cdot l^{-1}$ of butyric acid was initially added into the medium (confront with Fig. D1 of Appendix D given as auxiliary information). This value represents a 1.82-fold increase in glucose uptake competence using the corresponding control as reference. Additionally, this bacterium also showed the highest glucose uptake rate constant among all strains (~0.02 h^{-1}) at the same butyric acid concentration and revealed the highest amount of glucose consumed (38.2 $g \cdot l^{-1}$) in overall (65.5%). The other bacteria also exhibited a similar behavior in glucose uptake upon butyrate addition; yet, the consumption pattern was somewhat different for *C. beijerinckii* NCIMB 8052 which revealed its highest consumption rate (0.73 $g \cdot l^{-1} \cdot h^{-1}$) at 6.0 $g \cdot l^{-1}$ of butyric acid (see Table D5 in Appendix D); albeit in terms of rate constant the optimal value was attained at 4.0 $g \cdot l^{-1}$ of

butyric acid (Fig. 4.12a). These values corresponded to an increase of ~5.2-times in uptake efficiency in terms of glucose consumption rate considering the 6.0 $g \cdot l^{-1}$ of butyrate added over the control, even though in terms of rate constant the increase in glucose efficiency was ~5.7-times higher at 4.0 $g \cdot l^{-1}$ of butyric acid. Similar findings in butanol production and glucose consumption upon addition of butyric acid were also observed by Lee and co-workers (2008). Their work showed by using a suspended cell culture of *C. beijerinckii* NCIMB 8052 grown in serum bottles with modified CAB-medium, that butanol production increased almost 96% relative to control when 36 mM (~3.2 $g \cdot l^{-1}$) of butyrate was initially added into the medium. This corresponded to an impressive 25-fold increase in final butanol concentration. According to these authors the increase in both butanol production and glucose consumption rates could be derived from the fact that butyric acid has enhanced the buffering capacity of the fermentation broth, which in turn reflected in growth of the culture by preventing extremely acidic conditions from taking place (Lee *et al*., 2008b). In addition, the butyric acid could also have promoted and earlier shift to the solventogenic phase which might have reflected into a slow growth rate, supporting the results previously discussed in section 4.1.2.

In order to correlate the glucose consumed with the produced biomass, the specific glucose uptake rate was calculated in the range of 0.0–8.0 $g \cdot l^{-1}$ of butyric acid (Fig. 4.12b). This piece of information is especially useful since the specific glucose uptake rate is directly linked with cell growth and perturbations into the system are usually reflected in terms of biomass profiles those of which are particularly sensitive at the exponential growth phase (Görgens *et al*., 2005) and maximal biomass attained during growth. According to the Logarithmic Method described by the author, during fully exponential growth the linear section of the plot ln (glucose/net biomass formed) versus time (Fig. 3.1 from Materials and Methods) defines the “logarithmic” or “linear” substrate consumption rate which remains constant for the duration period associated with the ideal exponential cell growth. The graph reveals that upon increasing butyrate concentrations in the medium the specific glucose consumption rate increases up to the optimal level of butyrate concentration (4.0 $g \cdot l^{-1}$) decreasing afterwards. This behavior is particularly evident for the mutant strains ATCC 55025 and BA 101 while the other two remaining bacteria also behave the same way yet only from 2.0 $g \cdot l^{-1}$ of butyrate onwards. This general trend is probably owed to the fact that the inclusion of butyric acid in the medium aids to stimulate the consumption of glucose

associated with cell growth even though the specific growth rates for all bacteria decrease with increasing butyrate concentrations. Instead, glucose may being utilized for other cell purposes not directly involving growth such as maintenance effects and the synthesis of enzymes required for solventogenic functions. Above the optimal point all values decrease most probably due to inhibitory effects caused by the acids and the accumulation of ABE-solvents. The high values observed for the strains ATCC 824 and NCIMB 8052 at zero concentration of butyrate are due to high glucose utilization for growth functions mostly coupled with acids formation. These two strains showed independently their highest specific growth rates over the range of butyrate concentration studied. As butyric acid is gradually increased the specific cell growth rates drop and glucose is probably channelized to energize other cellular functions than growth.

Table 4.1. Effect of different concentrations of butyric acid added on the batch fermentation parameters for butanol (BuOH) and total ABE-solvents produced by the four clostridia strains.

Butyric Acid Concentration (g/l)	BuOH Production (g/l)	BuOH Yield (g/g)	BuOH Relative Yield	BuOH Productivity (g/l/h)	BuOH Relative Productivity	ABE-solvents Yield (g/g)	ABE-solvents Relative Yield
ATCC 824							
0.0	0.72 ± 0.076	0.072 ± 0.014	1.000	0.021 ± 0.006	1.000	0.159 ± 0.033	1.000
2.0	9.96 ± 0.386	0.253 ± 0.014	3.511	0.090 ± 0.018	4.221	0.379 ± 0.020	2.386
4.0	10.29 ± 0.338	0.290 ± 0.011	4.025	0.099 ± 0.023	4.653	0.454 ± 0.020	2.857
6.0	3.87 ± 0.114	0.268 ± 0.030	3.726	0.045 ± 0.010	2.131	0.332 ± 0.031	2.089
8.0	2.71 ± 0.036	0.219 ± 0.015	3.044	0.022 ± 0.003	1.023	0.282 ± 0.026	1.776
ATCC 55025							
0.0	0.332 ± 0.024	0.035 ± 0.0184	1.000	0.003 ± 0.000	1.000	0.054 ± 0.021	1.000
2.0	2.115 ± 0.086	0.192 ± 0.0252	5.477	0.026 ± 0.001	7.934	0.271 ± 0.043	5.050
4.0	5.529 ± 0.009	0.275 ± 0.0173	7.866	0.070 ± 0.006	21.610	0.379 ± 0.022	7.056
6.0	2.700 ± 0.014	0.226 ± 0.0366	6.469	0.036 ± 0.007	10.990	0.333 ± 0.068	6.197
8.0	1.788 ± 0.030	0.168 ± 0.0190	4.800	0.030 ± 0.005	9.246	0.251 ± 0.037	4.665
BA 101							
0.0	0.143 ± 0.003	0.040 ± 0.010	1.000	0.003 ± 0.001	1.000	0.169 ± 0.026	1.000
2.0	4.290 ± 0.065	0.248 ± 0.019	6.252	0.053 ± 0.010	21.320	0.385 ± 0.045	2.275
4.0	3.978 ± 0.172	0.291 ± 0.027	7.320	0.070 ± 0.004	28.040	0.423 ± 0.038	2.499
6.0	1.866 ± 0.029	0.206 ± 0.014	5.181	0.035 ± 0.010	13.960	0.269 ± 0.022	1.590
8.0	1.690 ± 0.077	0.204 ± 0.042	5.128	0.023 ± 0.004	9.080	0.260 ± 0.050	1.534
NCIMB 8052							
0.0	0.35	0.045	1.000	0.0028	1.000	0.096	1.000
2.0	4.61	0.211	4.698	0.0387	14.026	0.299	3.119
4.0	4.78	0.231	5.142	0.0452	16.382	0.327	3.410
6.0	4.08	0.186	4.127	0.0296	10.728	0.244	2.543
8.0	3.56	0.169	3.758	0.0293	10.619	0.199	2.072

Note: Values followed by ± are standard deviation of mean (errors) by using three independent experiments. Butanol yields are expressed in terms of consumed substrate $\left(Y_{P/S}\right)$.

Table 4.2. The effect of different concentrations of butyric acid on the butanol (BuOH) and ABE-solvents yields from biomass $\left(Y_{P/X}\right)$ for the four clostridia strains.

Butyric Acid Concentration (g/l)	Maximal Biomass, DCW (g/L)	BuOH Yield (g/g)	BuOH Relative Yield	ABE-solvents Yield (g/g)	ABE-solvents Relative Yield
ATCC 824					
0.0	1.745 ± 0.096	0.413 ± 0.023	1.000	0.952 ± 0.053	1.000
2.0	1.666 ± 0.092	5.978 ± 0.330	14.475	9.132 ± 0.505	9.597
4.0	1.360 ± 0.075	7.566 ± 1.056	22.438	11.904 ± 0.658	12.510
6.0	1.110 ± 0.061	3.485 ± 0.193	8.438	4.328 ± 0.239	4.549
8.0	0.916 ± 0.050	2.959 ± 0.164	7.165	3.758 ± 0.208	3.950
ATCC 55025					
0.0	1.238 ± 0.068	0.268 ± 0.015	1.000	0.413 ± 0.023	1.000
2.0	1.154 ± 0.063	1.833 ± 0.101	6.840	2.648 ± 0.146	6.411
4.0	1.032 ± 0.057	5.359 ± 0.295	19.996	7.471 ± 0.4116	18.090
6.0	0.871 ± 0.048	3.101 ± 0.171	11.571	4.561 ± 0.251	11.044
8.0	0.755 ± 0.041	2.366 ± 0.130	8.828	3.383 ± 0.186	8.192
BA 101					
0.0	0.715 ± 0.019	0.200 ± 0.005	1.000	0.669 ± 0.018	1.000
2.0	0.875 ± 0.023	4.905 ± 0.130	24.525	7.037 ± 0.187	10.509
4.0	0.797 ± 0.021	4.992 ± 0.132	24.960	7.013 ± 0.186	10.473
6.0	0.660 ± 0.017	2.828 ± 0.075	14.140	3.681 ± 0.098	5.498
8.0	0.600 ± 0.016	2.817 ± 0.075	14.085	3.593 ± 0.095	5.365
NCIMB 8052					
0.0	0.770 ± 0.074	0.453 ± 0.044	1.000	0.922 ± 0.090	1.000
2.0	1.007 ± 0.097	4.576 ± 0.446	10.109	6.739 ± 0.657	7.312
4.0	0.937 ± 0.090	5.104 ± 0.498	11.274	6.993 ± 0.682	7.587
6.0	0.883 ± 0.085	4.621 ± 0.451	10.206	6.597 ± 0.643	7.157
8.0	0.673 ± 0.065	5.283 ± 0.515	11.668	6.307 ± 0.615	6.843

Note: Errors for all strains represent the standard deviation (SD) associated with the two independent calibration curves correlating optical density and biomass concentration (DCW) obtained for each bacterial strain.

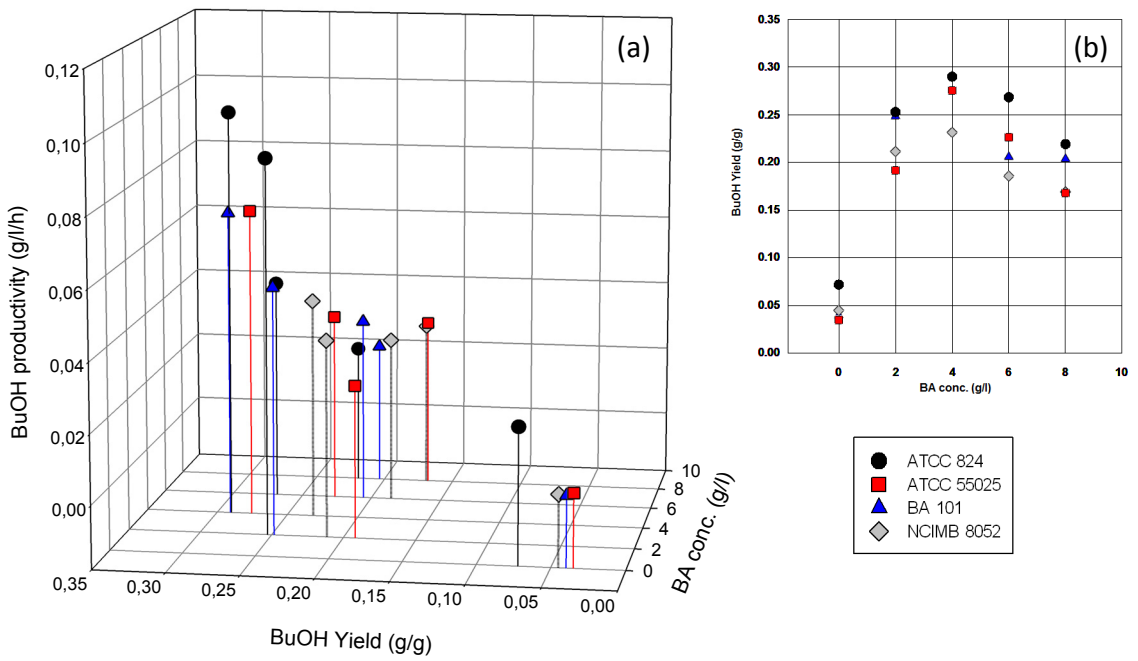

Figure 4.10. Butanol yield from substrate and productivity plotted as a function of butyrate concentration. (a) 3D-graph. Drop lines from each point designate the productivity level at each butyric acid concentration. (b) 2D-graph (top view) representing the distribution of points in the *xy*-plane. Legend: butyric acid (BA) concentration (*x*-axis); butanol yield from substrate (*y*-axis); and butanol productivity (*z*-axis). Butanol yields were calculated according to equation (6) as described in Materials and Methods.

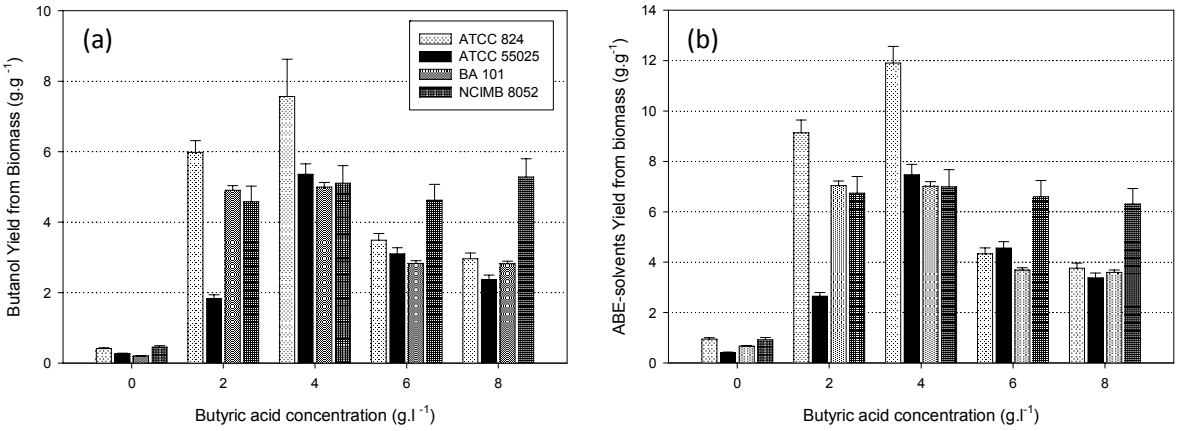

Figure 4.11. Butanol and total ABE-solvents yield from biomass plotted as a function of butyrate concentration for the four strains. (a) Butanol yield from biomass ($g_{butanol} \cdot g_{biomass}^{-1}$); (b) ABE-solvents yield from biomass ($g_{ABE} \cdot g_{biomass}^{-1}$). Corresponding values can be found in Table 4.2. Butanol and ABE-solvent yields were calculated according to equation (7) as described in Materials and Methods. Legend for both graphs is given on the inset of (a).

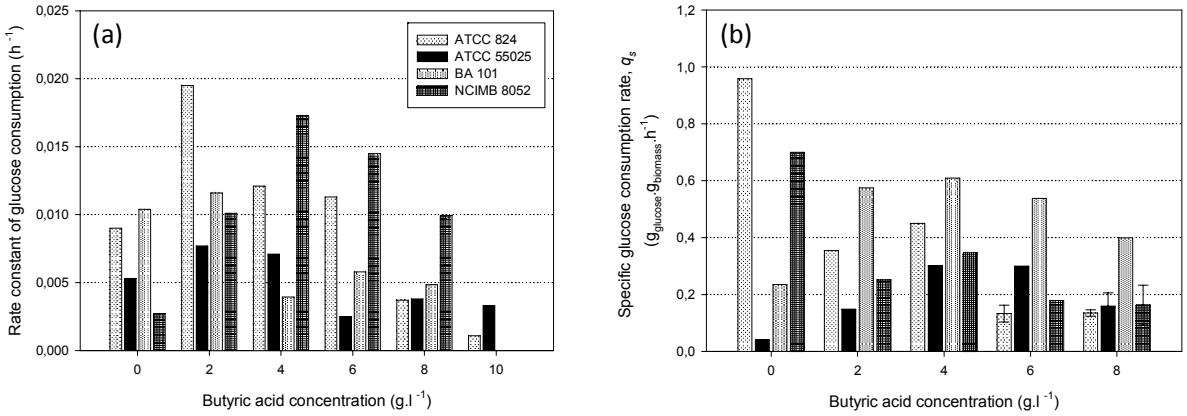

Figure 4.12. Kinetic parameters for glucose consumption expressed as a function of butyric acid concentration in the fermentation broth. Legend: (a) first-order rate constant for glucose utilization, k_s; (b) specific glucose consumption rate, q_s. Rate constants were estimated from the corresponding concentration decaying profiles presented in Appendix B for all bacteria. For comparison, the observable glucose consumption rate ($\Delta S/\Delta t$) as a function of butyrate concentrations is given in Fig. D1 from Appendix D. The specific glucose consumption rate (q_s) was calculated from the Logarithmic Method (check example in Appendix D5 and see Materials and Methods for details). Corresponding values are given in Table D5 from Appendix D for both graphs. Error bars in graph (b) represent slope oscillations (average) of several independent regression lines adjusted in the approximate linear range of the plot ln(glucose/net biomass formation) *versus* time. Legend for both graphs is given on the inset of (a).

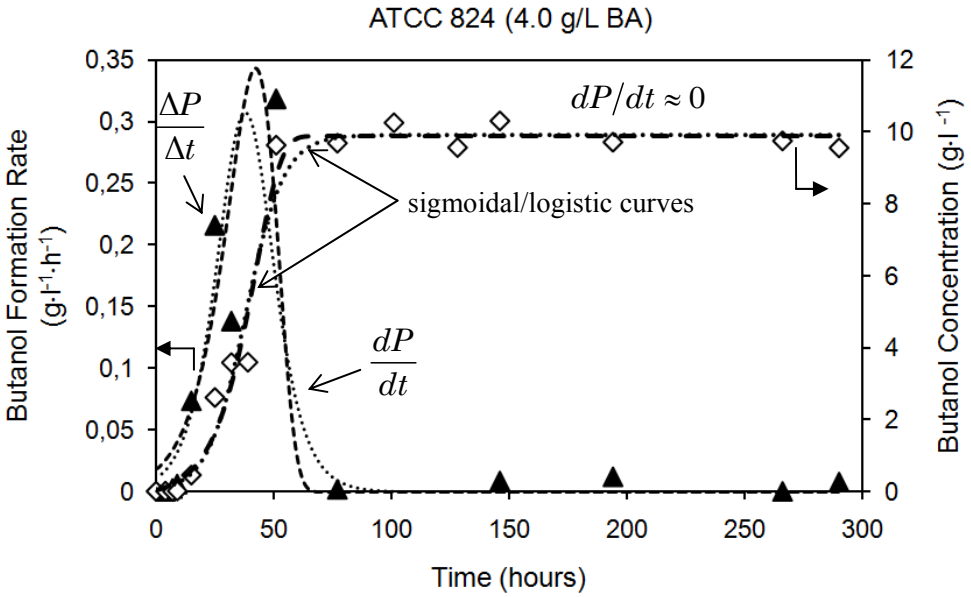

Figure 4.13. Rate of butanol production by *C. acetobutylicum* ATCC 824 during batch culture with an initial 4.0 g·l^{-1} butyrate concentration (illustrative example). Full triangles (▲) symbolize the average butanol formation rate ($\Delta P/\Delta t$) based on the experimental data of butanol concentration over time (◇). Thicker interpolating lines represent the two fitting curves to the discrete data whereas thinner ones reveal the instantaneous rate of butanol formation computed from the first derivative of each adjusted concentration curve (see subsection 3.7.1. of Materials and Methods).

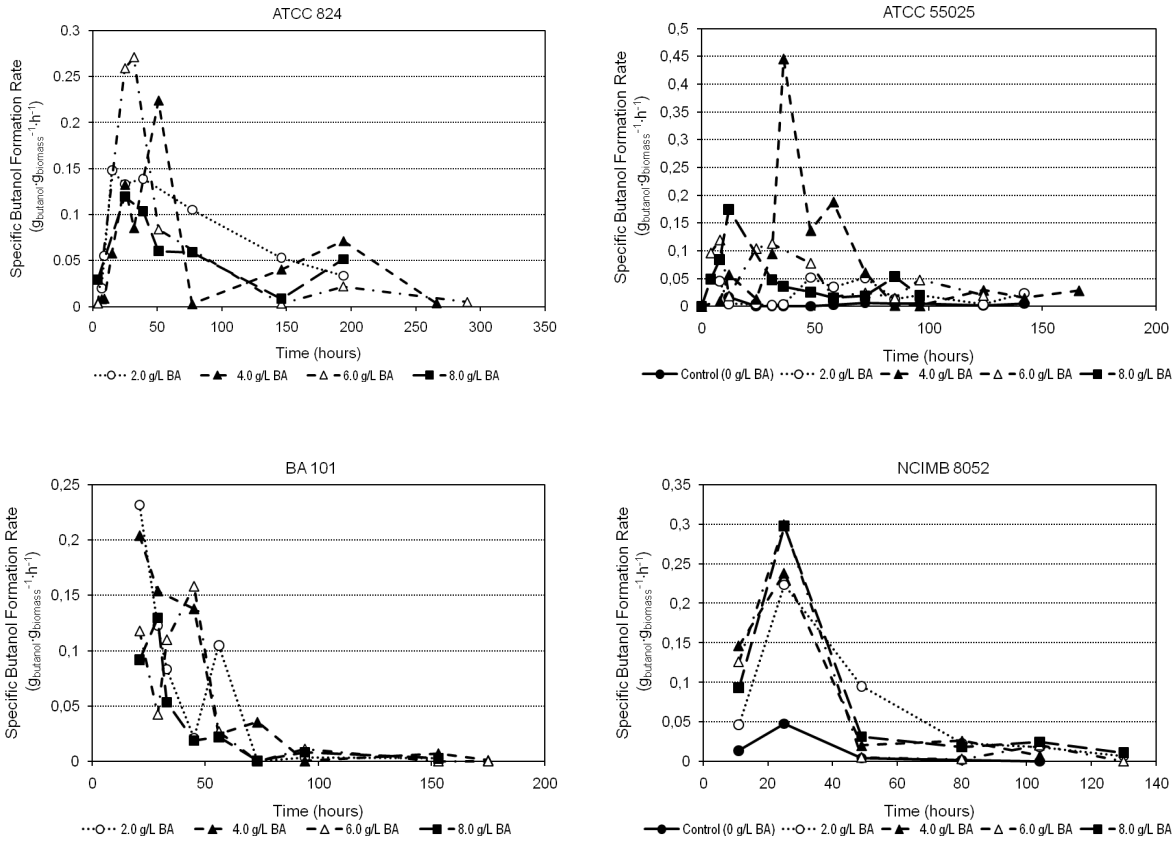

Figure 4.14. Influence of butyric acid on the kinetic profiles for specific rates of butanol formation for the four clostridia strains. The specific butanol production rate was calculated from equation 1 (see subsection 3.7.1. from Materials and Methods). For the strains ATCC 824 and BA 101 the corresponding control profiles are not shown due to difficulties in the calculation of the specific butanol production rate.

To better evaluate the precise effect of externally added butyric acid in the production of butanol, the specific butanol formation rates at each butyrate concentration were estimated and plotted as a function of fermentation time (Fig. 4.14). The individual evolution profiles for all bacteria explain the exact effect of butyrate on the cellular behavior since variations of concentration levels in the medium affect directly the cell metabolism. Additionally, the kinetic profiles can also point out the time frame where the increase in butanol is more pronounced.

It can be seen for all strains that the addition of butyric acid effectively increases the specific butanol formation rate indicating a clear switch from acidogenesis towards the solvent phase. This is particular evident for the strain NCIMB 8052 which shows a considerable increase after ~20-28 hours of fermentation when comparing to the control. In this case it is also apparent

that the formation of butanol seems to occur somewhat earlier than the remaining strains. It appears that the optimal butyrate concentration falls in the range of 4.0-6.0 $g \cdot l^{-1}$ of butyric acid for the strain ATCC 824 but for the strain ATCC 55025 the optimal value is clearly attained at 4.0 $g \cdot l^{-1}$ of butyrate showing the highest rate attainable among all bacteria (0.45 $g \cdot g^{-1} \cdot h^{-1}$). In Fig. 4.13 is illustrated a comparison between the observable and instantaneous butanol formation rates based on the butanol concentration profiles. All butanol concentration profiles were initially interpolated to obtain the approximate trend of data and then the lines converted to the corresponding rate profiles using a first-derivative transformation. As can be seen for this example the direct acceleration in butanol formation is evident up to the 50-hours of fermentation decreasing afterwards. Also, the graph shows no significant difference between both rate types, even though in some cases it was observed a short temporal displacement due to unavoidable calculation inaccuracies (results not shown); however, the same S-shaped pattern in butanol formation (logistic/sigmoidal profiles) and resulting rates were maintained for all situations evaluated. For the strain BA 101 the initial values for the specific butanol formation rate were underestimated given the low number of experimental points available to perform the calculations; therefore, it is not possible to evaluate when exactly the maximum rate occurred. However, globally, it is suggestive that butyric acid seems to favor the production of butanol in particular when 4.0–6.0 $g \cdot l^{-1}$ of butyrate is included into the medium. These results demonstrate that moderate butyric acid levels in the medium trigger the switch to soventogenesis resulting in higher butanol formation rates. A study mentioned in the literature also confirms these results. It is reported that the continuous addition of butyric acid unspecifically activates the formation of both butanol and acetone in *Clostridium acetobutylicum* strain 77 accelerating the cellular metabolism in the solventogenic phase, particularly when 50 $g \cdot l^{-1}$ of glucose were fermented (Ammouri *et al*., 1987).

In general, all the previous analysis reveal that butyric acid plays four main interdependent roles in clostridial fermentation systems: firstly, it is used as metabolic co-substrate for butanol synthesis by the cells; secondly, butyrate buffers the medium pH preventing it to drop below critical levels that compromise cell stability. The same work mentioned previously also states that butyrate addition prevented strain degeneration during an extended subculturing of *C.*

beijerinckii NCIMB 8052 (Lee *et al*., 2008b). Third, it inhibits cell growth by reducing the specific growth efficiency; and fourth, it appears to enhance the substrate consumption parameters even though the patterns for the sugar utilization rate are somewhat different among the four species. So, the cells unaffected by butyric acid addition consume glucose mainly for growth producing simultaneously butyrate as primary metabolite. As butyrate builds up in the system the medium pH drops with the cells shifting their metabolic state from acidogenesis to solventogenesis. However, if the pH drops below the critical level then the metabolic switch of the cells is negatively affected and acidogenesis is the dominant phase. In this case only residual levels of solvents are obtained. In contrast, when butyrate is added, it seems that a major fraction of the sugar is channelized to the generation of energy associated with the metabolic shift towards solventogenesis where new enzymes and other components are necessary, while cell growth uses only a smaller portion. This reflects into lower specific growth rates which are also conditioned progressively by cell inhibition effects due to increasing butyrate concentrations. In addition, as the butanol production pathway is induced by the added butyrate, the levels of butyryl-CoA are increased from acetoacetyl-CoA instead of forming acetoacetate. This results in a lower acetone production. Further details on the metabolic pathways for butanol and acid production can be found elsewhere (Desai *et al*., 1999 and Nöllin *et al*., 2001).

As summary, butyric acid addition seems to shorten the acidogenic phase with the cells consuming glucose mostly for solventogenic functions resulting in higher ABE-solvents production efficiencies, including butanol from sugar and co-substrate. Above the optimal butyrate concentration ABE-solvents production is decreased due to higher cell inhibition effects, suboptimal pHs and the carbon source is consumed mainly for energy generation most likely associated with cell maintenance effects and survival functions.

4.2. Batch Fermentation in Immobilized Cell System

4.2.1. Fermentation Study using a Fibrous-Bed Bioreactor (FBB)

As previously discussed, in a batch reactor using freely-suspended cells without any feed of butyrate, butanol productivity and yields are limited to low values due to residual butanol concentration caused by a dominant acidogenic phase. Additionally, it is general knowledge that low cell concentrations per unit of reactor volume reduce the volumetric productivity. In this part of the study it was preliminarily tested the influence of cell immobilization on the kinetic profiles for *C. beijerinckii* ATCC 55025 and BA 101 mutated bacteria since immobilization provides a good way for increasing cell concentration inside the reactor, among other advantages. The fermentation system was operated according to the schematic layout displayed in Fig. 4.15 and the kinetic profiles for several activities obtained for both mutated bacteria are depicted in Figs. 4.16A–B.

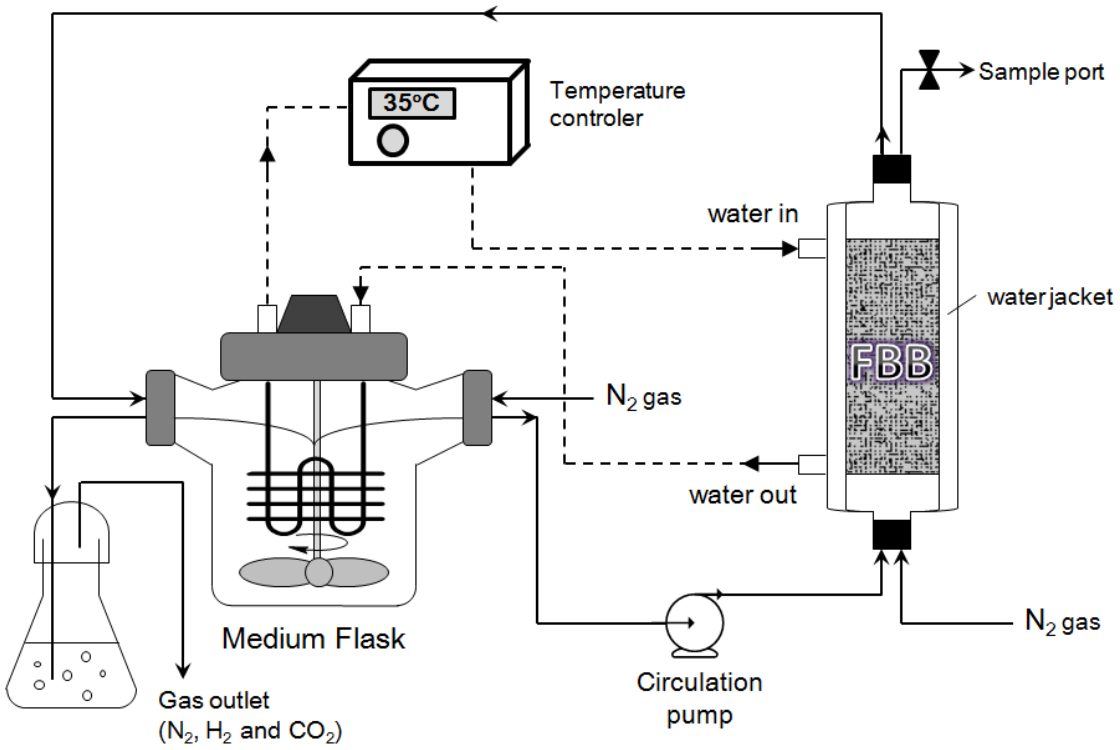

Figure 4.15. Schematic flow diagram of the Fibrous-Bed Bioreactor with medium recirculation operating in batch mode. Anaerobic fermentation conditions were maintained by preventing the ingress of air into the system through continuous injection of nitrogen gas. Purged gas was filtered in an Erlenmeyer flask by bubbling the gas in water as depicted.

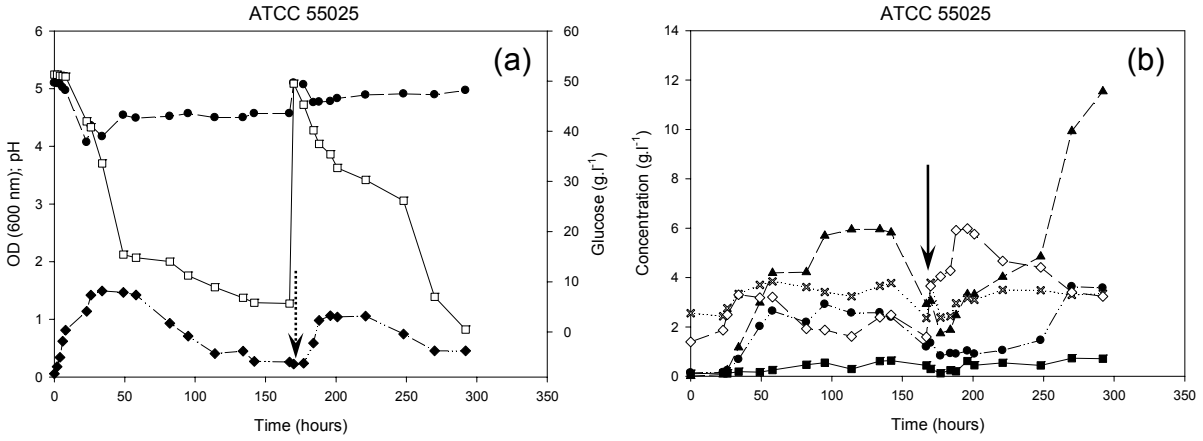

Figure 4.16A. Time–course studies of various activities for *C. beijerinckii* **ATCC 55025** fermentation in FBB; Legend: (a): medium pH (●), cell density (by OD_{600nm}) (◆), and glucose (□); (b): concentrations of butanol (▲), ethanol (■), acetic acid (×), butyric acid (◇), and acetone (✹). Arrows indicate the replacement of fermentation medium in the system with fresh P2-medium supplemented with sodium butyrate that resulted in a 4.0 $g \cdot l^{-1}$ butyrate concentration in the fermentation broth. First stage (167-hours of operation time); second stage (122-hours of fermentation with newly fresh P2-medium).

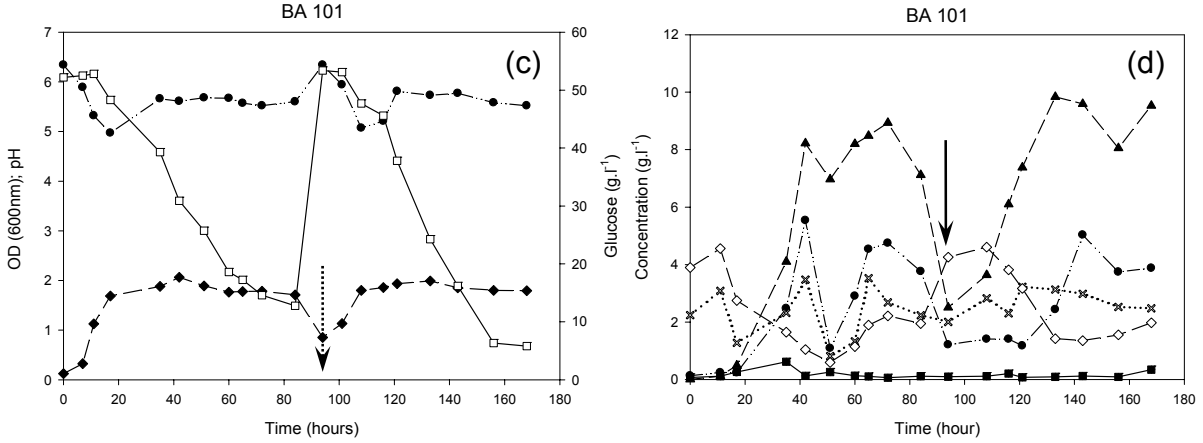

Figure 4.16B. Time–course studies of various activities for *C. beijerinckii* **BA 101** fermentation in FBB with an initial butyrate concentration of 4.0 $g \cdot l^{-1}$; Legend: (c): medium pH (●), cell density (by OD_{600nm}) (◆), and glucose (□); (d): concentrations of butanol (▲), ethanol (■), acetic acid (×), butyric acid (◇), and acetone (✹). Arrows indicate the replaced fermentation medium with fresh P2-medium supplemented with butyric acid that resulted in a 4.0 $g \cdot l^{-1}$ butyrate concentration in the fermentation broth. First stage (84-hours of fermentation); second stage (74-hours of fermentation with newly fresh P2-medium).

In graphs (a) and (b) from Fig. 4.16A up to the 167-hours of fermentation the system operated with no butyrate added initially into the medium. The initial amount once again resulted from inoculation effects where butyric acid was inevitably present. As the cells grow and immobilize onto the fibers, consuming glucose as energy source, they start producing organic acids that lower the medium pH inducing a shift from the acidogenic phase towards solventogensis. In this case the medium pH did not drop below 4.0 since the initial inoculated butyrate may have contributed into some extent to buffer the system and thereby inducing an earlier shift to solventogenesis. This resulted into higher amounts of butanol produced in the medium (~5.91±0.006 $g \cdot l^{-1}$) when compared to the values obtained in serum bottles (below 0.4 $g \cdot l^{-1}$), coupled with the fact that the present case uses an immobilized cell system over a suspended cell culture (serum bottles). Despite with the FBB the maximum cell density attained in the liquid phase being 1.48-times lower than the one obtained in serum bottles, it can be assumed the system in overall contains more active cells available per unit volume of reactor due to immobilization. One can see that in the period from 50–167 hours of fermentation, there was a substantial decrease in the average rate of glucose consumption (8.86-times lower) when compared with the initial phase (first 50-hours). This is probably associated with the metabolic switching from acidogenesis towards solventogenesis. By the time when ~90% of the initial glucose was consumed in the system the fermentation broth was replaced with newly fresh P2-medium containing an excess of butyrate necessary to achieve an initial butyrate concentration of 4.0 $g \cdot l^{-1}$ (second cycle of operation). The medium pH was controlled by adding a buffer solution containing sodium butyrate and butyric acid (see Materials and Methods). Again, following cell growth, the medium pH increased up to 5.0 followed by a lower pH (above 4.3) indicating the predominance of solventogenesis over acidogenesis. However, a closer look between 170–196 hours of fermentation one can see that butyric acid production is stimulated (5.95±0.035 $g \cdot l^{-1}$) at the expense of a steep glucose consumption rate (around 54.23 $g \cdot l^{-1} \cdot h^{-1}$ in average). After this point glucose uptake is somewhat slower (about 36.37 $g \cdot l^{-1} \cdot h^{-1}$) and butyric acid is consumed by the cells to produce butanol which accumulates progressively in the system reaching a maximum concentration of 11.54 $g \cdot l^{-1}$. At the final, the proportion ratio of ABE-production was roughly 7.5:15:1 (3:6:0.4) for 122-hours of fermentation time comparing to the control where the approximate stoichiometric ratio was found to be 3:6:1 (fermentation time of 167-hours).

For the culture of *C. beijerinckii* BA 101 in FBB the situation was slightly different from the previous one when the fermentation medium was replaced. In this case, the system started operating already with 4.0 $g \cdot l^{-1}$ of butyrate, while in the previous case (graphs (a) and (b)) only residual levels of butyrate were present when the fermentation was initiated. This was because with the strain ATCC 55025 the butanol results were more favorable than without added butyrate and due to the fact that in serum bottles the optimal concentration of butyric acid was found to be 4.0 $g \cdot l^{-1}$ for all strains and situations evaluated. In graphs (c) and (d) from Fig. 4.16B are represented the kinetic profiles obtained with an initial butyrate concentration of 4.0 $g \cdot l^{-1}$ followed by medium replacement at 84-hours of fermentation. As can be seen, the production of butanol in a double 80-hours fermentation period (averaged) increased considerably in both fermentation cycles (with and without medium replacement) reaching an average concentration of 9.38±0.45 $g \cdot l^{-1}$ per cycle (top concentration of 9.59 $g \cdot l^{-1}$), overall yield of 0.25±0.01 $g \cdot g^{-1}$/8.72±0.23 $g \cdot g^{-1}$ (from substrate/biomass) and 0.13 $g \cdot l^{-1} \cdot h^{-1}$ in productivity. These results particularly yield from substrate and volumetric productivity can be considered comparable to the ones obtained with *C. beijerinckii* ATCC 55025 at the same optimal concentration of butyric acid (see Table 4.3.). However, with *C. beijerinckii* ATCC 55025 the overall fermentation time necessary to produce the 11.54 $g \cdot l^{-1}$ of butanol was 122-hours whereas with BA 101 it took an average of 80-hours but at the cost of a lower titer of butanol formed (9.38 $g \cdot l^{-1}$). This reflects into similar volumetric productivities for both mutated strains even though the situations are entirely different. Moreover, considering the mean glucose consumption rate for the two periods for BA 101 (~0.56±0.12 $g \cdot l^{-1} \cdot h^{-1}$) over the second period for the first bacteria (~0.4 $g \cdot l^{-1} \cdot h^{-1}$) one can say that the strain BA101 consumed glucose ~1.4-times faster than strain ATCC 55025.

By comparing with the results obtained in serum bottles, the immobilized cell system with liquid recirculation showed better values in butanol production for both strains. The strain BA 101 exhibited a 2.36-fold increase in butanol concentration whereas in ATCC 55025 the butanol titer was approximately the double. However, butanol yield and productivity apparently were not so markedly different for both strains in each batch system at the optimal butyrate concentration. Indeed, it seems that immobilization in this case did not cause any noteworthy effect in these efficiency parameters at all. The yield in butanol from substrate obtained in serum bottles was slightly higher for BA 101 (~5.2%) while the productivity could be considered the

same (~0.07 $g \cdot l^{-1} \cdot h^{-1}$). In the immobilized cell system the same parameter pattern was observed with BA 101 showing a slightly better yield from substrate than ATCC 55025 (~8.0% higher) with equivalent productivities (see Tables 4.1 and 4.3 for comparison). Moreover, when comparing the strain ATCC 55025 both in serum bottles and immobilized cell system, when no butyrate was initially supplemented into the medium, one can see that both yield from substrate and productivity are much more favored with immobilization rather than using a suspended cell culture. In fact, the yield from substrate in this case showed to be 3.7-times higher by using immobilization when compared to the free-suspended system. The productivity also showed a very good improvement being in this case ~13-times higher than the free cell system. Additionally, by using the fibrous-bed bioreactor the results for strain ATCC 55025 are substantially higher at 4.0 $g \cdot l^{-1}$ of added butyrate then without the acid. Butanol titer in this case was almost doubled by using the optimal butyrate concentration. Yield from substrate and productivity exhibited a 1.8- and 2.5-fold increase, respectively, at 4.0 $g \cdot l^{-1}$ of butyrate than without the co-substrate initially added in the medium. The same trend in yield results from biomass for butanol and ABE-solvents was attained, showing the preference of optimal butyrate concentration over the control. In this case it was verified an almost 3-fold increase in yield from biomass for butanol and 1.5-fold increase for total ABE-solvents produced when compared with the control.

Table 4.3. Results for butanol and ABE-solvents production in Fibrous-Bed Bioreactor (FBB) for cells of *C. beijerinckii* ATCC 55025 and BA 101.

Butyric Acid Concentration (g/l)	BuOH Production (g/l)	BuOH Yield (g/g)	BuOH Relative Yield	BuOH Productivity (g/l/h)	BuOH Relative Productivity	ABE-Solvents Yield (g/g)	ABE-Solvents Relative Yield
ATCC 55025							
0.0	5.91	0.13	1.00	0.04	1.00	0.21	1.00
4.0	11.54	0.23	1.77	0.10	2.50	0.32	1.52
BA 101							
4.0	9.38 ± 0.45	0.25 ± 0.01	--------	0.130 ± 0.006	--------	0.380 ± 0.005	--------

Values followed by ± are standard deviation of mean (errors) of values obtained prior to and with replacement of fermentation medium. Yields are expressed in terms of consumed substrate $\left(Y_{P/S}\right)$.

Table 4.4. Yields from biomass $\left(Y_{P/X}\right)$ for butanol and ABE-solvents production in FBB for cells of *C. beijerinckii* ATCC 55025 and BA 101.

Butyric Acid Concentration (g/l)	BuOH Yield (g/g)	BuOH Relative Yield	ABE-Solvents Yield (g/g)	ABE-solvents Relative Yield
ATCC 55025				
0.0	7.08 ± 0.39	1.00	11.39 ± 0.63	1.00
4.0	19.40 ± 1.07	2.74	26.74 ± 1.47	2.35
BA 101				
4.0	8.72 ± 0.23	--------	13.29 ± 0.35	--------

Values followed by ± are standard deviation of mean (errors) of values obtained prior to and with replacement of fermentation medium followed by calculations with the inclusion of standard deviation of mean accounted for the two calibration curves correlating OD with DCW (strain BA 101). For the strain ATCC 55025, the values followed by ± indicate the standard deviation from mean accounted for the calibration curves that correlate optical density (OD) with biomass concentration (DCW).

Chapter 5 – Conclusions and Outlook

5. CONCLUSIONS AND OUTLOOK

5.1. Concluding Remarks

Examination of the effect of butyric acid on the batch fermentation performance of four different ABE-producing Clostridia strains was performed in this work. Through the addition of increasing butyrate concentrations in the media it was found that the butanol production parameters were significantly improved especially when the glucose based P2-medium was supplemented with 4.0 $g \cdot l^{-1}$ of butyrate. Above the optimal value cell growth inhibition predominates. The initial study carried out in serum bottles showed that butyric acid affects negatively the growth efficiency of the cell cultures with all specific growth rates declining with increasing butyrate concentrations. Yet, the buffering capacity of butyrate at low pHs induces an earlier shift from acidogenesis towards solventogenesis favoring butanol and ABE-solvents productions from co-substrate uptake. Multivariate data analysis was tentatively employed as a way to compare the different strains regarding their overall butyrate resistance during cell growth. According to the analysis, non-mutant C. *acetobutylicum* ATCC 824 appeared to be the most resistant strain towards increasing variations in butyric acid concentration up to ~6.0 $g \cdot l^{-1}$ of butyrate, also proving to be the most efficient butanol productive strain, and total ABE-solvents in the range of butyrate concentrations evaluated. Batch fermentations with this bacterium lead to butanol titers in the order of 10.3 $g \cdot l^{-1}$ at the optimal butyrate concentration, productivity around 0.1 $g \cdot l^{-1} \cdot h^{-1}$ and yields from substrate and biomass of 0.3 $g \cdot g^{-1}$ and 7.6 $g \cdot g^{-1}$, respectively. Nevertheless, these values were obtained at the expense of higher glucose consumption rate parameters and overall fermented glucose when compared with the other bacteria. The use of fibrous-bed bioreactor clearly seems to have enhanced butanol production when compared with the freely-suspended cell system. By using *C. beijerinckii* ATCC 55025 and BA 101 mutated bacteria it was possible to attain butanol concentrations about 11.5 $g \cdot l^{-1}$ and 9.4 $g \cdot l^{-1}$, respectively, those of which reach approximately twice the values obtained with the corresponding free system when the medium was initially supplemented with 4.0 $g \cdot l^{-1}$ of butyrate.

5.2. Future Prospects

Through the study presented here, it was demonstrated that the addition of butyrate to the media up to 4.0 $g \cdot l^{-1}$ results in superior butanol production efficiencies. However, no systematic evaluation of acetic acid influence was performed. Therefore, future work should focus on the following topics:

- Investigate for all clostridia strains using both batch fermentation regimes (serum bottles and immobilized cell system) the combined effect of butyrate and acetic acids in the production of butanol and ABE-solvents as well as cell growth patterns and changes in the metabolism. It would also be interesting to inspect if acetic acid by itself has any similar beneficial effect as butyric acid. If not it would highlight the idea of using butyric acid to increase butanol production.

- Characterize in detail the temporal switching towards the solvent phase and the influence of medium pH in the regulation of both metabolic stages and how this shift can be modulated through the addition of both organic acids, individually or combined.

- Establish a correlation between the sugar consumption profiles with cell growth patterns, formation and consumption of acids with concomitant production of ABE-solvents, especially on butanol formation.

Chapter 6 – References

6. BIBLIOGRAPHY

- Annous, B.A. and Blaschek, H.P. (1991). Isolation and Characterization of *Clostridium acetobutylicum* Mutants with Enhanced Amilolytic Activity. *Applied Environmental Microbiology*; 57: 2544-2548.
- Assobhei, O. *et al*., (1998). Effect of Acetic and Butyric Acids on the Stability of Solvent and Spore Formation by *Clostridium acetobutylicum* ATCC 824 during Repeated Subculturing. *Journal of Fermentation and Bioengineering*; 85(2): 209-212.
- Bahl, H., H. Mueller, S. Behrens, H. Joseph, and F. Narberhaus (1995). Expression of heat shock genes in *Clostridium acetobutylicum*. *FEMS Microbiol. Rev.*; 17:341–348.
- Bahl, H., W. Andersch, K. Braun, and G. Gottschalk (1982). Effect of pH and butyrate concentration on the production of acetone and butanol by *Clostridium acetobutylicum* grown in continuous culture. *European J. Appl. Microbiol. Biotechnol.*; 14: 17-20.
- Bochman, M. *et al*. (1999). Advanced Inorganic Chemistry. USA: John Wiley & Sons, Inc.
- Campos, E.J. *et al*., (2002). Production of Acetone Butanol Ethanol from Degermed Corn using *Clostridium beijerinckii* BA 101. *Applied Biochemistry and Biotechnology*; Vols. 98-100; 553-561.
- Chauvatcharin, S. *et al*., (1998). Metabolism Analysis and On-line Physiological State Diagnosis of Acetone-Butanol Fermentation. *Biotechnol. Bioeng.*; 58: 561-571.
- Chen, C.-K. and Blaschek, H.P. (1999). Acetate Enhances Solvent Production and Prevents Degeneration in *Clostridium beijerinckii* BA 101. *Appl. Microbiol. Biotechnol.*; 52: 170-173.
- Cornillot, E. *et al*., (1997). The Genes for Butanol and Acetone Formation in *Clostridium acetobutylicum* ATCC 824 Reside on a Large Plasmid Whose Loss Leads to Degeneration of the Strain. *Journal of Bacteriology*; 179: 5442-5447.
- Cornillot, E., and Soucaille, P. 1996. Solvent forming genes in Clostridia. *Nature*; 380:489.
- Davis, S.E. and Morton, S.A. III (2008). Investigation of Ionic Liquids for the Separation of Butanol and Water. *Separation Science and Technology*; 43: 2460-2472.
- de Mattos, M.J.T. *et al*., (1994). Metabolic Shift Analysis at High Cell Densities. *FEMS Microbiology Reviews*; 14: 21-28.

- Desai, R. P. *et al*., (1999). Metabolic Flux Analysis Elucidates the Importance of the Acid-formation Pathways in Regulating Solvent Production by *Clostridium acetobutylicum*. *Metabolic Engineering*; 1: 206-213.
- Donaldson, G.K. *et al*., (2007). Fermentative Production of Four Carbon Alcohols. International Patent: WO2007/041269.
- Doran, P.M., 1995. Bioprocess Engineering Principles. Academic Press; p. 257- 292.
- Dürre, P. (1998). New Insights and Novel Developments in Clostridial Acetone/Butanol/Isopropanol fermentation. *Applied Microbiology and Biotechnology*; 49: 639-648.
- Dürre, P. (2007). Biobutanol: an attractive biofuel. *Biotechnol. J.*; 2: 1525-1534.
- Dürre, P. (2008). Fermentative Butanol Production – Bulk Chemical and Biofuel. *Ann. N.Y. Acad. Sci*.; 1125: 353-362.
- Durre, P., R. J. Fischer, A. Kuhn, K. Lorenz, W. Schreiber, B. Sturzenhofecker, S. Ullmann, K. Winzer, and U. Sauer (1995). Solventogenic enzymes of *Clostridium acetobutylicum*: catalytic properties, genetic organization, and transcriptional regulation. *FEMS Microbiol. Rev.*; 17:251–262.
- Eckert, G. and Schugerl, K. (1987). Continuous Acetone-Butanol Production with Direct Product Removal. *Applied Microbiology and Biotechnology*; 27: 221-228.
- Esbensen, K.H. (2001): *Multivariate Data Analysis – in practice. An introduction to multivariate data analysis and experimental design.* 5.th Ed. (Oct. 2001); 600 p. CAMO AS Publ. ISBN 82-993330-2-4 (http://www.camo.com/introducer/).
- Evans, P.J. and Wang, H.Y. (1988). Enhancement of Butanol Formation by *Clostridium acetobutylicum* in the Presence of Decanol-Oleyl Alcohol Mixed Extractants. *Applied Environmental Microbiology*; 54: 1662-1667.
- Ezeji, T. C. *et al*., (2004)/a. Butanol Fermentation Research: Upstream and Downstream Manipulations. *The Chemical Record*; 4: 305-314.
- Ezeji, T.C. *et al*., (2004)/b. Acetone Butanol Ethanol (ABE) Production from Concentrated Substrate: reduction in substrate inhibition by fed-batch technique and product inhibition by gas stripping. *Appl. Microbiol. Biotechnol.*; 63: 653-658.

- Ezeji, T.C. *et al*., (2006). Butanol production from Corn. Alcoholic Fuels: *Fuels for Today and Tomorrow*. Edited by Minteer, S.D. new York, NY: Taylor & Francis Group; p.99-122.
- Ezeji, T.C. *et al*., (2007). Production of Acetone-butanol-ethanol (ABE) in a Continuous Flow Bioreactor Using Degermed Corn and *Clostridium beijerinckii*. *Process Biochemistry*; 42: 34-39.
- Ezeji, T.C. *et al*., (2007)/a. Bioproduction of Butanol from Biomass: from genes to bioreactors. *Current Opinion in Biotechnology*; 18: 220-227.
- Falbe, J. (1970). Carbon Monoxide in Organic Synthesis. Berlin-Heidelberg-New York; Springer Verlag.
- Fond, O. *et al*., (1985). The Role of Acids on the Production of Acetone and Butanol by Clostridium acetobutylicum. *Appl. Microbiol. Biotechnol.*; 22: 195-200.
- Geng, Q. and C.-H. Park (1994), Pervaporative butanol fermentation by *Clostridium acetobutylicum* B18. *Biotechnol. Bioeng.*; 43: 978-986.
- Girbal, L., and P. Soucaille (1998). Regulation of solvent production in *Clostridium acetobutylicum*. *Trends in Biotechnology;* 16:11–16.
- Godin, C. and Engasser, J.M. (1990). Two-stage Continuous Fermentation of Clostridium acetobutylicum: effects of pH and dilution rate. *Appl. Microviol. Biotechnol.*; 33: 269-273.
- Gottschalk, J.C. and J.G. Morris (1981). The Induction of Acetone and Butanol Production in Cultures of *Clostridium acetobutylicum* by Elevated Concentrations of Acetate and Butyrate. *FEMS Microbiol. Letters*; 12: 385-389.
- Gottwald, M. and G. Gottschalk (1985). The Internal pH of *Clostridium acetobutylicum* and its Effect on the Shift from Acid to Solvent Formation. *Arch. Microbiol.*; 143: 42-46.
- Groot, W.J. *et al*., (1991)/b. Integration of pervaporation and continuous butanol fermentation with immobilized cells I: experimental results. *Chem. Eng. J.*; 46: B1-B10.
- Groot, W.J. *et al*., (1992). Technologies for Butanol Recovery Integrated with Fermentation. *Process Biochemistry*; 27: 61-75.
- Groot. W.J. *et al*., (1991)/a. Integration of Pervaporation and Continuous Butanol Fermentation with Immobilized Cells II: mathematical modeling and simulations. *Chem. Eng. J.*; 46: B11-B19.

- Hansch, C., Leo, A., Hoekman, D., 1995. Exploring QSAR Hydrophobic, Electronic and Steric Constants. ACS, Washington, DC.
- Hansen, Alan C., Qin Zhang, Peter, W.L. Lyne. (2005). Ethanol diesel fuel blends – a review. *Bioresource Technol,* 96: 277-285.
- Harris, Daniel C. (2003). Quantitative Chemical Analysis. Sixth Edition. W.H. Freeman and Company. New York; p. 408-418.
- Hipolito, C.N. *et al*., (2008). Bioconversion of Industrial Wastewater from Palm Oil Processing to Butanol by *Clostridium saccharoperbutyllacetonicum* N1-4 (ATCC 13564). *Journal of Cleaner Production*; 16: 632-638.
- Holt, R.A. *et al*., (1984). Production of Solvents by *Clostridium acetobutylicum* Cultures Maintained at Neutral pH. *Applied Environmental Microbiology*; 48:1166-1170.
- Huber, G.W., Iborra, S., and Corma, A. (2006). Synthesis of transportation fuels from biomass: chemistry, catalysts and engineering. *Chem*. *Rev*.; 106: 4044–4098.
- Ishizaki, A. *et al*., (1999). Extractive Acetone-Butanol-Ethanol Fermentation using Methylated Crude Palm Oil as Extractant in Batch Culture of *Clostridium saccharoperbutylacetonicum* N1-4 (ATCC 13564). *J. Biosc. Bioeng.*; 87: 352-356.
- Izák, P. *et al*., (2008). Increased Productivity of Clostridium acetobutylicum fermentation of Acetone, Butanol, and Ethanol by Pervaporation Through Supported Ionic Liquid Membrane. *Applied Microbiology and Biotechnology*; 78: 597-602.
- Jain, M.K. *et al*., (1993). Mutant Strain of *C. acetobutylicum* and Process for Making Butanol. Patent: US005192673A
- James N. Miller and Jane C. Miller (2000). Statistics and Chemometrics for Analytical Chemistry. Fourth Edition, Prentice Hall; p.214-225.
- Johann F. Görgens, Willem H. Van Zyl, Johannes H. Knoetze, (2005). Reliability of methods for the determination of specific substrate consumption rates in batch culture. *Biochemical Engineering Journal*; 25: 109–112.
- Johnson, J. L., and J. S. Chen (1995). Taxonomic relationships among strains of *Clostridium acetobutylicum* and other phenotypically similar organisms. *FEMS Microbiol. Rev.*; 17:233–240.

- Johnson, J.L. *et al*., (1997). Cultures of "*Clostridium acetobutylicum*" from various collections comprise *Clostridium acetobutylicum*, *Clostridium beijerinckii*, and two other distinct types based on DNA–DNA reassociation. *Int. J. Syst. Bacterial.*; 47: 420-424.
- Jones, D. T., and S. Keis (1995). Origins and relationships of industrial solvent-producing clostridial strains. *FEMS Microbiol. Rev.*; 17:223–232.
- Karakashev, D. *et al*., (2007). Anaerobic Biotechnological Approaches for Production of Liquid Energy Carriers from Biomass. *Biotechnology Letters*; 29: 1005-1012.
- Kashket, E.R. and Cao, Z.Y. (1995). Clostridial Strain Degeneration. *FEMS Microbiol. Rev.*; 17: 307-315.
- Kirschner, M. (2006). *n*-Butanol. Chemical Market Reporter. January 30 – February 5, ABI/INFORM Global, p.42.
- Kourkoutas, Y. *et al*., (2004). Immobilization technologies and support materials suitable in alcohol beverages production: a review. *Food Microbiology*; 21: 377-397.
- Kristin Brekke (2007). Butanol – An Energy Alternative? *Ethanol Today*. March 2007; 36-39. Online sources: http://www.ethanoltoday.com/ and http://www.ethanol.org/pdf/contentmgmt/March_07_ET_secondary.pdf).
- Lee, S. F., C. W. Forsberg, and L. N. Gibbins (1985). Xylanolytic activity of *Clostridium acetobutylicum*. *Appl. Environ. Microbiol.*; 50:1068–1076.
- Lee, S.-M. *et al*., (2008)/b. Continuous Butanol Production using Suspended and Immobilized *Clostridium beijerinckii* NCIMB 8052 with Supplementary Butyrate. *Energy and Fuels*; 22: 3459-3464.
- Lee, S.Y. *et al*., (2008)/a. Fermentative Butanol Production by Clostridia. [Review]. *Biotechnology and Bioengineering*; 101(2): 209-228.
- Lenz, T.G. and Moreira, A.R. (1980). Economic Evaluation of the Acetone-Butanol Fermentation. *Ind. Eng. Chem. Prod. Res. Dev.*; 19; 478-483.
- Li, S.-M. (2008). Continuous Butanol Production using Suspended and Immobilized *Clostridium beijerinckii* NCIMB 8052 with Supplemented Butyrate. *Energy & Fuels*; 22: 3459-3464.
- Lima, N., and Mota, M. (2003). Biotecnologia – Fundamentos e aplicações. Biocatálise aplicada Lidel-Edições Técnicas, Lda.

- Lin, Y. L. and Blaschek, H. P. (1983). *Applied Environmental Microbiology*; 45: 966.
- Lin, Y.L. and Blaschek H.P. (1983). Butanol production by a butanol tolerant strain of *Clostridium acetobutylicum* in extruded corn browth. *Appl. Environ. Microbiol.*; 45: 966-973.
- Lipnizki, F. *et al*., (2000). Use of Pervaporation-bioreactor Hybrid Process in Biotechnology. *Chemical Engineering and Technology*; 23: 569-577.
- Liu, J. and Fan, L.T. (2004). Downstream Process Synthesis for Biochemical Production of Butanol, Ethanol, and Acetone from Grains: Generation of Optimal and Near-Optimal Flowsheets with Conventional Operating Units. *Biotechnol. Prog*.; 20: 1518-1527.
- Maddox, I. S., N. Qureshi, K. Roberts-Thomson (1995), Production of acetone-butanol-ethanol from concentrated substrates using *Clostridium acetobutylicum* in an integrated fermentation-product removal process. *Process Biochem.*; 30(3): 209-215.
- Maddox, I.S. (1989). Biotechnology and Genetic Engineering Reviews; Vol. 7, p. 190.
- Maddox, I.S. (1989). The Acetone-Butanol-Ethanol Fermentation: recent progress in technology. *Biotechnol. Genet. Eng. Rev.*; 7: 189-220.
- Maddox, I.S. *et al*., (1995). Production of Acetone-Butanol-Ethanol from Concentrated Substrates using *Clostridium acetobutylicum* in an Integrated Fermentation-Product Removal Process. *Process Biochemistry*; 30(3): 209-215.
- Madigan, M., *et al*., (1997). Brock, Biology of Microorganisms. International Edition, Eight Edition, Prentice Hall International Inc.
- Matsumura, M. *et al*., (1988). Energy saving effect of pervaporation using oleyl alcohol liquid membrane in butanol purification. *Bioprocess Engineering* (discontinued); 3: 93-100. (continued by *Bioprocess and Biosystems Engineering*).
- Matta-El-Ammouri, G. *et al*., (1987). Effects of Butyric and Acetic Acids on Acetone-Butanol Formation by Clostridium acetobutylicum. *Biochemie*; 69: 109-115.
- Mermelstein, L.D. and Papoutsakis, E.T. (1993). Metabolic Engineering of Clostridium acetobutylicum ATCC 824 for Increased Solvent Production by Enhancement of Acetone Formation Enzyme Activities using Synthetic Acetone Operon. *Biotechnol. Bioeng.*; 42: 1053-1060.
- Mes-Hartree, M. and Saddler, J.N. (1982). Butanol Production of *Clostridium acetobutylicum* Grown on Sugars found in Hemicellulose Hydrolysates. *Biotechnology Letters*; 4(4): 247-252.

- Mitchell, W. J. (1998). Physiology of carbohydrate to solvent conversion by Clostridia. *Adv. Microb. Physiol.*; 39:31–130.
- Mollah, A. H. and D. C. Stuckey (1993), Maximizing the production of acetone-butanol in an alginate bead fluidized bed reactor using *Clostridium acetobutylicum*. *J. Chem. Tech. Biotechnol.*; 56: 83-89.
- Monot, F. *et al*., (1984). Influence of pH and Undissociated Butyric Acid on the Production of Acetone and Butanol in Batch Cultures of *Clostridium acetobutylicum*. *Applied Microbiology and Biotechnology*; 19: 422-426.
- Mulchandani, A. and B. Volesky (1994). Production of acetone-butanol-ethanol by *Clostridium acetobutylicum* using a spin filter perfusion bioreactor. *J. Biotechnol.*; 34:51-60.
- Mutschlechner, O., *et al*., (2000). Continuous two-stage ABE fermentation using *Clostridium beijerickii* NRRL B592 operating with a growth rate in the first stage vessel close to its maximum value. *J. Mol. Microbiol. Biotechnol.*; 2: 101-105.
- Nair, R.V. *et al*., (1999). Regulation of sol locus genes for Butanol and Acetone formation in *Clostridium acetobutylicum* ATCC 824 by a putative transcriptional repressor. *Journal of Bacteriology*; 181: 319-330.
- Nimcevic, D. *et al*., (1998). Solvent Production by *Clostridium beijerinckii* NRRL B592 Growing on Different Potato Media. *Applied Microbiology and Biotechnology*; 50: 462-428.
- Niven, R.K. (2005). Ethanol in gasoline: environmental impacts and sustainability review article. Renewable and Sustainable Energy Reviews; 9: 535-555.
- Nölling J. *et al*., (2001). Genome Sequence and Comparative Analysis of the Solvent-Producing Bacterium *Clostridium acetobutylicum*. *Journal of Bacteriology*; 183(16): 4823-4838.
- Papoutsakis, E. P. (2008). Engineering Solventogenic Clostridia. *Current Opinion in Biotechnology*; 19: 420-429.
- Papoutsakis, E. T., and G. N. Bennett (1999). Molecular regulation and metabolic engineering of solvent production by *Clostridium acetobutylicum*. *Bioprocess Technol.*; 24:253–279.
- Parekh, M. and Blaschek, H.P. (1999). Butanol Production by Hypersolvent-producing Mutant Clostridium beijerinckii BA 101 in Corn Steep Water Medium Containing Maltodextrin. *Biotechnology Letters*; 21: 45-48.

- Parekh, M. *et al*., (1998). Development of a Cost-effective Glucose-corn Steep medium for Production of Butanol by *Clostridium beijerinckii*. *Journal of Industrial Microbiology and Biotechnology*; 21: 187-191.
- Park, C.-H., M. R. Okos, and P. C. Wankat (1989). Acetone-butanol-ethanol (ABE) fermentation in an immobilized cell trickle bed reactor. *Biotechnol. Bioeng.*; 34: 18-29.
- Petitdemange, H., C. Cherrier, J. M. Bengone, and R. Gay (1997). Study of the NADH and NADPH-ferredoxin oxidoreductase activities in *Clostridium acetobutylicum*. *Can. J. Microbiol.* 23:152–160.
- Philips, J.A. and Humphrey A.E. (1985). In Biotechnology and Bioprocess Engineering. T.K. Ghose, Ed. United India Press, New Dehli; p. 157.
- Pierrot, P. *et al*., (1986). Continuous Acetone-Butanol Fermentation with High Productivity by Cell Ultrafiltration and Recycling. *Biotechnology Letters*, 8(4): 253-256.
- Qureshi, N and Blaschek, H.P. (2005). Butanol production from Agricultural Biomass. *Food Biotechnology*. 525-551 (Taylor & Francis Group plc).
- Qureshi, N. and Blascheck, H.P. (2000). Butanol Production Using *Clostridium beijerinckii* BA 101 Hyper-Butanol Producing Mutant Strain and Recovery by Pervaporation. *Applied Biochemistry and Biotechnology*; 84-86: 225-235.
- Qureshi, N. and Blaschek, H.P. (1999). Production of Acetone Butanol Ethanol (ABE) by a Hyper-Producing Mutant Strain of *Clostridium beijerinckii* BA 101 and Recovery by Pervaporation. *Biotechnol. Prog.*; 15: 594-602.
- Qureshi, N. and Blaschek, H.P. (2001)/a. ABE Production from Corn: a recent economic evaluation. *Journal of Industrial Microbiology and Biotechnology*; 27: 292-297.
- Qureshi, N. and Blaschek, H.P. (2001)/d. Recovery of Butanol from Fermentation Broth by Gas Stripping. *Renewable Energy*; 22: 557-564.
- Qureshi, N. and Blaschek, H.P., (2001)/c. Evaluation of Recent Advances in Butanol Fermentation, Upstream and Downstream processing. *Bioprocess and Biosystems Engineering*; 24: 219-226.
- Qureshi, N. and I. S. Maddox (1995). Continuous production of acetone-butanol-ethanol using immobilized cells of *Clostridium acetobutylicum* and integration with product removal by liquid-liquid extraction. *Journal of Fermentation and Bioengineering*; 80(2): 185-189.

- Qureshi, N. *et al*., (2000). Continuous solvent production by *Clostridium beijerinckii* BA101 immobilized by adsorption onto brick. *World Journal of Microbiology & Biotechnology* 16: 377-382.
- Qureshi, N. *et al*., (2001)/b. Soy Molasses as Fermentation Substrate for production of Butanol using *Clostridium beijerinckii* BA 101. *Journal of industrial Microbiology and Biotechnology*; 26: 290-295.
- Qureshi, N. *et al*., (2007). Butanol Production from Wheat Straw Hydrolysate using *Clostridium beijerinckii*. *Bioprocess Biosyst. Eng.*; 30: 419-427.
- Qureshi, N. *et al*., (2008). Butanol Production by *Clostridium beijerinckii*. Part I: Use of Acid and Enzyme Hydrolyzed Corn Fiber. *Bioresource Technology*; 99: 5915-5922.
- Qureshi, N. *et al*., (2008)/a. Butanol Production from Wheat Straw by Simultaneous Saccharification and Fermentation using *Clostridium beijerinckii*: Part I – Batch Fermentation. *Biomass and Bioenergy*; 32: 168-175.
- Qureshi, N. *et al*., (2008)/b. Removal of Fermentation Inhibitors from Alkaline Peroxide Pretreated and Enzymatically Hydrolysed using *Clostridium beijerinckii* in Batch Reactors. *Biomass and Bioenergy*; 32: 1353-1358.
- Ramey, D. and Yang, S.-T. (2004). Production of Butyric Acid and Butanol from Biomass – Final Report. *U.S. Department of Energy, Morgantown, WV*.
- Robinson, Richard K. Encyclopedia of Food Microbiology, Volumes 1-3. (pp: 445-450). Elsevier (2000).
- Scotcher and Bennett (2005). SpoIIE Regulates Sporulation but Does Not Directly Affect Solventogenesis in *Clostridium acetobutylicum* ATCC 824. *Journal of Bacteriology*; 187(6): 1930-1936.
- Shang-Tian Yang (2008). Methods for Producing Butanol. Patent: US 20080248540A1.
- Shota Atsumi, Taizo Hanai and James C. Liao (2008). Non-fermentative pathways for synthesis of branched-chain higher alcohols as biofuels. *Nature*; 451, 86-89 doi: 10.1038/nature06450.
- Silva, M.N. and S.-T. Yang (1995). Kinetics and Stability of a Fibrous-bed Bioreactor for Continuous Production of Lactic Acid from Unsupplemented Acid Whey. *Journal of Biotechnology*; 41: 59-70.

- Swodenk , W. (1983). Ethanol als Rohstoff für die chemische Industrie. *Chem . Ing. Tech.*; 55: 683-688.
- Syed, Qurat-ul-Ain *et al*., (2008). Enhanced Butanol Production by Mutant Strains of *Clostridium acetobutylicum* in Molasses Medium. *Turkish Journal of Biochemistry*; 33(1): 25-30.
- T.C. Ezeji, N. Qureshi and H.P. Blaschek (2003). Production of acetone, butanol and ethanol by *Clostridium beijerinckii* BA101 and in situ recovery by gas stripping. *World Journal of Microbiology & Biotechnology*; 19: 595–603.
- Tashiro, Y. *et al*., (2004). High Butanol Production by *Clostridium saccharoperbutylacetonicum* N1-4 in Fed-Batch Culture with pH-Stat Continuous Butyric Acid and Glucose Feeding Method. *Journal of Bioscience and Bioengineering*; 98(4): 263-268.
- Terracciano, J.S. and Kashket, E.R. (1986). Intracellular Conditions required for Initiation of Solvent Production by *Clostridium acetobutylicum*. *Applied and Environmental Microbiology*; 52(1): 86-91.
- Wackett, L.P. (2008). Biomass to Fuels via Microbial Transformations. *Current Opinion in Chemical Biology*; 12: 187-193.
- Weyer, E. R., and Rettger, L.F. (1927). A comparative study of six different strains of the organism commonly concerned in large-scale production of butyl alcohol and acetone by the biological process. *Journal of Bacteriology*; 14:399–424.
- Wilkinson, S.R. *et al*., (1995). Molecular Genetics and the Initiation of Solventogenesis in *Clostridium beijerinckii* (formerly *Clostridium acetobutylicum*) NCIMB 8052. *FEMS Microbiol. Rev.*; 17: 275-285.
- Woods, D.R. (1995). The Genetic Engineering of Microbial Solvent Production. *Trends in Biotechnology*; 13: 259-264.
- Yang, X. and G. T. Tsao (1995). Enhanced acetone-butanol fermentation using repeated fed-batch operation coupled with cell recycle by membrane and simultaneous removal of inhibitory products by adsorption. *Biotechnol. Bioeng*.; 47: 444-450.

- Yu, E.K.C. and Saddler, J.N. (1983). Enhanced Acetone-Butanol Fermentation by *Clostridium acetobutylicum* grown in D-xylose in the Presence of Acetic or Butyric Acid. *FEMS Microbiology Letters*; 18: 103-107.
- Zverlov, V.V. *et al*., (2006). Bacterial Acetone and Butanol Production by Industrial Fermentation in the Soviet Union: use of hydrolyzed agricultural waste for birefinary. *Applied Microbiology and Biotechnology*; 71: 587-597.

Additional Sources of References:

[1] Biobutanol website: http://www.biobutanol.com/

[2] http://blogs.princeton.edu/chm333/f2006/biomass/2007/01/biobutanol.html

[3] http://www.genomenewsnetwork.org/resources/sequenced_genomes/genome_guide_p1a.shtml

[4] http://www.cheric.org/kdb/kdb/hcprop/showprop.php?cmpid=821

[5] http://cetiner.tripod.com/Properties.htm

Appendices & Supporting Information

Appendix A – Bioreactor Construction, Start-Up and Operation

A1. Fibrous-Bed Bioreactor (FBB) Construction:

Figure A2 shows a picture of the experimental set-up used in this work. The immobilized cell bioreactor (FBB) was made of a packed glass column containing a water jacket. The fibrous-bed matrix was constructed by winding a piece of cotton towel affixed to the surface of a stainless-steel wire mesh in a spiral configuration with 2-5 mm gaps between each turn of the spiral layer (schematic drawing in Fig. A1 below) and the coiled set placed inside the column for cell immobilization. The packed glass column was then sealed with rubber stoppers at both ends and connected to a 1.0 liter spinner-flask fermentor through a recirculation loop. The FBB was kept at the optimal bacterial growth temperature (35ºC) by the recirculation of water with temperature control through the water jacket in the glass column.

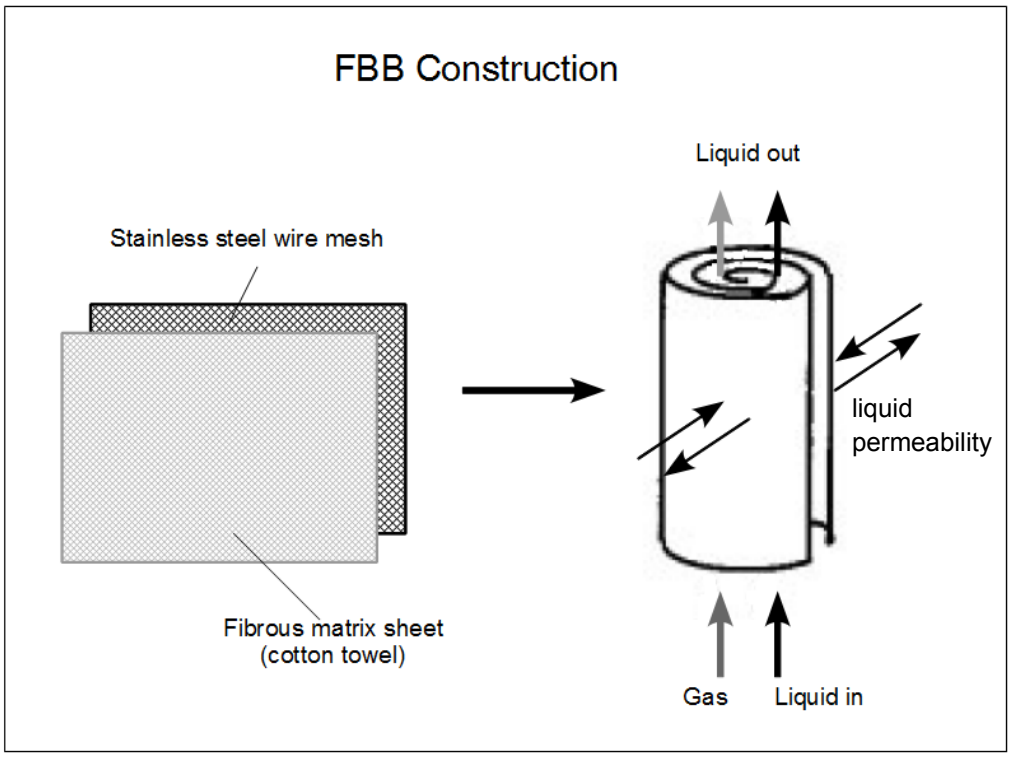

Figure A1. Construction of spiral wound fibrous matrix showing exchange of liquid medium.

Figure A2. Experimental set-up image of the fibrous-bed immobilized cell bioreactor system used in this study. See Fig. 4.15 displayed in section 4.2.1 for flow diagram details about the operation mode.

A2. FBB Start-Up and Operation:

Before use, the bioreactor was sterilized by autoclaving at 121ºC and 15-psig for 1-hour, held overnight at room temperature and sterilized again for 30 min for complete sterilization. The spinner-flask (μ-Carrier BELLCO 1965-00500) containing initially solution of dextrose in distilled water was sterilized in the exact same conditions. A sterilized solution of yeast extract

together with the other solutions that make the P2-medium were introduced separately in the stirrer-flask. Yeast extract solution was added by purging nitrogen gas while the other solutions were independently injected aseptically via a 0.2 μm pore size membrane filter (Nalgene Lab ware Div., Nalgene/Sybron Corp., Rochester, N.Y.). The column reactor was already aseptically connected to the sterile stirrer/spinner-flask fermentor through a recirculation loop. The entire system contained ~1.0 liter of the sterile P2-medium (supplemented or not with 4.0 $g \cdot l^{-1}$ of butyric acid). Unless stated otherwise, the system temperature was maintained at 35ºC by continuous water recirculation through jacket of FBB and heat-exchanger coils inside the stirrer-flask, agitation speed of 120 rpm, and the initial medium pH was adjusted up to a certain value by adding 6.0 N HCl solution. Total anaerobic conditions inside the system were reached by sparging the medium with sterile nitrogen gas for 1-hour using a 5.0 mm disc filter. To start the fermentation, 50 ml of cell suspension inoculum previously-grown in serum bottles were introduced into the spinner-flask and allowed to grow for 26-hours for the strain ATCC 55025 until the cell concentration reached an optical density ($OD_{600\ nm}$) of ~1.4. For the strain BA 101 the cell density was ~1.9 in OD after 35-hours of cell growth. Cell immobilization and fermentation were carried out simultaneously by recirculation of the fermentation broth through the fibrous bed at a pumping rate of ~25 $ml \cdot min^{-1}$ in order to allow the cell attachment and immobilization onto the fibrous-bed matrix. After 17–27 hours of continuous recirculation the majority of cells were immobilized and no significant changes in cell density was observed in the circulating fermentation broth. The reaction system was operated at a repeated 2-cycle batch mode. Initial pH values in the system with added butyrate (4.0 $g \cdot l^{-1}$) were adjusted to 5.0 and 6.4 for the strains ATCC 55025 and BA 101, respectively, by using a corresponding sodium butyrate/butyric acid buffer solution. After the first cycle of operation, when the glucose level in the fermentation broth was stabilized to a minimum value, the exhausted medium was entirely replaced with fresh sterile P2-medium supplemented with glucose (~50 $g \cdot l^{-1}$) plus butyrate (4.0 $g \cdot l^{-1}$) to start a new batch run. The media inside the stirring-vessel was always kept anaerobic by continuous bubbling with filtered oxygen-free nitrogen. The media inside the FBB was also kept oxygen free through continuous injection of filtered nitrogen gas. Samples were withdrawn intermittently at the product outlet and immediately frozen until analysis could be performed.

Appendix B – Kinetic Profiles with Increasing Concentrations of Butyric Acid:

B1. Kinetic profiles obtained in Serum Bottles for *Clostridium acetobutylicum* ATCC 824

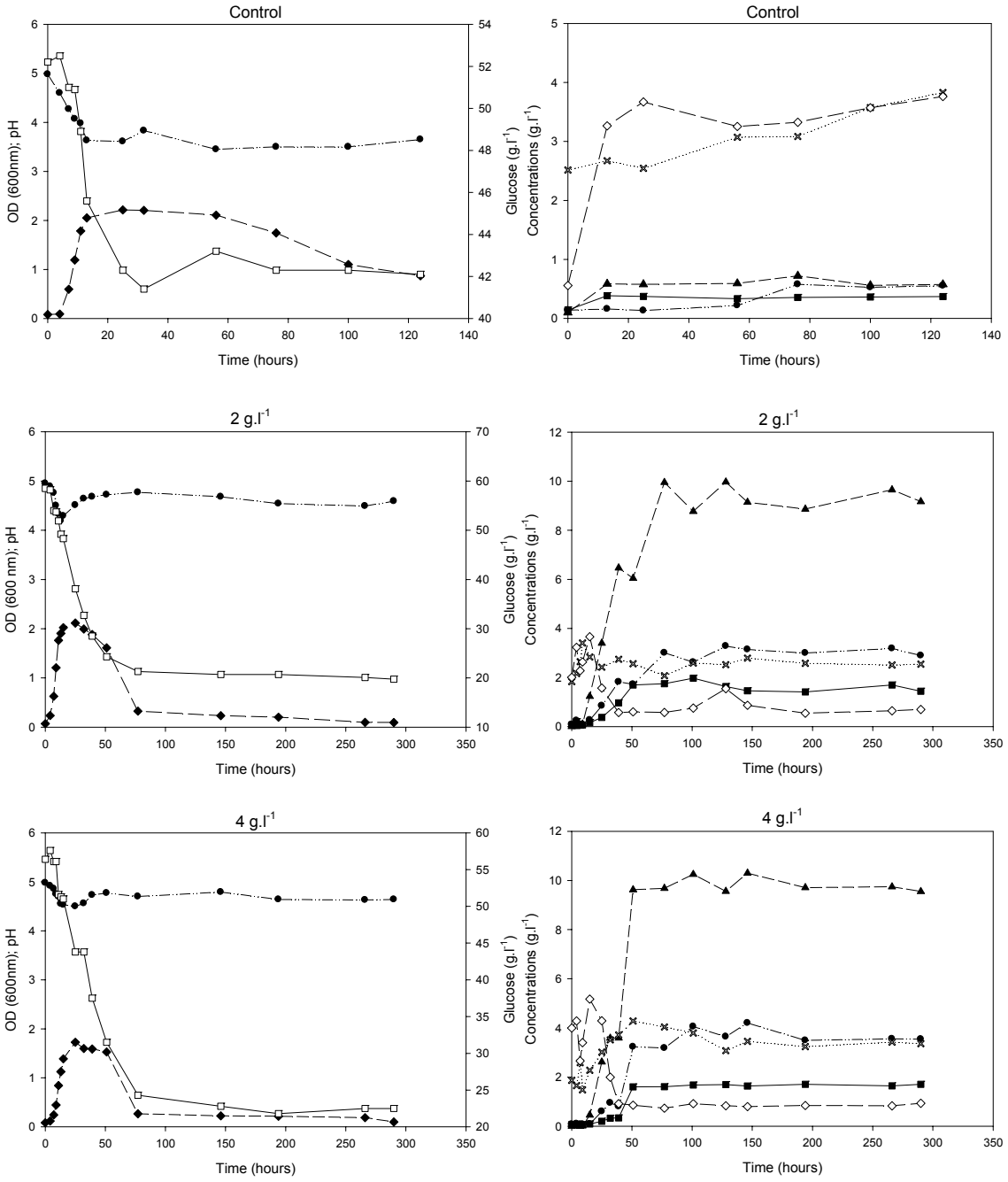

Figure B1-1. Time–course studies of various activities for *C. acetobutylicum* **ATCC 824** batch fermentation as a function of added butyric acid concentrations (above each graph); Legend: medium pH (●), cell density (by OD_{600nm}) (◆), glucose (□), butanol (▲), ethanol (■), acetic acid (✕), butyric acid (◇), and acetone (✹).

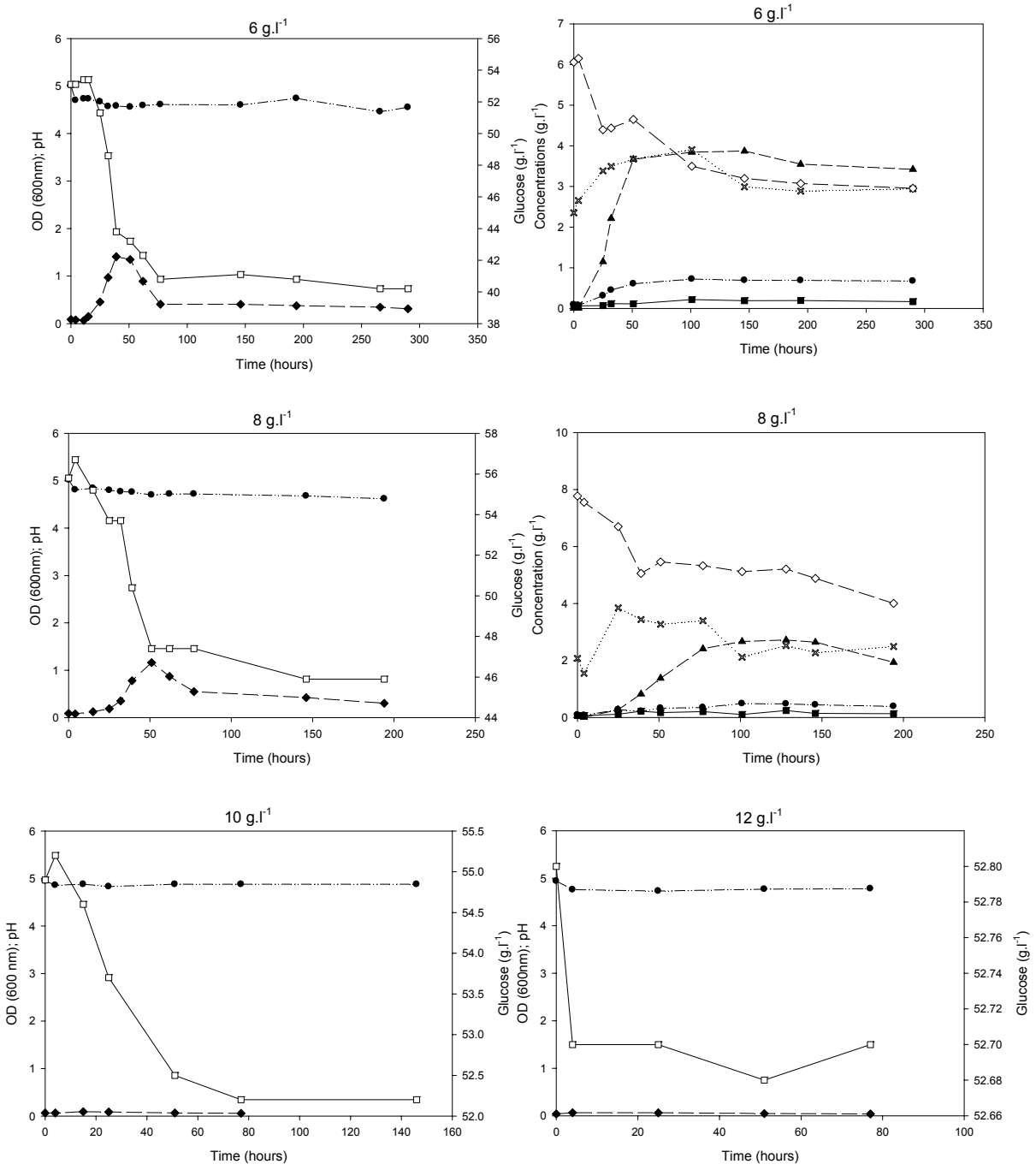

Figure B1-2. Time–course studies of various activities for *C. acetobutylicum* **ATCC 824** batch fermentation as a function of added butyric acid concentrations (above each graph); Legend: medium pH (●), cell density (by OD_{600nm}) (◆), glucose (□), butanol (▲), ethanol (■), acetic acid (×), butyric acid (◇), and acetone (✹). No observable cell growth was obtained for butyrate concentrations of 10.0 and 12.0 $g \cdot l^{-1}$, therefore no ABE-solvents production was found.

B2. Kinetic profiles obtained in Serum Bottles for *Clostridium beijerinckii* ATCC 55025

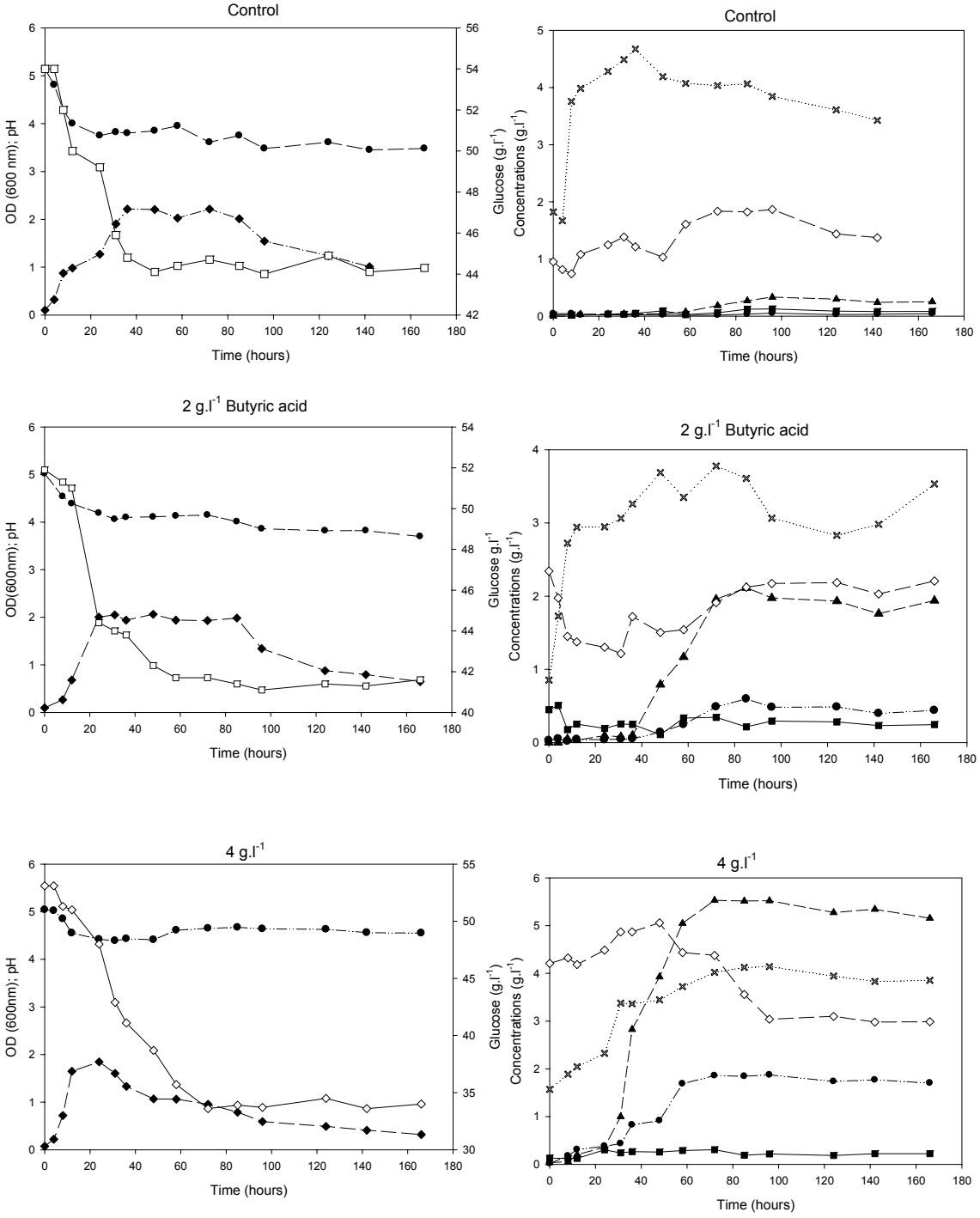

Figure B2-1. Time–course studies of various activities for *C. beijerinckii* **ATCC 55025** batch fermentation as a function of added butyric acid concentrations (above each graph); Legend: medium pH (●), cell density (by OD_{600nm}) (◆), glucose (□), butanol (▲), ethanol (■), acetic acid (×), butyric acid (◇), and acetone (✹).

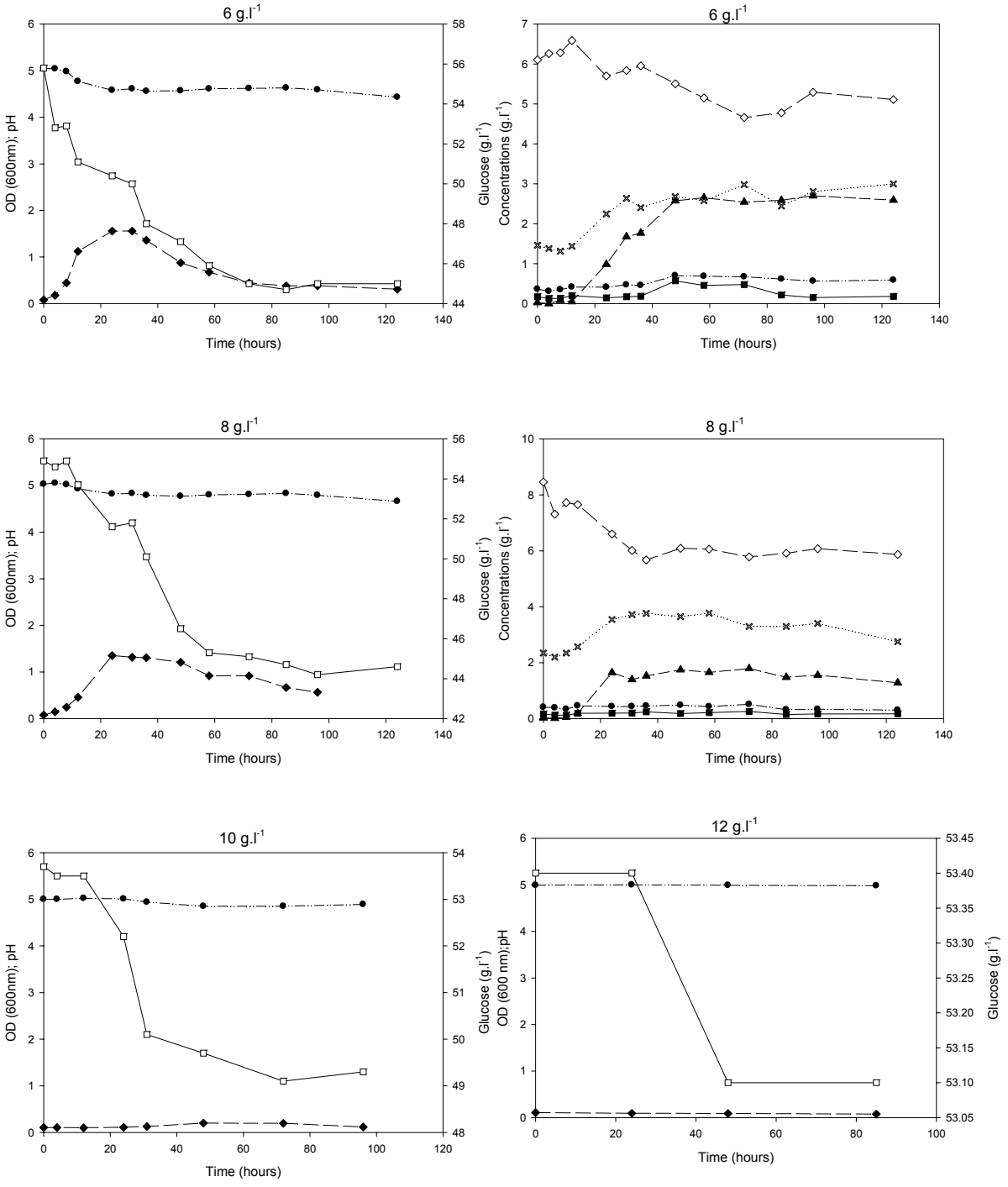

Figure B2-2. Time–course studies of various activities for *C. beijerinckii* **ATCC 55025** batch fermentation as a function of added butyric acid concentrations (above each graph); Legend: medium pH (●), cell density (by OD_{600nm}) (◆), glucose (□), butanol (▲), ethanol (■), acetic acid (×), butyric acid (◇), and acetone (✹). No observable cell growth was obtained for butyrate concentrations of 10.0 and 12.0 g·l^{-1}, therefore no ABE-solvents production was found.

B3. Kinetic profiles obtained in Serum Bottles for *Clostridium beijerinckii* BA 101

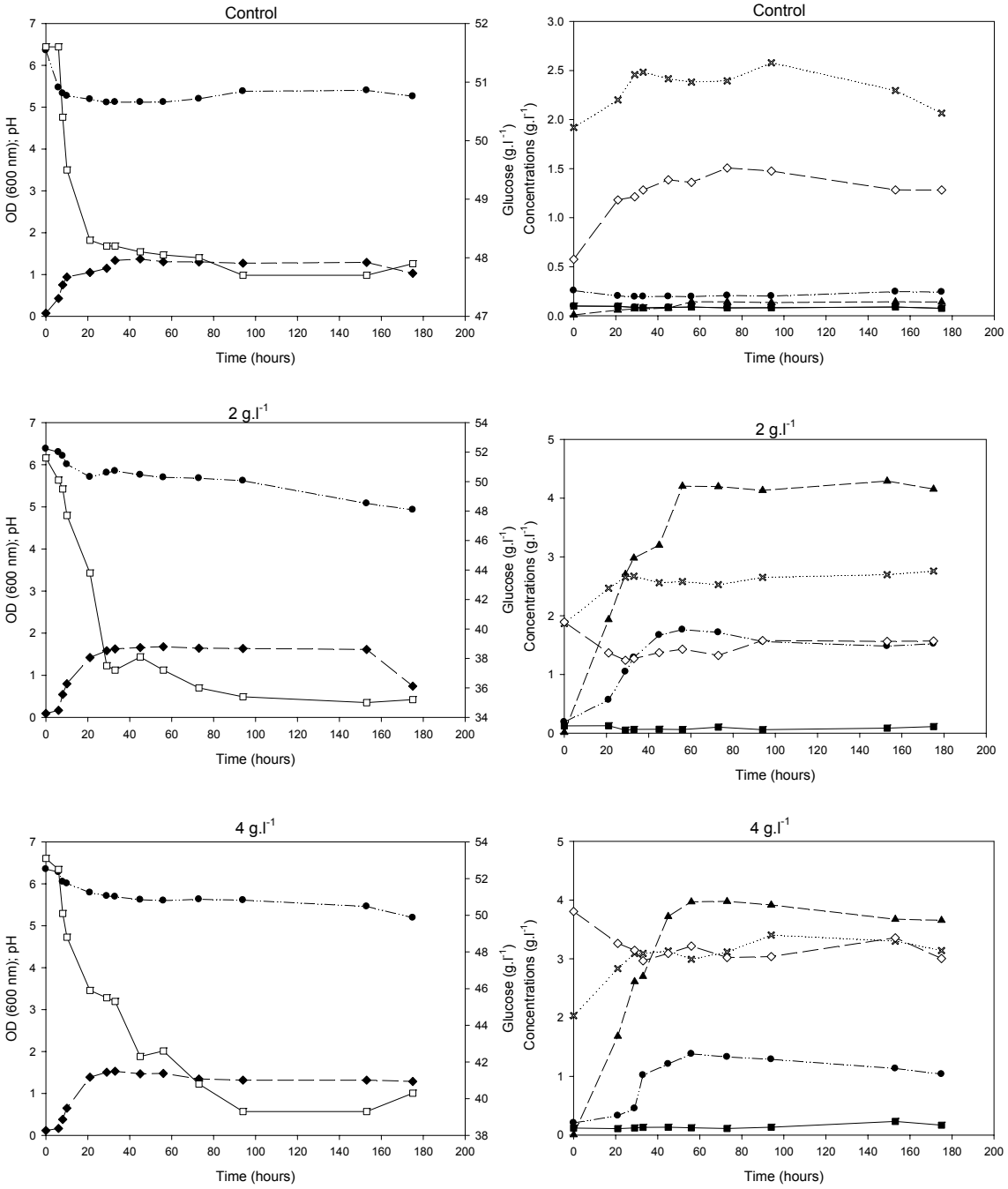

Figure B3-1. Time–course studies of various activities for *C. beijerinckii* **BA 101** batch fermentation as a function of added butyric acid concentrations (above each graph); Legend: medium pH (●), cell density (by OD_{600nm}) (◆), glucose (□), butanol (▲), ethanol (■), acetic acid (✕), butyric acid (◇), and acetone (✹).

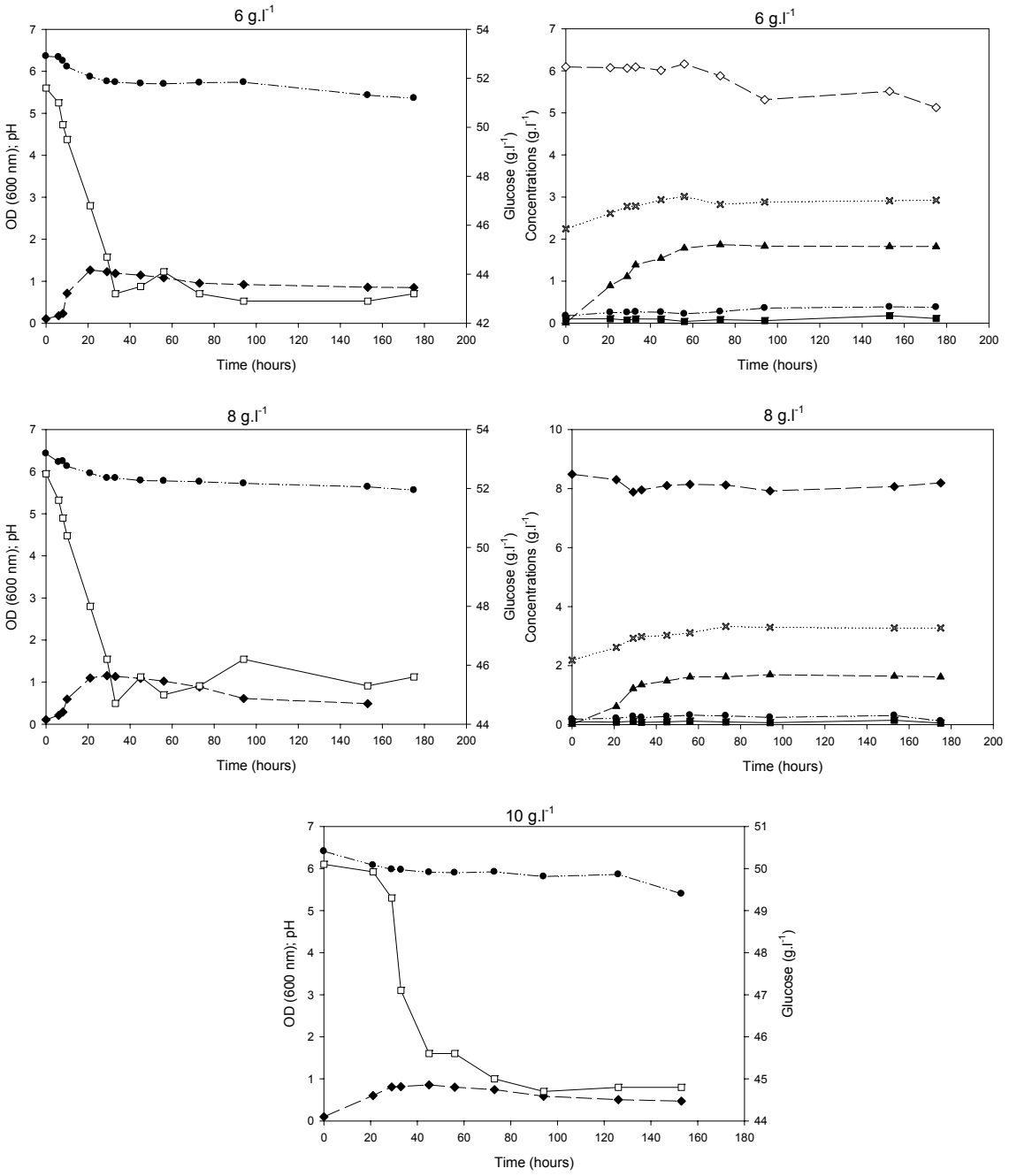

Figure B3-2 Time–course studies of various activities for *C. beijerinckii* **BA 101** batch fermentation as a function of added butyric acid concentrations (above each graph); Legend: medium pH (●), cell density (by OD_{600nm}) (◆), glucose (□), butanol (▲), ethanol (■), acetic acid (✕), butyric acid (◇), and acetone (✹). No observable cell growth was obtained for butyrate concentrations of 10.0 g·l^{-1}, therefore no ABE-solvents production was found.

B4. Kinetic profiles obtained in Serum Bottles for *Clostridium beijerinckii* NCIMB 8052

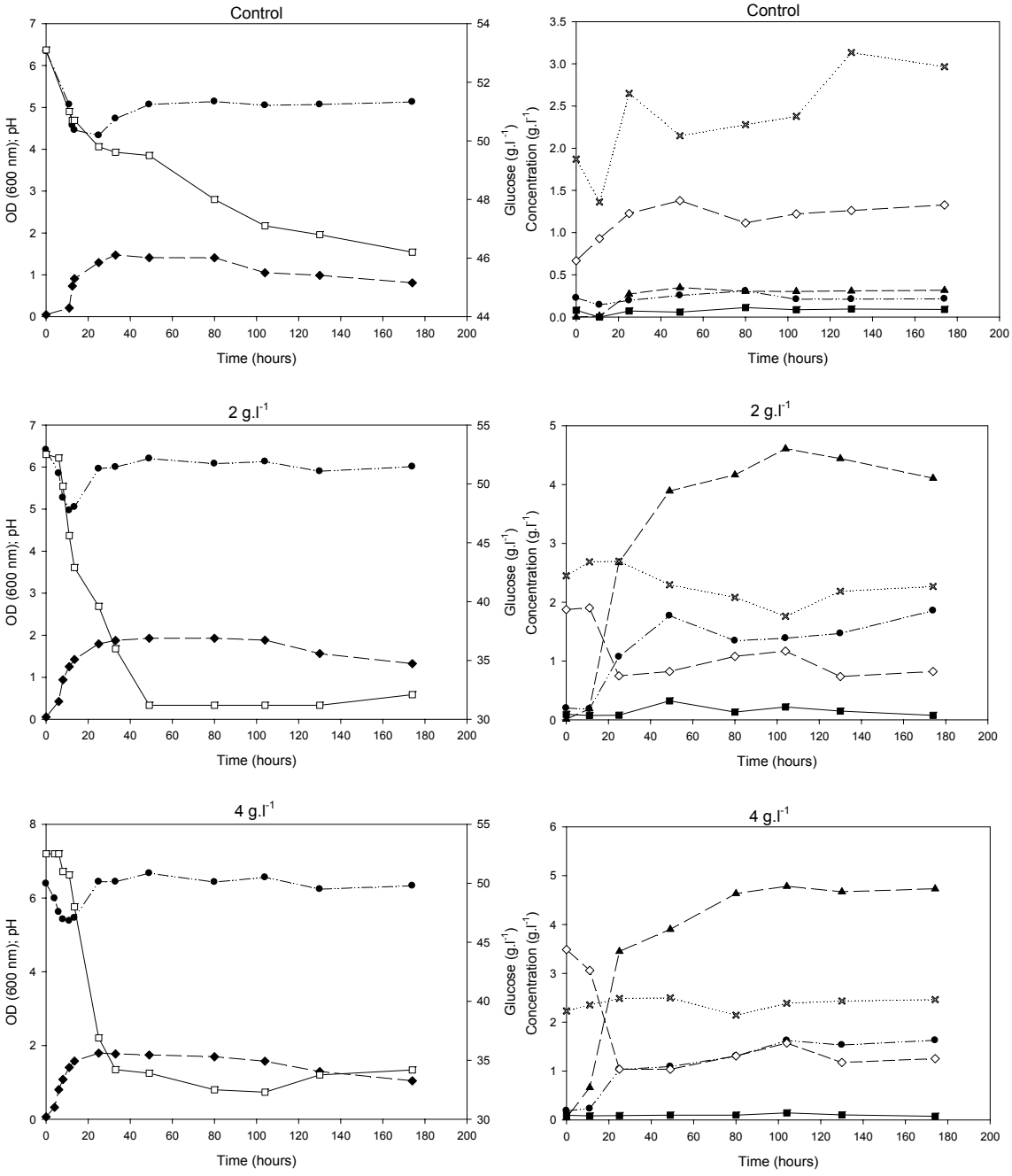

Figure B4-1. Time–course studies of various activities for *C. beijerinckii* **NCIMB 8052** batch fermentation as a function of added butyric acid concentrations (above each graph); Legend: medium pH (●), cell density (by OD_{600nm}) (◆), glucose (□), butanol (▲), ethanol (■), acetic acid (×), butyric acid (◇), and acetone (✹).

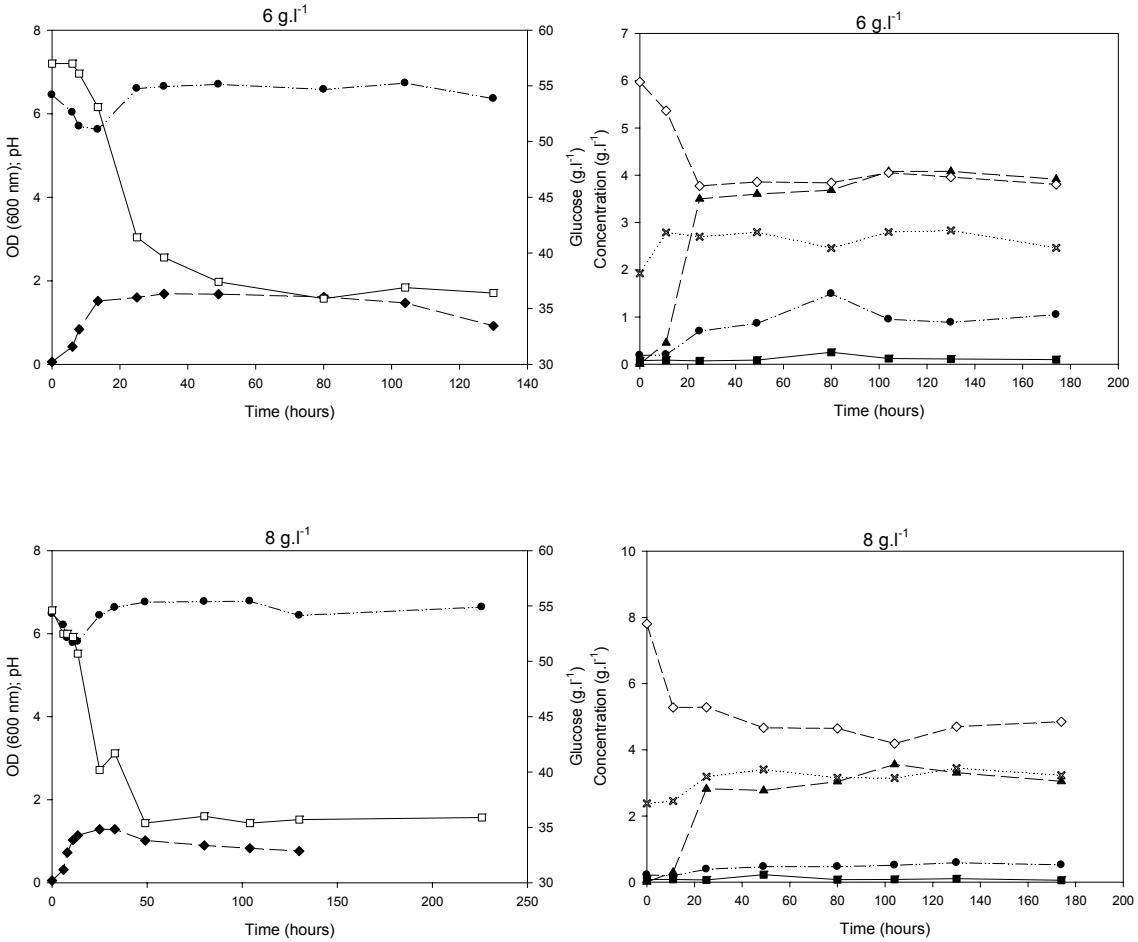

Figure B4-2. Time–course studies of various activities for *C. beijerinckii* **NCIMB 8052** batch fermentation as a function of added butyric acid concentrations (above each graph); Legend: medium pH (●), cell density (by OD_{600nm}) (◆), glucose (□), butanol (▲), ethanol (■), acetic acid (×), butyric acid (◇), and acetone (✹). No observable cell growth was obtained for butyrate concentrations of 10.0 and 12.0 g·l^{-1}, therefore no ABE-solvents production was found.

Appendix C – Calibration Curves and Multivariate Data Analysis

C1. Correlation lines between Optical Density (OD) and Biomass Concentration (dry cell weight, DCW):

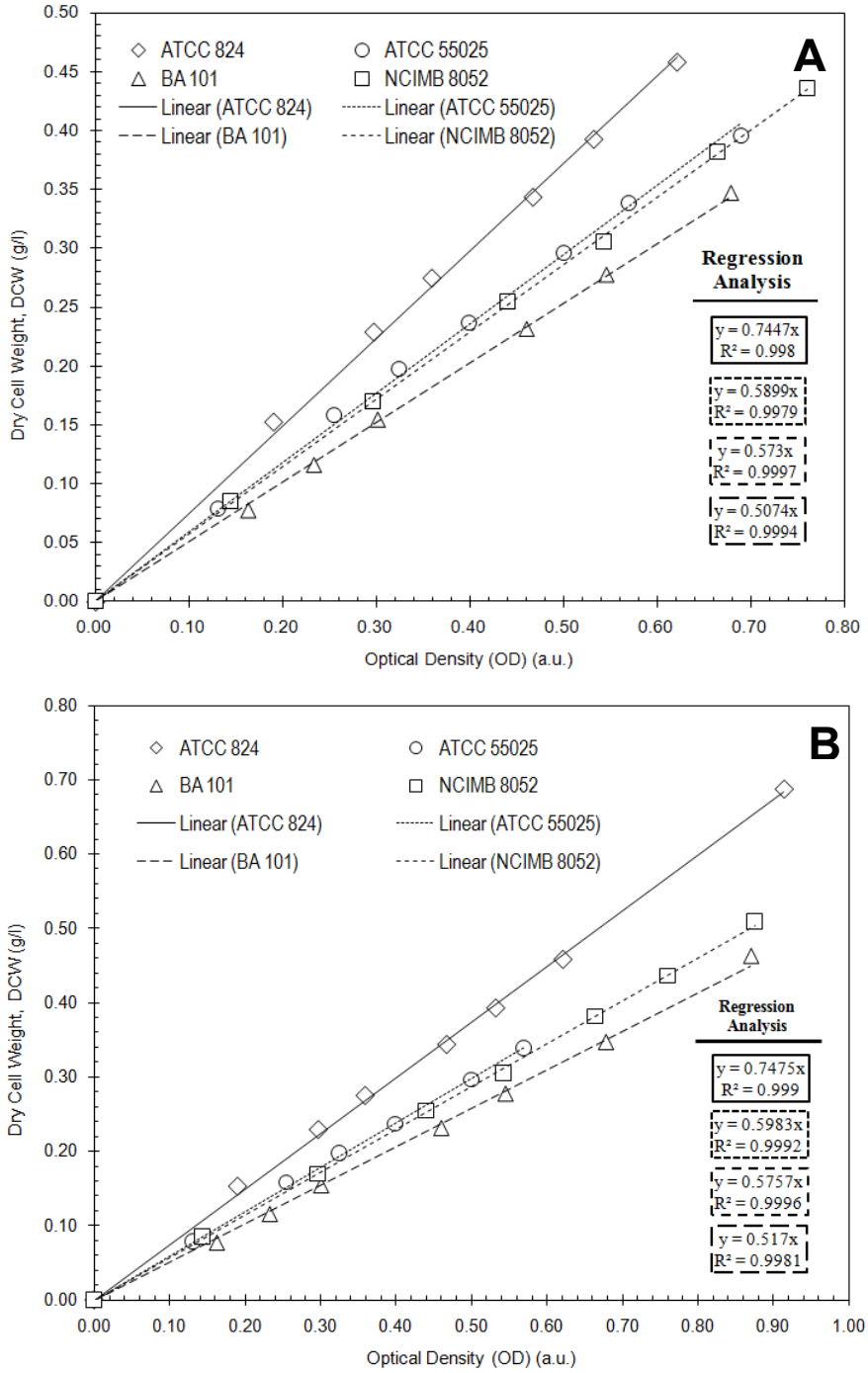

Figure C1. Linear correlations between dry cell weight (DCW) and optical density (OD_{600nm}) for the four bacterial strains. The analysis was repeated twice (graph A – first time, and graph B – second time).

C2. Specific growth rate estimation:

The maximal specific growth rates for each bacterial strain were calculated according to the following example given for the *C. acetobutylicum* ATCC 824 fed with P2-medium containing 4.0 g·l^{-1} of butyric acid:

1. Linearization (integration) of the kinetic growth profiles of OD_{600} over time using the natural logarithm transformation[1]:

   $x(t) = x_0 \cdot \exp(\mu \cdot t) \Rightarrow \ln x(t) = \mu \cdot t + \ln x_0 \Leftrightarrow y = m \cdot x + b$ (Straight line equation)

   Where: $x(t)$ = biomass concentration at every time t; x_0 = initial biomass concentration; and μ_{max} = maximum specific growth rate (h^{-1}). Specific growth rate: $\mu = \frac{1}{x(t)} \cdot \frac{dx}{dt}$; and $OD(t) \propto x(t)$ according to the Lambert-Beer law: $Abs = \varepsilon_{600\ nm} \cdot c \cdot l$ (Harris, 2003).

2. Choice of the most approximate linear range of data points corresponding to the exponential growth phase of bacteria;
3. Linear regression (calibration) of the linearized data (see graph below);
4. The straight line slope ($m = \mu_{max}$) gives the maximal specific growth rate (h^{-1});
5. In some cases, where the minimum requirement of three experimental data points was not satisfied, the following alternative expression was utilized which accounts only for two extreme points (at the beginning and at the end of the exponential phase, respectively):

$$\mu_{max} = \frac{\Delta \ln OD}{\Delta t} = \frac{\ln OD_f - \ln OD_i}{t_f - t_i}$$

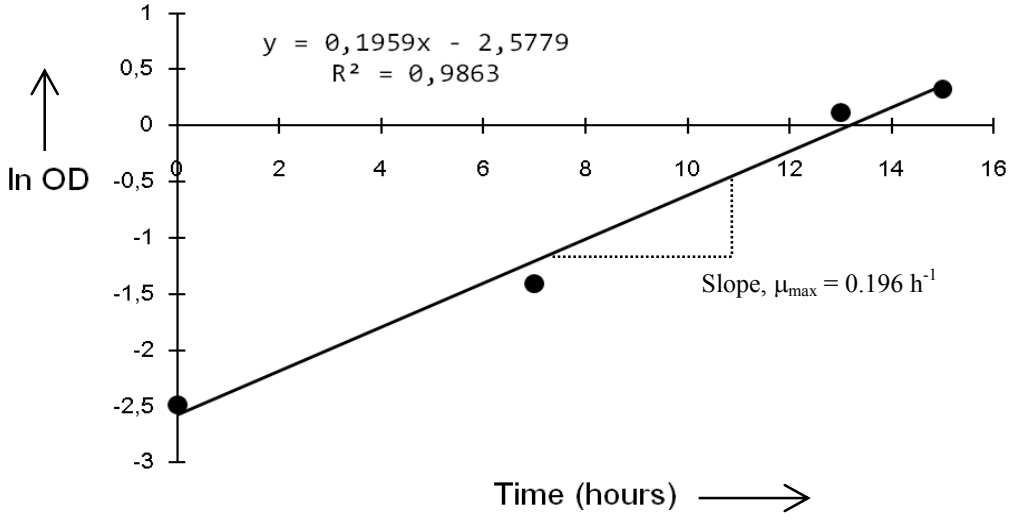

[1] For simplification purposes, it was assumed that all bacteria followed the exponential law of cell growth in a batch culture according to a first-order kinetic model (Brock, 1997).

C3. Butanol yields with and without butyric acid as co-substrate:

Graph #1 – Calibration lines for Butanol Yields ($Y_{P/S}$) based on substrate consumed

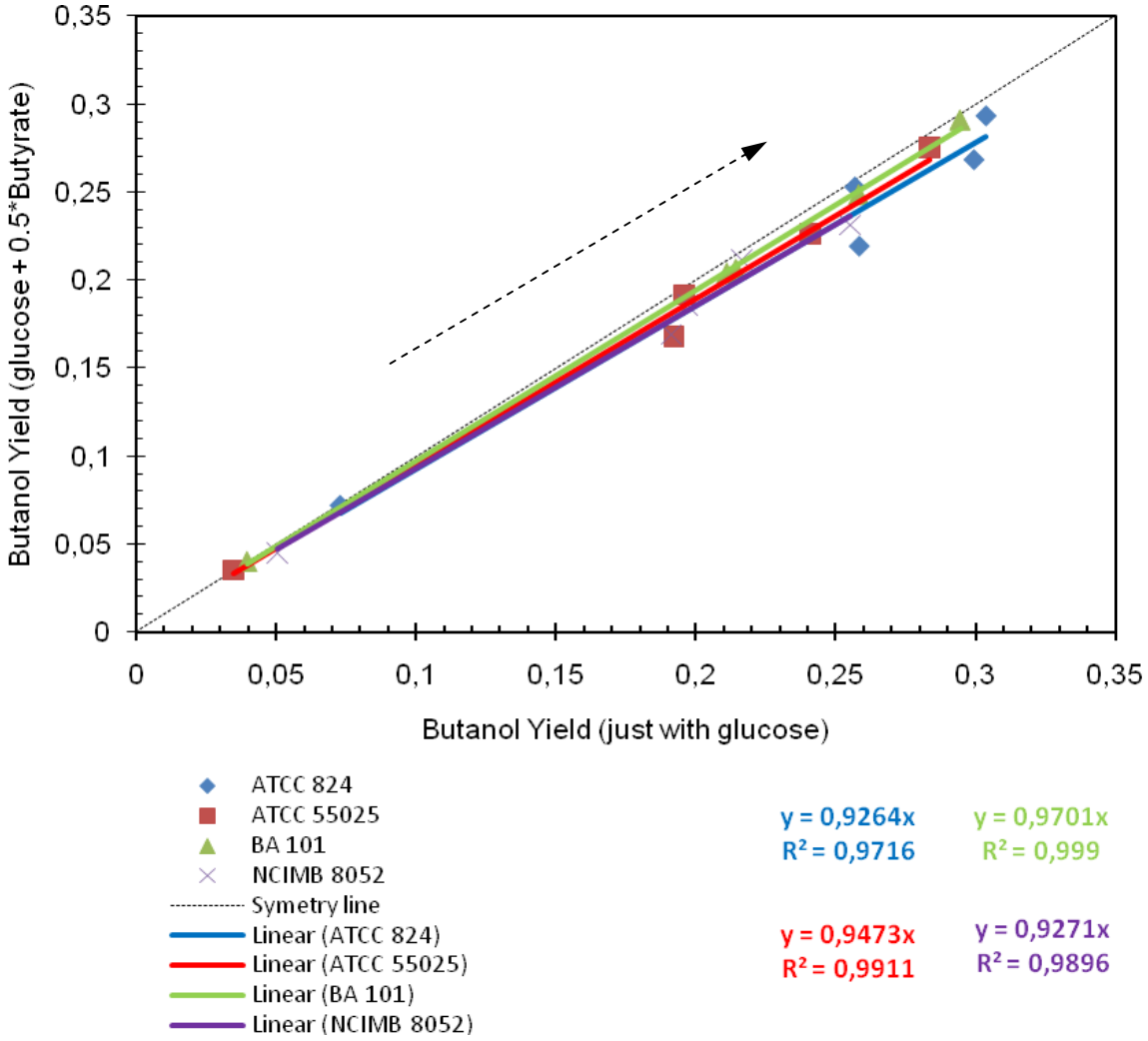

Figure C3. Plot of butanol yield calculated with the inclusion of half butyrate consumed as co-substrate *versus* the yield from glucose utilized only as limiting substrate. Individual calibration lines indicate the balanced deviation error from the ideal symmetry line as a function of increasing butyrate concentrations in the medium (0.0–8.0 g·l^{-1} butyric acid) for the four clostridia strains. Arrow indicates ascending order of initial butyrate concentrations for each strain. Deviation errors from ideality showed an overall average value of 4.6%±2.2 ($\bar{x} \pm SD$) accounted for all strains. Balanced deviation errors were calculated individually for each strain for all concentrations of butyric acid using each regression line slope as a measure of variation from ideality (symmetry line slope = 1.0).

C4. ABE-solvents yields with and without butyric acid as co-substrate:

Graph #2 – Calibration lines for the Yields ($Y_{P/S}$) of ABE-solvents based on substrate consumed

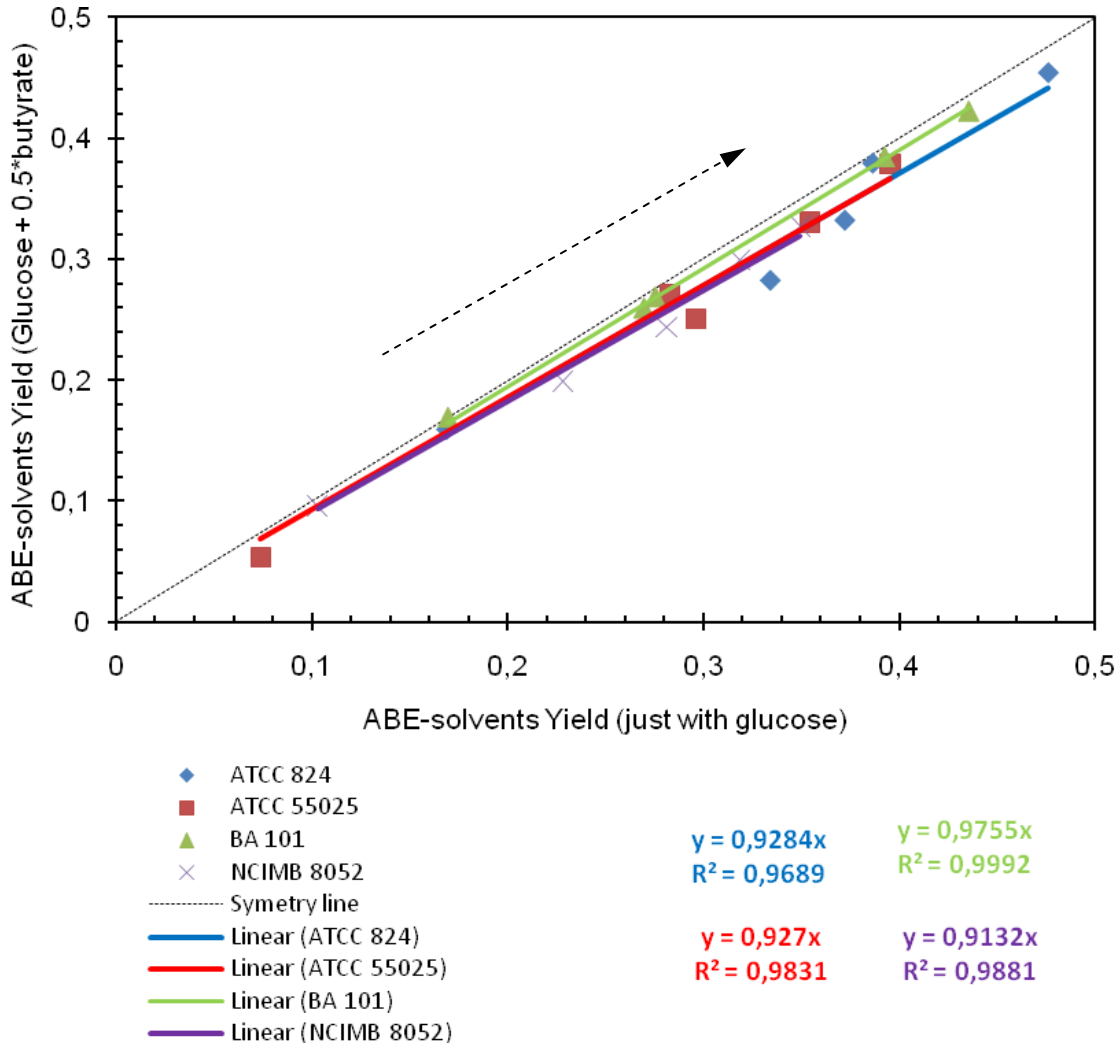

Figure C4. Plot of ABE-solvents yield calculated with the inclusion of half butyrate consumed as co-substrate *versus* the yield from glucose utilized only as limiting substrate. Individual calibration lines indicate the balanced deviation error from the ideal symmetry line as a function of increasing butyrate concentrations in the medium (0.0–8.0 $g \cdot l^{-1}$ butyric acid) for the four clostridia strains. Arrow indicates ascending order of initial butyrate concentrations for each strain. Deviation errors from ideality showed an overall average value of 6.4%±2.7 ($\bar{x} \pm SD$) accounted for all strains. Balanced deviation errors were calculated individually for each strain for all concentrations of butyric acid using each regression line slope as a measure of variation from ideality (symmetry line slope = 1.0).

C5. Principal Component Analysis (PCA) and Hierarchical Clustering (HC):

```
------------------------------------------------------------
Principal Component Analysis and Clustering Analysis:
------------------------------------------------------------

DATE: 27/06/2009

Input data:
```

	Butyric acid concentration (g/L)						
Bacteria	0.0	2.0	4.0	6.0	8.0	10.0	12.0
ATCC 55025	0.252	0.1576	0.1346	0.1232	0.0948	0.0286	0.00045
ATCC 824	0.2516	0.2265	0.1959	0.0956	0.0762	0.0253	0.001
BA 101	0.2614	0.1732	0.1534	0.1031	0.0794	0.0669	0
NCIMB 8052	0.1263	0.1151	0.0905	0.0852	0.0525	0	0

multivariate data

Values represent specific growth rates (in reciprocal hours).

Principal Component Analysis (PCA) for input data:

PCA Calculated from Correlation Matrix by SVD
(Eingenanalysis of the correlation matrix)

	PC1	PC2	PC3
Eigenvalue	4.3551	1.7402	0.9047
Proportion	0.622	0.249	0.129
Variance (%)	62.2	24.9	12.9
Cumulative (%)	62.2	87.1	100.0

PCA *dimensionality reduction*

Eigenvectors

Variable	PC1	PC2	PC3
0.0 g/L	0.468	-0.137	0.118
2.0 g/L	0.406	0.389	0.144
4.0 g/L	0.420	0.337	0.190
6.0 g/L	0.298	-0.490	-0.465
8.0 g/L	0.405	-0.338	-0.310
10.0 g/L	0.307	-0.339	0.658
12.0 g/L	0.304	0.497	-0.430

Scatter plot (PC scores):

Bacteria:	PC1	PC2	PC3
ATCC 55025	0.91026	-1.13144	-1.0945
ATCC 824	1.47701	1.74254	-0.0614
BA 101	0.70449	-0.90437	1.2277
NCIMB 8052	-3.09176	0.29327	-0.0718

univariate data

Hierarchical Cluster Analysis from input data:

Complete Linkage
Euclidean Distance

Amalgamation Steps

Step	Number of clusters	Similarity level	Distance level	Clusters joined		New cluster	Number of obs. in new cluster
1	3	73.75	0.053	1	3	1	2
2	2	51.27	0.098	1	2	1	3
3	1	0.00	0.201	1	4	1	4

Final Partition

Number of clusters: 1

	Number of observations	Within cluster sum of squares	Average distance from centroid	Maximum distance from centroid
Cluster1	4	0.029	0.078	0.129

Note: In order to make natural variables carry equal weight, all raw input data were autoscaled on a 0-to-1 basis (zero mean and unit variance) prior to PCA and HC analysis (scaling and centering).

Appendix D – Kinetic Parameters for Glucose Consumption

D1. Observable glucose uptake rate:

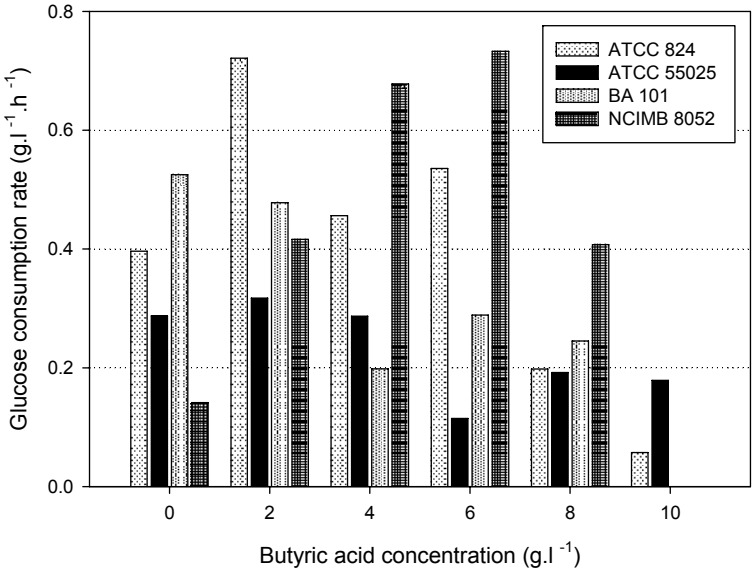

Figure D1. The observable glucose consumption rate (ΔS/Δt) expressed as a function of butyric acid concentration in the medium. Corresponding values are given in Table D5.

D2. Determination of k_s and $\frac{\Delta S}{\Delta t}$:

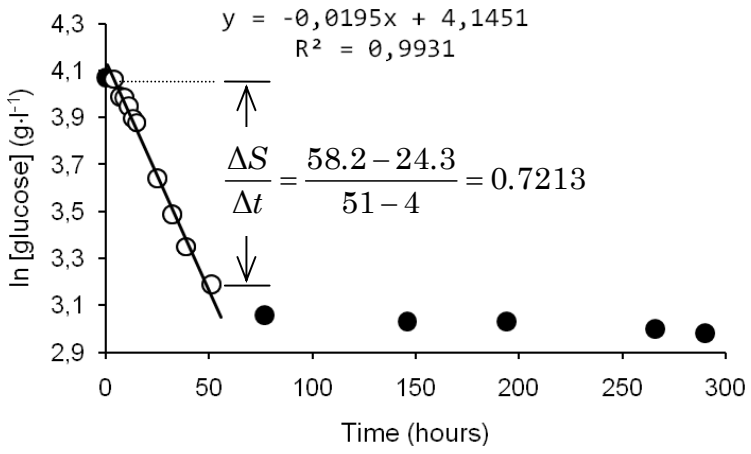

$$\frac{\Delta S}{\Delta t} = \frac{58.2 - 24.3}{51 - 4} = 0.7213$$

Figure D2. Graphical estimation of the first-order rate constant for glucose uptake using the semi-logarithmic plot of glucose concentration over time. The calibration line slope gives the value of k_s for the selected range. The corresponding observable consumption rate (ΔS/Δt) was calculated from the glucose concentration values at the beginning and at the end of the linear range of data. This example is given for the strain ATCC 824 affected by 2.0 g·l^{-1} of butyric acid in the medium.

D3. Correlation level between the observable glucose uptake rate (ΔS/Δt) and the corresponding glucose consumption rate constant (k_s):

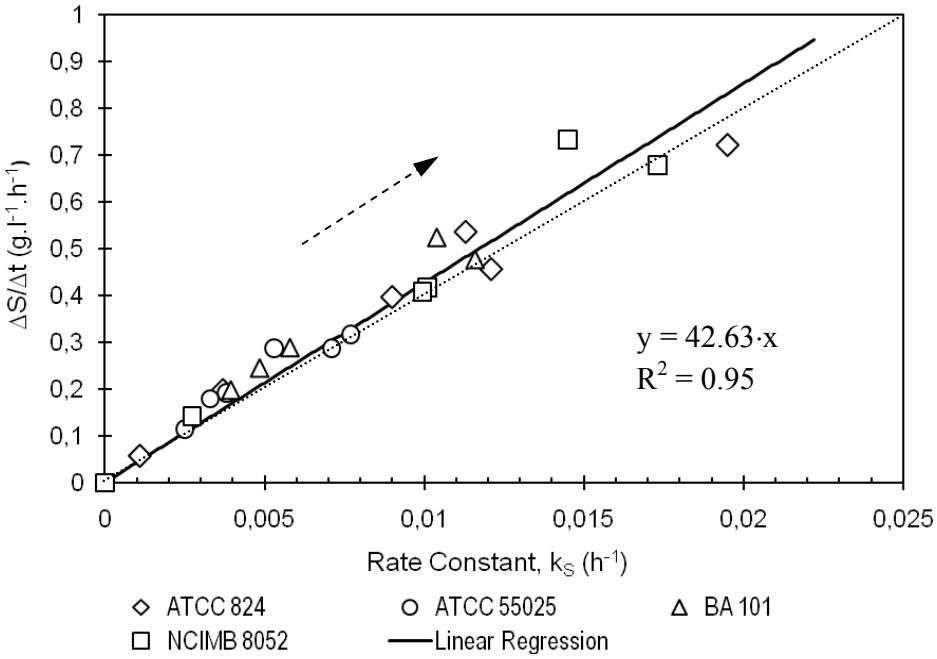

Figure D3. Linear correlation of the observable glucose uptake rate with the first-order consumption rate constant, accounted simultaneously for all bacteria at increasing concentrations of butyric acid. Arrow indicates the increasing direction of butyric acid concentration. Calibration error from ideality (symmetry line slope = 40) shows a deviation value of 6.58%.

D4. Determination of the specific glucose consumption rate (q_s) using the Logarithmic Method:

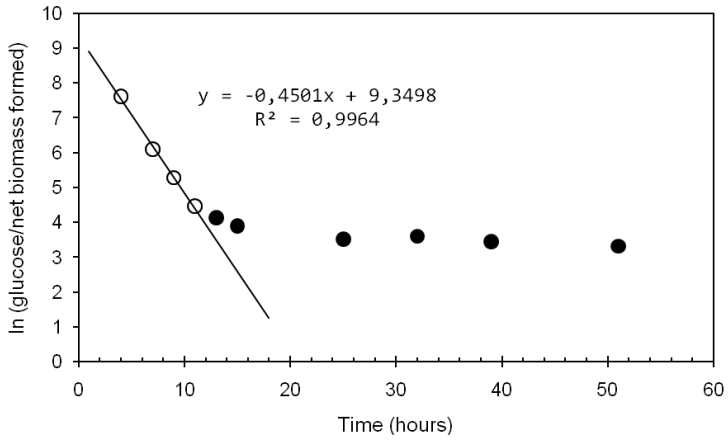

Figure D4. Graphical estimation of the specific glucose consumption rate using the Logarithmic Method. The slope of the calibration line at the linear range of data indicates the specific uptake rate. Example given for the strain ATCC 824 affected with 4.0 g·l^{-1} of butyric acid in the medium.

D5. Glucose consumption parameters:

Table D5. Kinetic parameters of glucose utilization for each bacterial strain as a function of butyrate concentration.

Butyric Acid Concentration (g/l)	Rate Constant, k_s (h^{-1})	Glucose Uptake Rate, ($\Delta S/\Delta t$) (g/l/h)	Specific Glucose Uptake Rate, q_s (g/g/h)	Glucose Utilized (global) (g/l)	Glucose Consumed (%)
ATCC 824					
0.0	0.009	0.396	0.958	9.73	18.63
2.0	0.020	0.721	0.355	38.20	65.50
4.0	0.012	0.456	0.450	34.73	60.94
6.0	0.011	0.536	0.133 ± 0.030	13.05	24.51
8.0	0.004	0.198	0.135 ± 0.012	10.35	18.40
10.0	0.001	0.057	n.d.	3.05	5.54
ATCC 55025					
0.0	0.005	0.288	0.041	9.68	17.92
2.0	0.008	0.317	0.149	10.47	20.17
4.0	0.007	0.287	0.302	19.10	35.91
6.0	0.003	0.115	0.300	10.90	19.53
8.0	0.004	0.192	0.159 ± 0.047	10.40	18.94
10.0	0.003	0.179	n.d.	4.50	8.38
BA 101					
0.0	0.010	0.525	0.235	3.80	7.36
2.0	0.012	0.478	0.575	16.50	31.98
4.0	0.004	0.198	0.609	13.30	25.05
6.0	0.006	0.289	0.538	8.55	16.57
8.0	0.005	0.245	0.399	7.05	13.43
10.0	0.000	0.000	----	----	----
NCIMB 8052					
0.0	0.003	0.142	0.700	6.90	13.00
2.0	0.010	0.416	0.252	20.85	39.71
4.0	0.017	0.678	0.347	19.09	36.36
6.0	0.015	0.733	0.179	20.60	36.14
8.0	0.010	0.407	0.163 ± 0.070	18.80	34.43
10.0	0.000	0.000	----	----	----

Legend: n.d.: non-defined (difficult to estimate). Errors represent slope fluctuations from several regression lines adjusted in the approximate linear range of the plot ln(glucose/net biomass formation) *versus* time. The quotient ($\Delta S/\Delta t$) denotes the observable glucose consumption rate based on the extreme values of the same range of data used to estimate the specific glucose uptake rate.